**Distribution Agreement**

In presenting this thesis or dissertation as a partial fulfillment of the requirements for an advanced degree from Emory University, I hereby grant to Emory University and its agents the non-exclusive license to archive, make accessible, and display my thesis or dissertation in whole or in part in all forms of media, now or hereafter known, including display on the world wide web. I understand that I may select some access restrictions as part of the online submission of this thesis or dissertation. I retain all ownership rights to the copyright of the thesis or dissertation. I also retain the right to use in future works (such as articles or books) all or part of this thesis or dissertation.

Signature:

_____ _____

Abraham Mathai Date

Glutamatergic Inputs to the Monkey Subthalamic Nucleus:
A Comparison of Relative Abundance, Synaptology and Functional Connectivity in Normal versus Parkinsonian Conditions

By
Abraham Mathai
Doctor of Philosophy

Graduate Division of Biological and Biomedical Sciences
Neuroscience

_____
Yoland Smith
Advisor

_____
John Paul Bolam
Committee Member

_____
Mahlon Delong
Committee Member

_____
Dieter Jaeger
Committee Member

_____
Thomas Wichmann
Committee Member

Accepted:

_____
Lisa A. Tedesco, Ph.D.
Dean of the James T. Laney School of Graduate Studies

_____
Date

# Glutamatergic Inputs to the Monkey Subthalamic Nucleus: A Comparison of Relative Abundance, Synaptology and Functional Connectivity in Normal versus Parkinsonian Conditions

By

Abraham Mathai

Bachelor of Engineering – Electronics & Telecommunication, University of Pune, 2003

Master of Science – Biomedical Engineering, New Jersey Institute of Technology, 2008

Advisor: Yoland Smith, Ph.D.

An abstract of

a dissertation submitted to the Faculty of the

James T. Laney School of Graduate Studies of Emory University

in partial fulfillment of the requirements for the degree of

Doctor of Philosophy

in Graduate Division of Biological and Biomedical Sciences, Neuroscience

2013

# ABSTRACT

Glutamatergic Inputs to the Monkey Subthalamic Nucleus:
A Comparison of Relative Abundance, Synaptology and Functional Connectivity in Normal versus Parkinsonian Conditions

By Abraham Mathai

Abnormal activity in the subthalamic nucleus (STN) has been linked to motor and non-motor abnormalities in Parkinson's disease. In addition to abundant GABAergic inputs from the external globus pallidus, the STN also receives significant glutamatergic afferents from the cerebral cortex, thalamus and brainstem. Although the sources of these excitatory afferents have been recognized, their pattern of synaptic connectivity and relative prevalence in normal and pathological conditions are unknown. Hence, we undertook an ultrastructural analysis of the abundance and synaptology of glutamatergic terminals in the STN of normal and 1-methyl-4-phenyl-1,2,3,6-tetrahydropyridine treated parkinsonian monkeys, using vesicular glutamate transporters 1 and 2 as markers of cortical (vGluT1) or sub-cortical (vGluT2) glutamatergic inputs. Because the STN is functionally divided into a "motor" sector and a "non-motor" territory, that receive inputs from different regions, the distribution and density of vGluT1- and vGluT2-positive terminals were compared between these two regions in normal and parkinsonian conditions.

In the normal STN, vGluT1-positive terminals (~14,000/$mm^2$) were more abundant than vGluT2-positive terminals (~10,300/$mm^2$). vGluT1-immunoreactive terminals innervated dendritic spines (~30%) and dendritic shafts (~70%); whereas, vGluT2-immunoreactive terminals almost exclusively targeted dendritic shafts (~90%). The dendritic shaft innervation sites of both glutamatergic inputs were mostly situated on the distal parts of STN dendrites. Notably, we found that the relative density of both vGluT1- and vGluT2-positive terminals significantly decreased by almost half in parkinsonian monkeys compared with controls. Still, the innervation patterns of both vGluT1- and vGluT2-immunopositive inputs on STN dendritic trees were quite similar between the normal and parkinsonian states. No major differences were observed in the relative abundance and synaptology of these glutamatergic inputs between the motor and non-motor STN.

Furthermore, preliminary electrophysiology data from 2 monkeys showed that fewer pallidal neurons responded to electrical stimulation of the internal capsule with the characteristic early excitation (<12ms) typically mediated by corticosubthalamic activation. These data suggest that partial degeneration of cortical inputs to the STN may affect transmission along the cortico-subthalamo-pallidal network in parkinsonism.

Whether the loss of glutamatergic inputs to the STN in parkinsonism is a primary pathological phenomenon or a compensatory mechanism is unclear.

# Glutamatergic Inputs to the Monkey Subthalamic Nucleus: A Comparison of Relative Abundance, Synaptology and Functional Connectivity in Normal versus Parkinsonian Conditions

By

Abraham Mathai

Bachelor of Engineering – Electronics & Telecommunication, University of Pune, 2003

Master of Science – Biomedical Engineering, New Jersey Institute of Technology, 2008

Advisor: Yoland Smith, Ph.D.

A dissertation submitted to the Faculty of the

James T. Laney School of Graduate Studies of Emory University

in partial fulfillment of the requirements for the degree of

Doctor of Philosophy

in Graduate Division of Biological and Biomedical Sciences, Neuroscience

2013

# ACKNOWLEDGEMENTS

I would like to express my sincere gratitude to my advisor, Dr. Yoland Smith for his invaluable guidance and continuous support of my doctoral study and research. I sincerely appreciate his contribution in making my Ph.D. experience a productive and stimulating one. I could not have asked for a more inspirational and supportive mentor. In fact, he has always encouraged me to pursue research ideas beyond the scope of my doctoral dissertation. Two key characteristics I would like to emulate from him are to be a "good human being" and an "affable yet extraordinary scientist".

I would like to thank Dr. Thomas Wichmann, who for all practical purposes has been my co-advisor. A true gentleman and a thoroughbred physician-scientist with an eye-for-detail, he has always encouraged me to push my boundaries to near perfection. I consider him to be my role model in the professional sphere and I hope to follow his career path.

I would also like to thank the rest of my thesis committee: Dr. Mahlon Delong, Dr. John Paul Bolam, and Dr. Dieter Jaeger for their insightful comments and careful review of my research. Their timely inputs and constructive comments have enabled me to successfully complete my doctoral work. I also take this opportunity to make mention of my gratitude to my former committee member, Dr. James Greene. In addition, I would like to thank Dr. Stewart Factor who graciously allowed me to shadow him in his movement disorders clinic to learn the clinical aspects of Parkinson's disease.

I would like to thank Mr. Jean-Francois Paré and Ms. Susan Jenkins for their untiring support that has enabled me to complete the anatomical component of my research studies. I am also grateful for the support I received from all my other colleagues in the Smith lab, especially Dr. Gunasingh Masilamoni and Mr. Robert Moot.

Additionally, I would like to thank Dr. Yuxian Ma and Mr. Damien Pittard, who have contributed immensely to the electrophysiological part of my studies. I am also grateful for the support I received from all the other members of the Wichmann lab, especially Dr. Xing Hu and Dr. Adriana Galvan.

I would like to thank the members of the Emory Neuroscience Program, in particular Ms. Sonia Hayden and Mr. Gary Longstreet, for supporting me during the tenure of my doctoral studies.

Last but certainly not the least, I would like to thank the ones who matter the most to me, for their unwavering support and at times, personal sacrifices to enable me to accomplish this milestone.

Firstly, I would like to thank my Lord and Savior, Jesus Christ – the Author and Perfecter of my faith, for everything. Unequivocally, I have been able to get this far only by His grace. Secondly, I would like to thank my dear wife, Reeba for her unshakeable support and personal sacrifices which have helped me see this day. Along with the delicious meals and sleepless nights staying awake with me, she is the real reason that I had a timeline for graduating within approximately five years. It is said that behind every successful man, there is a woman. Well, in my case, I had a loving woman with a "knife

to my back" warning me that if I took longer to graduate, "she would defend the thesis for me". Thirdly, I would like to thank my loving parents, Mr. K. A. Mathai and Mrs. Lilly Mathai for bringing me into this world, for raising me up in a loving family and for their unfailing trust in me. If I had not seen my father's personal struggle with Parkinson's disease, my motivation to pursue my doctoral studies wouldn't have been this resolute. My role model, his humility, integrity and diligence are virtues I aspire to uphold. In trying times, I derive strength from the immense courage with which he combats all adversities. Certainly, I wouldn't have seen this moment if not for the pillar of my family – my dear mother. She has held the fabric of my family all this while; and admirably ever since my father's tryst with Parkinson's disease since the past twenty three years. Her selfless nurture and strict yet loving parenting have made me what I am today. Adorned with a peaceful smile even in the face of hardships, her faith and hope encourage me to stay calm. In a world where families are crumbling and the sacred bonds of marriage are being ripped apart, I thank my father and mother for providing my sister and me with a tight-knit family and for setting an example by which I should live. I would also like to thank my dear sister, Annie, who is my best friend for her love, support and prayers. Even though we used to fight over the last crumbs of a bar of chocolate while growing up, she is the first person to cry when I fail. Although she is younger than me by two years, I often wonder whether we are "conjoined twins born years apart". I would also like to thank my cute two-year old nephew, David, who brightens my day each time I speak to him. The songs I sing to him and the responses thereof in his toddler voice puts life into perspective. I would also like to thank my mother-in-law, Mrs. Susan Thomas for encouraging me during my doctoral studies and for wholeheartedly supporting my career decisions.

Finally, I would like to thank Uncle Gary and Aunt Kay for hosting my wife and me for the better part of our stay in Atlanta. They have truly been our "family away from family" and have provided us a "home away from home". I would also like to thank my aunt, Chinnamma and my friends, Sangjin, Reni, Thenu, Ashish, Rama, Shyno, Hendry and Rajesh for their support and well wishes.

## TABLE OF CONTENTS

# LIST OF TABLES

# LIST OF FIGURES

# 1. Introduction

## 1.1. Functional Circuitry of the Basal Ganglia

### 1.1.1. General Organization of the basal ganglia

The basal ganglia are a set of tightly interconnected forebrain structures situated deep underneath the cerebral cortex, which participate in both motor and non-motor functions. Comprised of the striatum, external and internal segments of the globus pallidus (GPe & GPi), subthalamic nucleus (STN), substantia nigra pars reticulata (SNr) and substantia nigra pars compacta (SNc), the basal ganglia are intricately connected to process complex information (Wichmann and DeLong, 1996). The basal ganglia network receives inputs from various cortical and sub-cortical sources, and it delivers a tonic inhibitory output to its main targets – the thalamus and brainstem via the GPi and SNr. Within its complex circuitry, the basal ganglia network processes the information it receives, and then generates a corresponding output. This processing is done using several neurotransmitters, which adds to the complexity of information processing within the basal ganglia. Most widely used among them is the inhibitory neurotransmitter γ-aminobutyric acid (GABA), which is employed by projection neurons of the striatum, GPe, GPi and SNr, whereas, the projection neurons arising from the STN use the excitatory neurotransmitter glutamate; and the output neurons of the SNc release the neurotransmitter dopamine. In addition to projections neurons, the basal ganglia nuclei also contain some interneurons, which use neurotransmitters like GABA and acetylcholine. The complex connectivity of basal ganglia nuclei coupled by the usage of

distinct neurotransmitters with opposing effects enables the basal ganglia circuitry to mediate a wide spectrum of functions (Fig. 1.1).

### 1.1.2. Basal ganglia circuits

Anatomical and functional studies modeling the circuitry of the basal ganglia, have led to a strong hypothesis about the role of the basal ganglia in processing information. Fundamental to this model is the presence of two main projection systems called the "direct" and "indirect" pathways within the basal ganglia (Albin et al., 1989; Mink and Thach, 1993; Mink, 1996; Nambu et al., 2002). The direct pathway refers to the monosynaptic connection from the striatum to the GPi/SNr; whereas the indirect pathway is the polysynaptic pathway where the order of connectivity is striatum – GPe – STN – GPi/SNr (Albin et al., 1989) (Fig. 1.1). Subsequently, the GPi/SNr, also called the output nuclei of the basal ganglia, project to the thalamus and brainstem. The thalamic neurons which receive afferents from the basal ganglia output nuclei further project back to the cerebral cortex.

The direct and indirect pathways are activated by excitatory inputs from the neocortex and thalamus. Activation of the direct pathway results in the inhibition of GPi/SNr neurons, whereas triggering of the indirect pathway produces an opposing excitation of these neurons. Any imbalance between the functioning of the direct and indirect pathways results in a shift in the basal ganglia output and its subsequent regulation of the thalamus and brainstem. The polarity of the imbalance determines the direction of the activity shift. If the resulting basal ganglia output is more inhibitory than that seen in

healthy conditions, it is thought to result in hypokinetic conditions, whereas reduced basal ganglia output supposedly causes hyperkinetic movements (Albin et al., 1989; Wichmann and DeLong, 1996).

In addition to the direct and indirect striatofugal pathways, there are other significant pathways in the basal ganglia circuitry such as the corticosubthalamic pathway, also called the hyperdirect pathway (Monakow et al., 1978; Nambu et al., 1996), reciprocal connections of the GPe and STN (Shink et al., 1996), pallidostriatal projections (Mallet et al., 2012), connections from the GPe to GPi/SNr (Hazrati et al., 1990; Hazrati and Parent, 1991) and the nigrostriatal dopaminergic projections (Albin et al., 1989) (Fig. 1.1).

### 1.1.3. Parallel processing in the basal ganglia

Another notable feature of basal ganglia organization is that there are functionally distinct, parallel, non-overlapping channels of the cortico–basal ganglia–thalamo–cortical loops devoted to the processing of motor, oculomotor, limbic and prefrontal information (Alexander et al., 1986; Alexander et al., 1990; Middleton and Strick, 1994, 2002). Such a parallel flow of functionally distinct information is possible due to the presence of devoted topographical territories within each basal ganglia nucleus, the thalamus and cortex which are sequentially linked along the course of these loops. For example, the motor circuit originating in cortical areas involved in the planning and execution of movements, such as the primary motor, supplementary motor and premotor cortices, target the posterior two-thirds of the putamen. Striatal projection neurons from these territories of the putamen further project to the caudal and ventrolateral two-thirds of the

pallidum. Pallidosubthalamic projections emanating from the ventrolateral two-thirds of the GPe terminate in the dorsolateral STN. The motor territories of the GPi project to the ventralis lateralis pars oralis (VLo), the ventralis anterior pars parvocellularis (VApc) and centromedian (CM) nuclei of the thalamus. From here, the information is relayed back to the motor and pre-motor cortices.

Though the basal ganglia network is generally organized along segregated parallel circuits that process functionally distinct information, the functional integration of information typically occurs at the cortical level. In addition to cortical integration, there is also some evidence for the convergence of functionally distinct information within the basal ganglia nuclei (Joel and Weiner, 1994; Haber et al., 2000; Miyachi et al., 2006). Another feature of the cortico–basal ganglia–thalamo–cortical circuit is that at some points in the network, information flows through intricate feedback and feedforward loops. For example, in the striatum the less abundant GABAergic interneurons receive excitatory inputs from the neocortex and, in turn, directly inhibit medium spiny neurons (MSNs), thereby forming a feedforward mechanism (Tepper et al., 2008). On the contrary, the interconnections of MSNs by their local axon collaterals constitute a feedback circuit (Tepper et al., 2008). In addition to feedback mechanisms by local axon collaterals, some of the feedback within the basal ganglia network is enabled by reciprocal connections of basal ganglia nuclei, as seen between the striatum and GPe and that amongst the GPe and STN (Fig. 1.1).

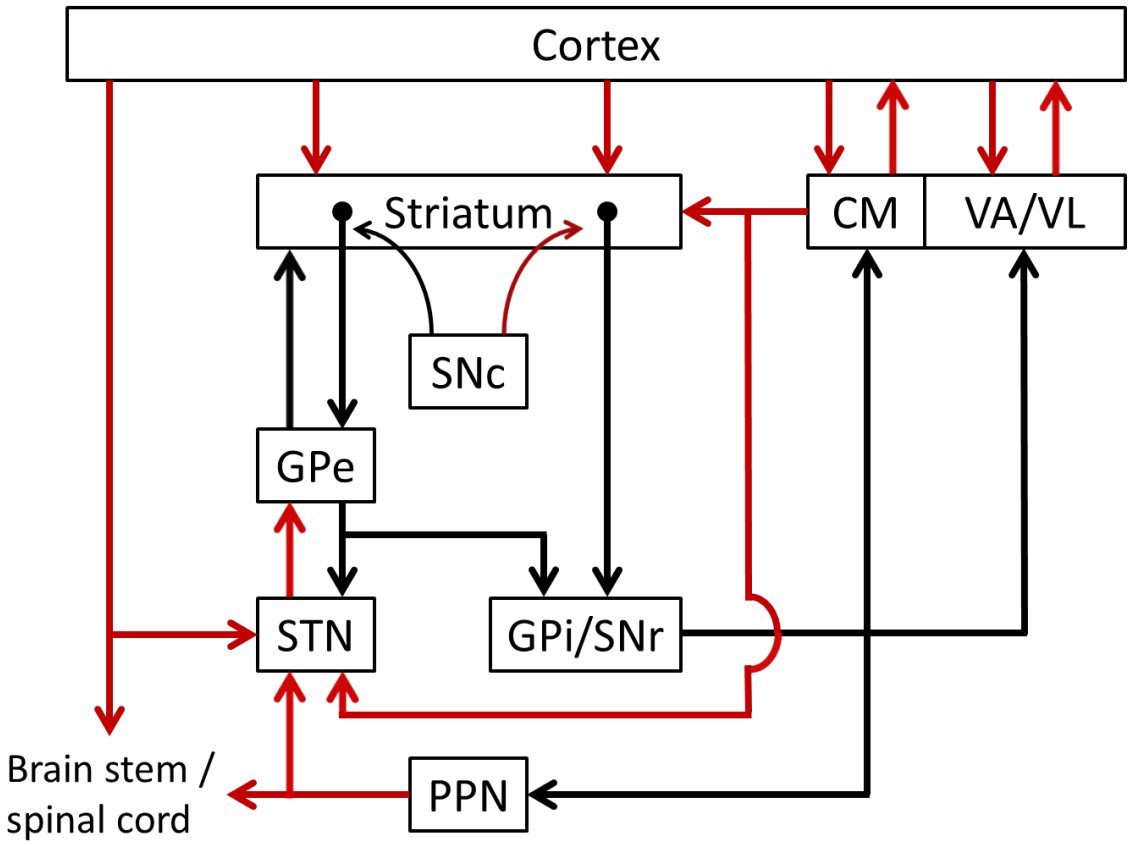


**Figure 1.1: Simplified schematic diagram showing the functional circuitry of the basal ganglia.**

Figure adapted from (Wichmann and DeLong, 2003). Red arrows indicate excitatory connections and black arrows depict inhibitory connections. Note: Some connections have been omitted for simplicity. Abbreviations: CM – centromedian nucleus of the thalamus, VA/VL – ventral anterior and ventral lateral nuclear complex of the thalamus, SNc – substantia nigra pars compacta, SNr – substantia nigra pars reticulata, GPe – external segment of globus pallidus, GPi – internal segment of globus pallidus, STN – subthalamic nucleus, PPN – pedunculopontine nucleus.

1.1.4. Regulation of basal ganglia function by dopamine: Implications in pathological conditions

Dopaminergic signaling in the brain is involved in the regulation of movements, error prediction of reward, motivation, cognition and learning (Arias-Carrion and Poppel, 2007). SNc dopaminergic neurons project extensively to the striatum (Wichmann and DeLong, 1996) and to a lesser degree innervate the extrastriatal basal ganglia nuclei (Rommelfanger and Wichmann, 2010). Importantly, the nigrostriatal dopaminergic projection regulates the balance between the functioning of the direct and indirect pathways, which is necessary for mediating normal basal ganglia function.

In Parkinson's disease, dopaminergic neurons in the SNc progressively degenerate. The ensuing loss of striatal dopamine results in a decreased direct pathway drive and increased indirect pathway activity, thereby causing an imbalance in the activity of the direct and indirect pathways. This imbalance is thought to contribute to the symptoms of Parkinson's disease, such as akinesia, bradykinesia and resting tremor (Wichmann and DeLong, 2003).

## 1.2. Organization of the STN

The STN (formerly called 'corpus Luysi') is an almond-shaped structure in the basal ganglia, which plays a key role in the functional circuitry of the basal ganglia. The STN is a rather homogenous nucleus comprised almost exclusively of glutamatergic neurons (Yelnik and Percheron, 1979). These glutamatergic neurons receive inputs from the GPe,

cortex, thalamus, brainstem and SNc; and they project to the GPe, GPi/SNr and brainstem (Fig 1.1).

### 1.2.1. Functional topography of the STN

Based on its reciprocal connections with the GPe, the STN is topographically divided into various functional regions concerned with motor, associative and limbic functions (Fig. 1.2). In primates, the dorsolateral sector of the nucleus is defined as its motor region, whereas the ventral region and ventromedial pole of the STN are known as its associative and limbic regions, respectively (Shink et al., 1996; Smith, 2011).

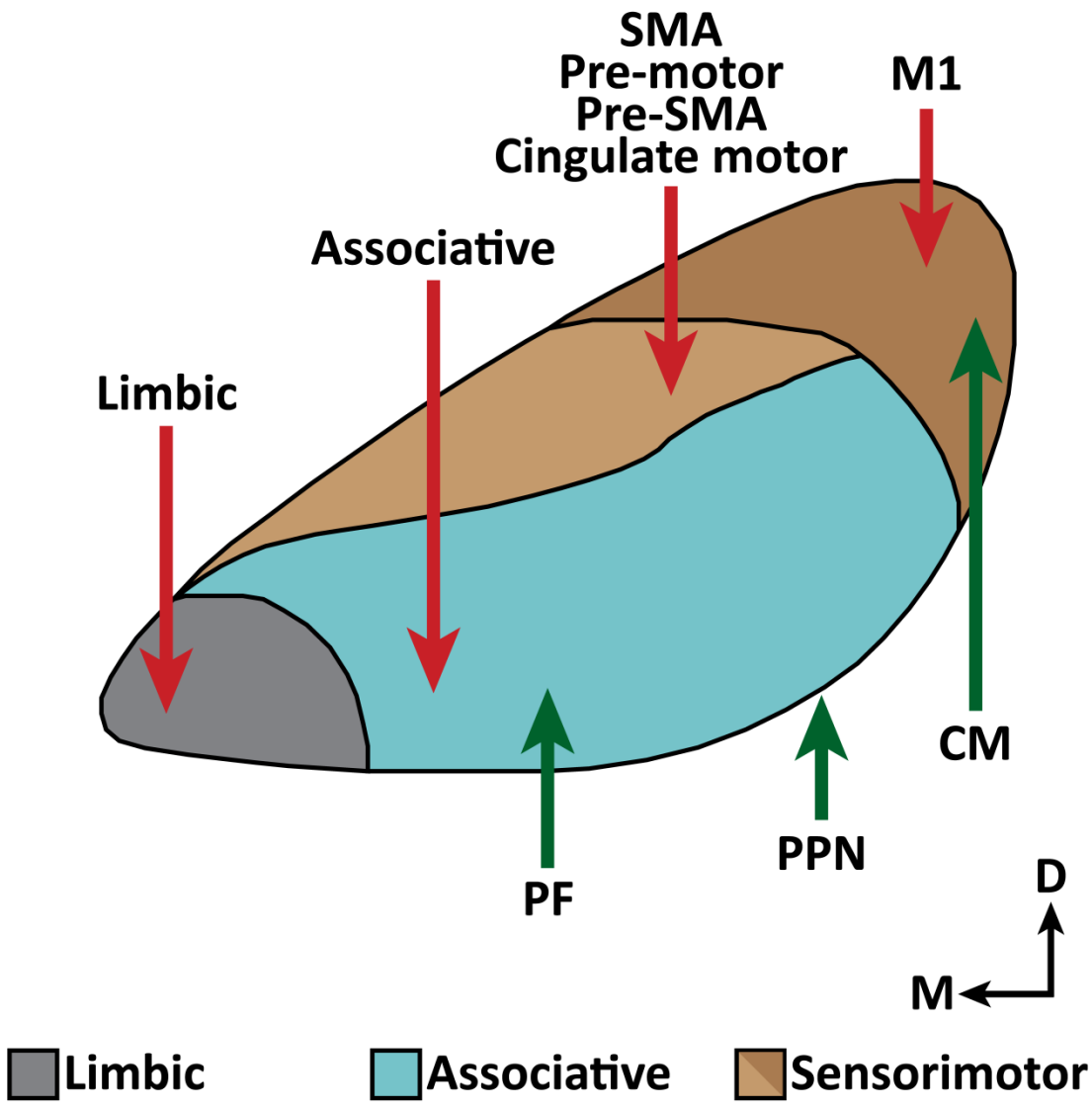


**Figure 1.2: Schematic diagram showing the topographical organization of various cortical and sub-cortical glutamatergic afferents with respect to the functional territories of the STN**

Figure adapted from (Smith, 2011). Red lines indicate cortical inputs and green lines depict sub-cortical inputs. Abbreviations: M1 – primary motor area, SMA – supplementary motor area, CM – centromedian nucleus of thalamus, PF – parafascicular nucleus of thalamus, PPN – pedunculopontine nucleus, D – dorsal, M – medial.

### 1.2.2. Morphology of STN neurons

The STN is a fairly homogenous nucleus comprised almost exclusively of glutamatergic projection neurons. The STN neurons have either a radiating or elongated fusiform morphology in both primates and rodents (Rafols and Fox, 1976; Yelnik and Percheron, 1979; Afsharpour, 1985). All Golgi impregnation studies of the primate, cat and rodent STNs have reported the presence of Golgi type I neurons, which morphologically depict projection neurons (Rafols and Fox, 1976; Iwahori, 1978; Yelnik and Percheron, 1979; Afsharpour, 1985). Also, a few studies have reported the existence of Golgi type II local interneurons in the STN (Rafols and Fox, 1976; Iwahori, 1978). A recent study of the human STN revealed a scarce, but noteworthy presence of GABAergic interneurons (Levesque and Parent, 2005).

The morphological characteristics of the projection neurons of the STN have been studied extensively. Some of these neurons have many dendritic spines, while others have a few. Also, the dendrites of these neurons are confined within the boundaries of the nucleus in cats and primates (Rafols and Fox, 1976; Iwahori, 1978; Yelnik and Percheron, 1979); and therefore, the STN is considered as a closed nucleus. However, in the rat STN, dendrites extend beyond the confines of the nucleus; and hence, the rat STN is categorized as an open nucleus (Hammond and Yelnik, 1983; Kita et al., 1983; Afsharpour, 1985). An interesting feature of STN neurons is that some of their dendrites extend to great distances, as far as 750 μm away from the soma (Rafols and Fox, 1976). Considering the small size of the nucleus, the radial distances covered by these neurons are noteworthy. In fact, the dendritic domain of an individual STN neuron can cover

about half, one-fifth, and one-ninth of the STN in the cat, monkey and human, respectively (Yelnik and Percheron, 1979).

### 1.2.3. Glutamatergic afferents to the STN

#### *1.2.3.1. Cortical glutamatergic inputs*

Along with the striatum, the STN is another input station within the basal ganglia network which receives cortical glutamatergic inputs (Monakow et al., 1978; Nambu et al., 1996; Mathai and Smith, 2011). Corticosubthalamic projections arise from motor, associative and limbic cortices and innervate their respective functional domains within the STN topographical map (Nambu et al., 1996; Haynes and Haber, 2013) (Fig. 1.2). Motor, associative and limbic cortical inputs target the dorsolateral, ventral and ventromedial sectors of the primate STN, respectively. These inputs mainly target distal dendritic shafts and dendritic spines on STN neurons in the rat (Bevan et al., 1995). Little is known about the synaptic organization of the corticosubthalamic inputs in primates and this question is one of the main topics of study of this thesis (see chapters 2 & 3). Though the cortical inputs innervating the STN are not as profuse as the ones which terminate in the striatum, they still deliver a powerful excitatory drive to the STN (Nambu et al., 2002; Jahfari et al., 2011; Haynes and Haber, 2013). Compared with transmission from the cerebral cortex to the GPi via the direct and indirect pathways, information flow along the cortex-STN-GPi pathway has a significantly shorter latency (< 12 ms) (Nambu et al., 2000). Hence, the cortex-STN-GPi connection has been called the “hyperdirect” pathway of the basal ganglia. Electrical stimulation of the cerebral cortex results in a triphasic

"excitation-inhibition-excitation" response in pallidal neurons (Kita, 1992; Nambu et al., 2000) due to the activation of the hyperdirect, direct and indirect pathways, respectively. According to some authors, this temporal pattern of activation of the different basal ganglia circuits forms the basis for a center-surround model of action selection mediated by the cortico-basal ganglia-thalamocortical circuits (Mink, 1996; Nambu et al., 2002). According to this model, cortical activation results in a direct excitation of glutamatergic neurons of the STN. In turn, these STN neurons deliver a broad excitation to the basal ganglia output nuclei (GPi/SNr) through the diffuse subthalamopallidal projections (Smith et al., 1990). Subsequently, the inhibitory output of the basal ganglia inhibits large areas of the thalamus and cortex, thereby inhibiting regions pertaining to the desired motor program and its competing programs. This chain of transmission via the hyperdirect pathway is the fastest conduction route from the cortex to the basal ganglia output nuclei. After the surround inhibition is provided by the hyperdirect pathway to the thalamus, a specific disinhibition is mediated through the direct pathway, which supposedly selects the desired motor programs. Then, a surround inhibition is elicited by activation of the indirect pathway. The proposed role of the hyperdirect pathway in the action selection model has gained a lot of attention over the past decade or so (Nambu et al., 2002). However, it is not clear whether the basal ganglia are even required to select actions, let alone the proposed sequential chain of activation of the hyperdirect-direct-indirect pathways to mediate action selection. In fact, parkinsonian patients with a surgical lesion of the GPi, which is the most prominent motor-related output nucleus of the basal ganglia network, do not generally report problems with selection of action programs (Gross, 2008).

*1.2.3.2. Sub-cortical glutamatergic inputs*

Apart from the cortical afferents, the STN also receives glutamatergic inputs from the centromedian (CM) and parafascicular (PF) thalamic nuclei (Sadikot et al., 1992), pedunculopontine nucleus (PPN) (Lavoie and Parent, 1994a; Bevan and Bolam, 1995) (Fig. 1.2). In rats, the STN also receives glutamatergic inputs from axon collaterals of local neurons (Kita et al., 1983). In monkeys, afferents from the CM terminate in the dorsolateral STN, while the afferents from the PF target the ventral STN (Sadikot et al., 1992), a pattern consistent with the functional topography of the STN as described earlier. In rats, these thalamic inputs to the STN primarily target proximal dendrites and dendritic spines (Bevan et al., 1995). Neuronal tracing studies in both rats and monkeys have not characterized their exact topographical organization of the pedunculosubthalamic connections thus far (Lavoie and Parent, 1994a; Bevan and Bolam, 1995). However, it is known that the pedunculosubthalamic inputs target both dendritic shafts and spines in the rat STN (Bevan and Bolam, 1995). Also, it must be noted that some of the glutamatergic neurons in the PPN also co-express choline acetyltransferase (ChAT) (Lavoie and Parent, 1994b).

A detailed characterization of the synaptic connectivity of cortical and sub-cortical glutamatergic afferents to various functional regions of the monkey STN remains to be established (see chapter 3).

*1.2.3.3. Vesicular glutamate transporters as specific markers of cortical and sub-cortical glutamatergic afferents to the basal ganglia*

The predominant excitatory neurotransmitter of the central nervous system, glutamate, is packaged into synaptic vesicles by proteins called the vesicular glutamate transporters (vGluTs). In mammals, the family of vGluTs consists of three highly homologous proteins: vGluT1-3. Throughout the brain, the expression of particular vGluTs is complementary (Fremeau et al., 2004). vGluT1 mRNA is richly expressed in the cerebral cortex, hippocampus, dentate gyrus and medial amygdala, whereas vGluT2 mRNA is predominantly present in the thalamus, hypothalamus, brainstem and basolateral amygdala (Fig. 1.3). However, there are few exceptions to this generally complementary expression of vGluT1 and vGluT2 mRNA between various brain regions. In the thalamus, subsets of neurons co-express both vGluT1 and vGluT2 mRNA (Barroso-Chinea et al., 2007; Barroso-Chinea et al., 2008). Also, neurons in layer IV of the cortex express the vGluT2 mRNA (Fremeau et al., 2001). Lastly, vGluT3 mRNA is less abundant and widely expressed throughout the brain, often in non-glutamatergic neurons (Gras et al., 2002).

Although there are subsets of neurons which co-express vGluT1 and vGluT2 mRNA, typically only either of their respective proteins is expressed in the glutamatergic terminals within the striatum (Fujiyama et al., 2004; Fujiyama et al., 2006). Thus, corticostriatal and thalamostriatal terminals can be distinguished based on the complementary expression of vGluT1 and vGluT2 proteins, respectively (Fujiyama et al., 2004; Fujiyama et al., 2006; Raju et al., 2006; Raju et al., 2008). This complementary expression pattern of vGluT1 and vGluT2 proteins is also seen in other regions of the

adult nervous system (Hur and Zaborszky, 2005; Kubota et al., 2007; Liguz-Lecznar and Skangiel-Kramska, 2007), with a few exceptions where both isoforms are co-expressed (Li et al., 2003) (Fig. 1.3). Hence, vGluT1 and vGluT2 are considered the most reliable markers to distinguish between glutamatergic inputs of cortical versus sub-cortical origin (Liguz-Lecznar and Skangiel-Kramska, 2007).

Another important point to consider is whether the almost exclusive expression of the vGluT1- and vGluT2-isoform in cortical and sub-cortical afferents, respectively, can account for a different influence of these two types of inputs to the basal ganglia. In fact, physiological studies indicate that vGluT1-immunopositive neurons tend to have lower release probability and less short term depression compared with vGluT2-containing neurons (Weston et al., 2011).

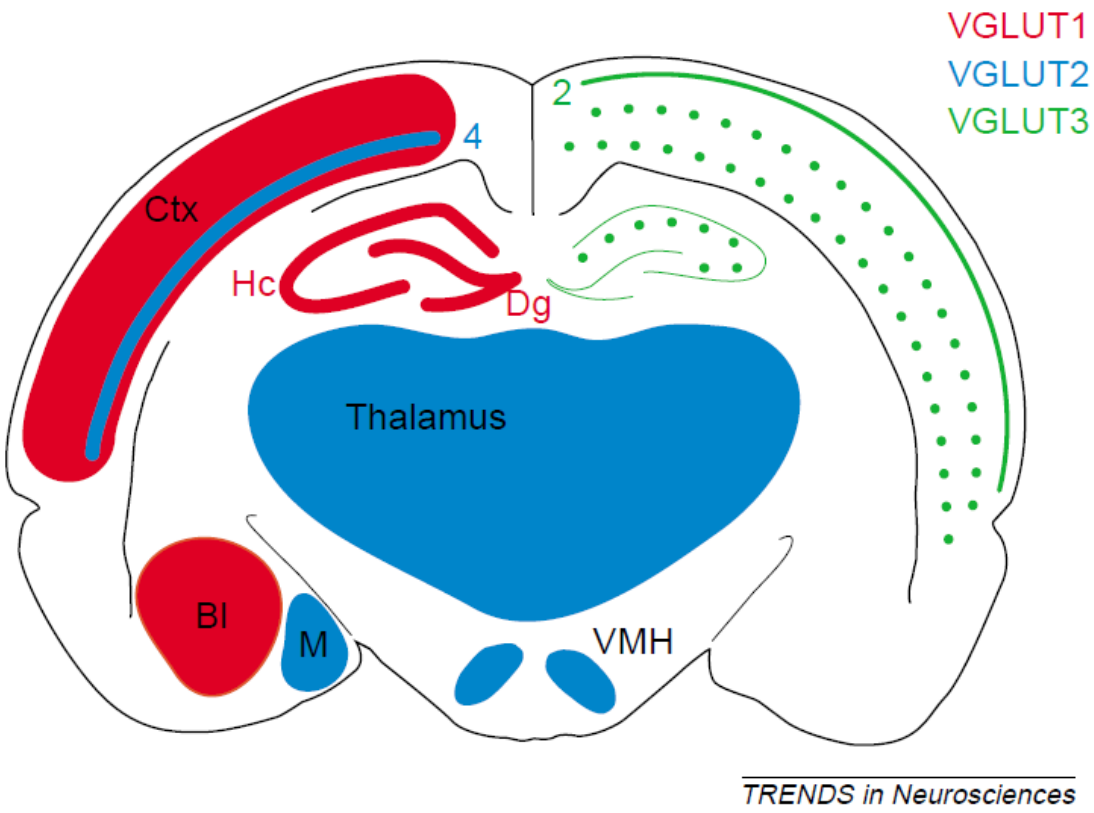


**Figure 1.3: Expression of vGluT1-3 mRNA in neuronal cell bodies across the central nervous system**

Figure directly reproduced with permission from (Fremeau et al., 2004). Abbreviations: Ctx – cerebral cortex, Hc – hippocampus, Dg – dentate gyrus, Bl – basolateral nucleus of amygdala, M – medial nucleus of amygdala, VMH – ventromedial nucleus of hypothalamus. Numbers indicate cortical layers and dots illustrate sparse distribution of cell bodies. The brainstem is not shown in this figure.

### 1.3. Pathophysiology of the STN in Parkinson's disease

In addition to dopamine loss in the striatum, which is a hallmark characteristic of Parkinson's disease, a lesser-known feature is dopaminergic denervation in the extrastriatal nuclei of the basal ganglia (Rommelfanger and Wichmann, 2010). In this context, there is a significant loss of the modest nigral dopaminergic inputs to the STN in parkinsonian patients (Hornykiewicz, 1998) and in 1-methyl-4-phenyl-1,2,3,6-tetrahydropyridine (MPTP)-induced parkinsonian monkeys (Pifl et al., 1990; Rommelfanger and Wichmann, 2010). In addition to the loss of dopaminergic afferents of the STN, there are wide-ranging aberrations in functional activity of STN neurons. In parkinsonism, STN neurons have increased spike rates (Fig. 1.4), and they fire in a more correlated, rhythmic and synchronous manner with GPe neurons compared with that seen in normal conditions (Bergman et al., 1994; Bevan et al., 2002; Wichmann and DeLong, 2003). Since prominent changes in STN activity are seen during wide-ranging brain oscillations (Magill et al., 2000), it is often assumed that pathological rate and pattern changes in STN neuronal activity in Parkinson's disease may directly contribute to the disease symptoms (Bevan et al., 2002; Bevan et al., 2006).

The firing pattern of STN neurons is primarily generated intrinsically due to the presence of several non-synaptic ion channels, such as voltage-gated $Na^+$ channels, voltage-gated $Ca^{2+}$ channels and small conductance $Ca^{2+}$ -dependent $K^+$ channels (Beurrier et al., 1999; Bevan and Wilson, 1999; Do and Bean, 2003; Hallworth et al., 2003; Do and Bean, 2004). Extrinsic inputs to STN neurons are thought to contribute subtly to these largely intrinsically generated STN activity patterns (Bevan et al., 2006).

While changes in the intrinsic membrane properties could cause major changes in STN neuronal activity, any pathological changes in the extrinsic inputs to the STN would also contribute to changes in its activity (Wilson and Bevan, 2011). It is known that there is a proliferation of the GABAergic GPe-STN inputs in the dopamine denervated state (Fan et al., 2012). However, a detailed description of pathological changes occurring to cortical and sub-cortical glutamatergic inputs to the STN in parkinsonism needs to be done (see chapters 2 & 3).

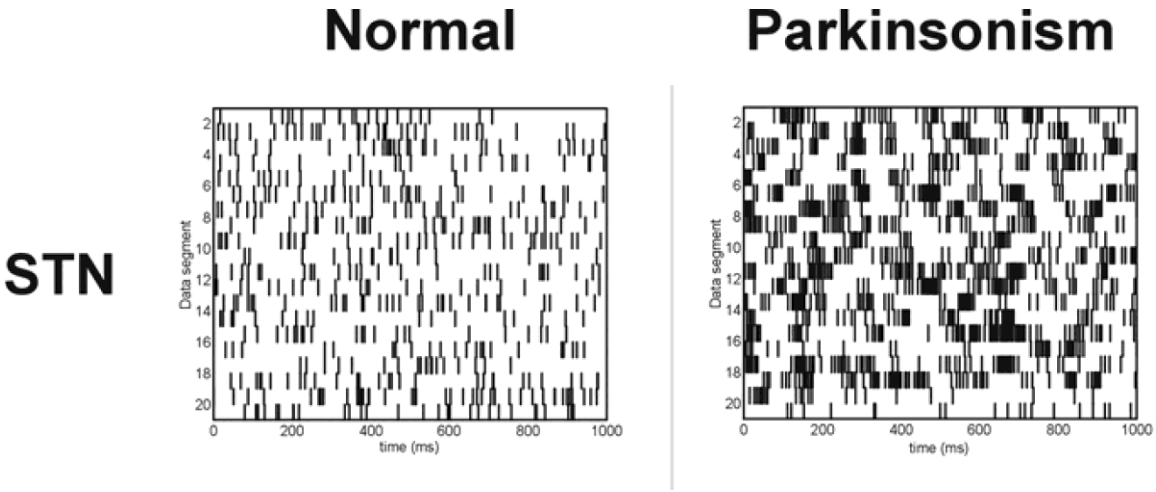


**Figure 1.4: Raster plots of spontaneous neuronal activity of STN neurons in normal and parkinsonian monkeys**

Partial reproduction of a figure taken with permission from (Wichmann and DeLong, 2003). Each raster generated from 20 consecutive 1000 ms data segments. Obvious differences seen in both the firing rates and firing patterns of the neurons recorded in normal versus parkinsonian conditions.

### 1.4. STN deep brain stimulation (DBS) as a treatment for Parkinson's disease

Traditionally, dopamine replacement strategies have been the first line of treatment of the symptoms of Parkinson's disease. Levodopa and dopamine receptor agonists have been effectively used to treat parkinsonian symptoms for decades (Smith et al., 2012). However, as the disease progresses, there are major complications induced by these pharmacological interventions. In patients with advanced Parkinson's disease, the effects of these drugs are quite unreliable with extended periods called OFF times, when the drugs do not relieve the motor symptoms. Also, even during the ON times when the drugs are effective, there can be troublesome side effects such as involuntary movements, which are at times more debilitating and hazardous than the disease symptoms. Therefore, effective pharmacological management of parkinsonian symptoms is highly challenging in advanced parkinsonian patients.

Around two decades ago, neuroscientists showed that surgical lesioning of the STN could reverse the symptoms of parkinsonism in MPTP-treated monkeys (Bergman et al., 1990). The basis for this approach was the assumption that silencing an overactive STN in parkinsonism would reduce the pathological hyper-inhibitory basal ganglia output, thereby, reversing the ensuing hypokinetic symptoms. Moreover, this approach had its underpinnings in the pathophysiology of another movement disorder known as hemiballismus, in which lesions of the STN in otherwise healthy adults results in large amplitude, uncontrolled movements (Guridi and Obeso, 2001). While lesioning the STN has been effective in reversing the hypokinetic symptoms of parkinsonian patients (Dierssen et al., 1961; Gill and Heywood, 1997), the irreversible nature of the procedure gives very limited options for post-operative remediation (Alvarez et al., 2009). An

alternative approach of silencing STN activity using high frequency electrical stimulation was undertaken, wherein it was initially proposed that the stimulation would inactivate the STN neurons by a depolarization block (McIntyre et al., 2004). Later, some studies suggested that STN-DBS activates/inhibits surrounding fibers of passage, including the antidromic stimulation of inputs from the cerebral cortex (Li et al., 2007), thereby causing global network changes. Though the exact mechanism of action of STN-DBS is not yet clear (McIntyre et al., 2004), it is a popular treatment for advanced Parkinson's patients since the procedure can be adjusted and even reversed post-operatively. However, it must be noted that in addition to its therapeutic benefits, STN-DBS can produce some cognitive and limbic side-effects (Bronstein et al., 2011).

### 1.5. Specific Aims

It has been well established that there are major pathophysiological changes occurring to STN neurons in parkinsonism (Fig. 1.4). In part, these changes could be attributed to changes in the membrane properties of STN neurons (Wilson and Bevan, 2011); while some could be due to changes in the activity of extrinsic inputs to the STN. A recent study showed that the GPe-STN connection, which is a very prominent input to the STN, is substantially strengthened in the dopamine-denervated state, most likely through complex morphological changes of GPe terminals (Fan et al., 2012). Moreover, there are significant functional changes occurring to the cortical glutamatergic afferents to the STN in animal models of PD and the human disease. In 6-hydroxydopamine (6-OHDA) treated parkinsonian rats, corticosubthalamic neurons show lower metabolic activity (Orieux et al., 2002), and there are exaggerated beta oscillations between the cortex and

STN (Mallet et al., 2008). In the human disease, the cortex and STN show increased functional connectivity (Baudrexel et al., 2011), and their activities are pathologically synchronized (Shimamoto et al., 2013). The functional changes occurring to the corticosubthalamic system in parkinsonism could underlie the development of pathological oscillations within the STN, which are thought to contribute to the genesis of the motor symptoms of PD (Wilson and Bevan, 2011). Also in the case of the sub-cortical glutamatergic afferents to the STN, inputs originating from the PF and PPN have increased metabolic activity in parkinsonian rats (Orieux et al., 2000). However, it is unknown whether there are underlying morphological changes occurring to these glutamatergic inputs in parkinsonism, as was found for cortical and thalamic inputs to the striatum (Villalba and Smith, 2013). Also, some studies have shown that during STN-DBS, cortical afferents to the STN are antidromically stimulated (Li et al., 2007; Rektor et al., 2009). If some of the effects of STN-DBS could be attributed to antidromic stimulation of STN inputs, it is important to know the detailed synaptic organization and relative abundance of these afferents in normal and parkinsonian states to understand better the possible sources of STN pathophysiology in PD and the potential mechanisms of action of STN-DBS. To address these problems, I have written this thesis devoted to the following specific aims:

### 1.5.1. Specific Aim 1

To compare the relative abundance, synaptology and functional connectivity of the motor corticosubthalamic system in normal versus parkinsonian monkeys. (Chapter 2)

### 1.5.2. Specific Aim 2

To compare the relative abundance and synaptology of cortical and sub-cortical glutamatergic afferents in the motor and non-motor regions of the STN in normal and parkinsonian monkeys. (Chapter 3)

# 2. Cortical Innervation of the Subthalamic Nucleus Decreases in Experimental Parkinsonism

## 2.1. Introduction

The basal ganglia receive inputs from functionally diverse regions of the cerebral cortex via two main stations, the striatum and the subthalamic nucleus (STN) (Mathai and Smith, 2011). Both systems originate from wide areas of the cerebral cortex and provide topographically organized inputs to various regions of the striatum and STN (Parent and Hazrati, 1995; Nambu et al., 1996; Haynes and Haber, 2013). Compared with the corticostriatal system which represents the most prominent afferent to striatal projection neurons, and accounts for the largest number of axon terminals in the mammalian striatum, the corticosubthalamic projection is more modest. Corticosubthalamic axons target dendritic spines and distal dendritic shafts of STN neurons in rats (Bevan et al., 1995); whereas its dendritic innervation pattern has not been characterized in primates. Despite its sparse nature, the corticosubthalamic projection is recognized as a powerful source of excitation to STN neurons through which cortical inputs regulate basal ganglia output activity in the internal globus pallidus (GPi) and substantia nigra pars reticulata (SNr) (Nambu et al., 2000). Because of its rapid transmission (compared to the slower trans-striatal “direct” and “indirect” pathways), the corticosubthalamo-pallidal route has been called the “hyperdirect” pathway of the basal ganglia.

Although abnormal STN neuronal activity has long been known as a key pathophysiological feature of parkinsonism (Bergman et al., 1994; Bevan et al., 2002; Wichmann and DeLong, 2003), our understanding of the exact substrate(s) that underlies these changes remains incomplete, but most likely involves altered transmission and functional interactions between γ-aminobutyric acid (GABA) -ergic inputs from the external pallidal segment (GPe) (Fan et al., 2012) and glutamatergic afferents from the cerebral cortex. While activity changes in the corticosubthalamic system are increasingly recognized to occur in parkinsonism (Orieux et al., 2002; Mallet et al., 2008; Baudrexel et al., 2011; Shimamoto et al., 2013), the network alterations that underlie such dysfunctions remain poorly understood.

Thus, we combined ultrastructural and electrophysiological approaches in the non-human primate model of PD to further characterize the anatomical and physiological integrity of the corticosubthalamic system in the parkinsonian state. Initially, we assessed changes in the density and pattern of dendritic innervation of STN neurons by cortical terminals (labeled with antibodies against the vesicular glutamate transporter 1-vGluT1) (Fremeau et al., 2001; Raju et al., 2008) between normal and parkinsonian monkeys. Subsequently, we characterized the functional integrity of the cortico-subthalamo-pallidal system in awake normal and MPTP-treated parkinsonian monkeys with electrophysiologic techniques. Our findings revealed a significant loss of the corticosubthalamic projection, together with a decreased drive of this system upon pallidal neurons, in MPTP-treated parkinsonian monkeys. Preliminary results of this study have been presented in abstract form (Mathai et al., 2010; Mathai et al., 2011).

## 2.2. Methods

### 2.2.1. Animals

All experiments were performed in accordance with the National Institutes of Health's "Guide for the Care and Use of Laboratory Animals" (Garber et al., 2010), the United States Public Health Service Policy on Humane Care and Use of Laboratory Animals (amended 2002), and were approved by the Biosafety Committee and the Animal Care and Use Committee of Emory University.

Fourteen adult rhesus monkeys (Macaca Mulatta, 4.4-15.0 kg, 2-11 years old, 8 males & 6 females) were used. The monkeys were raised in the breeding colony of the Yerkes National Primate Research Center. The animals had ad libitum access to food and water. Twelve of the monkeys were used in the anatomical studies. Six of these were rendered parkinsonian following chronic administration of MPTP (see below).

The remaining two monkeys were used in the electrophysiological studies. Prior to experimentation, these animals were acclimated to the laboratory, and trained to permit handling by the experimenter and to sit quietly in a primate restraint chair, using positive reinforcement techniques (McMillan et al., 2010). Electrophysiology data in the normal state were collected from the left hemispheres, while data from the right hemispheres were collected after the animals displayed stable parkinsonian motor symptoms (see description below).

2.2.2. Induction of Parkinsonism

Monkeys were rendered parkinsonian by weekly administration of MPTP (0.2-0.8 mg/kg/week; Sigma-Aldrich, St. Louis, MO, USA; cumulative doses, 3.2-19.4 mg/kg; treatment time range, 1-8 months) until moderate parkinsonian motor signs developed. As described in previous studies (Wichmann et al., 2001; Kliem et al., 2010; Masilamoni et al., 2011; Hadipour-Niktarash et al., 2012), the animal's behavior was analyzed in an observation cage. One side of the cage was made of Plexiglas to facilitate an unobstructed view of the monkey. The cage was equipped with 8 infrared beams, which allowed us to assess the severity and stability of the MPTP-induced motor disability by recording the monkey's spontaneous movements using an automated infrared beam break counting system (infrared emitters and detectors made by Banner Engineering Corp., Minneapolis, MN). In addition, the video records of the animal's behavior were scored using a Parkinsonism Rating Scale (PRS) which rated bradykinesia, freezing, extremity posture, trunk posture, the presence and severity of tremor, the frequency of arm movements, finger dexterity, home cage activity, and balance, each on a 0-3 scale. Monkeys were considered to be stably parkinsonian if their motor deficits remained stable for at least 6 weeks after the last administration of MPTP. The extent of MPTP-induced nigrostriatal dopaminergic denervation was later assessed anatomically (see below) (Fig. 2.1).

### 2.2.3. Animal euthanasia and tissue fixation

At the time of euthanasia, the monkeys were deeply anesthetized with an overdose of pentobarbital (100mg/kg, i.v.) and transcardially perfused with cold, oxygenated Ringer's solution. Following this, the animals were perfused with 2 liters of a fixative – either 4% paraformaldehyde + 0.1% glutaraldehyde in phosphate buffer (PB; 0.1M, pH 7.4) or 2% paraformaldehyde + 3.75% acrolein in PB. After fixation, the brains were removed from the skull, cut into 10 mm thick blocks in the frontal plane and immersed in fixative (2% or 4% paraformaldehyde in PB, 0.1M, pH 7.4) overnight at 4 ºC. Both fixative recipes and post-fixation procedures provided adequate ultrastructural preservation and antibody penetration in the tissue for both light (LM) and electron microscopic (EM) observations.

### 2.2.4. Anatomical Experiments

#### *2.2.4.1. Tissue processing*

Sixty µm-thick coronal sections were cut from the tissue blocks in cold phosphate-buffered saline (PBS; 0.01M, pH 7.4) using a vibrating microtome. These sections were stored in an anti-freeze solution (30% ethylene glycol and 30% glycerol in PB) at -20 ºC, until ready for immunohistochemistry. Prior to light or electron microscopy immunohistochemical processing, sections were treated with sodium borohydride (1% in PBS) for 20 minutes, followed by washes in PBS.

*2.2.4.2. STN volume measurements*

To estimate the volume of the STN, every twelfth section containing the STN (total: 3 sections/animal) was selected from 3 normal and 3 parkinsonian monkeys. These sections were Nissl-stained, mounted onto gelatin-coated slides and coverslipped with Permount. The borders of the STN were delineated using a light microscope (DMRB, Leica Microsystems, Inc., Bannockburn, IL, USA) at 2.5x magnification. The volume of the STN was estimated with the Cavalieri method (StereoInvestigator 10.0 software, MBF Bioscience, Williston, VT, USA).

*2.2.4.3. Visualization of vGluT1 with pre-embedding immunoperoxidase staining for LM observations*

For LM studies, brain tissue from the monkeys (3 normal, 3 parkinsonian) used to determine the STN volume was used. Sections containing the STN were pre-incubated for 1 hour at room temperature (RT) in PBS containing 10% normal goat serum (NGS), 1% bovine serum albumin (BSA), and 0.3% Triton X-100. These sections were then incubated for 24 hours at RT in PBS containing 1% NGS, 1% BSA and 0.3% Triton X-100, and the primary antibody, anti-vGluT1 (raised in guinea pig; 1:5000 dilution; EMD Millipore, Billerica, MA, USA) (Raju et al., 2008). After thorough rinses with PBS, the sections were further incubated for 1.5 hours at RT in PBS containing 1% NGS, 1% BSA and 0.3% Triton X-100, and the secondary antibody, biotinylated anti-guinea pig IgGs (raised in goat; 1:200 dilution; Vector Laboratories, Burlingame, CA). After three rinses with PBS, the sections were incubated for 1.5 hours at RT in avidin-biotin peroxidase complex (ABC) solution (1:100; Vectastain standard ABC kit; Vector Laboratories) in

PBS, followed by rinses in PBS and Tris buffer (50 mM; pH 7.6). Sections were then treated with a solution containing 0.025% 3,3'-diaminobenzidine tetrahydrochloride (DAB; Sigma-Aldrich), 10 mM imidazole, and 0.005% hydrogen peroxide in Tris buffer for 10 minutes at RT. Later, they were thoroughly rinsed with PBS, placed onto gelatin-coated slides, and coverslipped with Permount.

*2.2.4.4. Quantitative Analysis of vGluT1 immunostaining at the light microscopic level*

At high magnification (>40x), a large number of immunolabeled pleomorphic processes, most likely corresponding to vGluT1-containing terminals were seen in the STN (Fig. 2.2 C). A Leica DMRB light microscope (Leica Microsystems) and the StereoInvestigator software were used to assess the relative prevalence of these labeled terminal-like profiles in the dorsolateral part of the STN (Fig. 2.2 B). While viewing the tissue at low magnification (2.5x), we placed a 500 µm x 500 µm region of interest (ROI) in the dorsolateral STN (Fig. 2.2 A). A virtual grid (consisting of 80 x 80 µm square elements) was randomly placed in the ROI with StereoInvestigator's Optical Fractionator probe, such that each ROI contained approximately 36-49 grid squares. At the left hand top corner of each virtual square, a square dissector frame (10 x 10 µm), with a height of 24 µm, allowing 3 µm guard zone both above and below the counting frame was positioned (Villalba et al., 2013). Under a 100x oil immersed objective, we counted the labeled processes in each counting frame. After gently moving the focal plane back and forth, we distinctly identified each labeled process, ensuring that no element was overlooked or counted twice. Automated software-based control of the microscope's X-Y stage enabled us to sample all counting frames within the ROI. Finally, we calculated the volumetric

density of immunolabeled varicosities after dividing the total number of counted varicosities by the volume occupied by the counting frames.

*2.2.4.5. Double Immuno EM for vGluT1 and vGluT2*

Glutamatergic inputs to the STN originate from the cerebral cortex (Nambu et al., 1996; Haynes and Haber, 2013), the thalamus (Sadikot et al., 1992), the brainstem pedunculopontine tegmental nucleus (Lavoie and Parent, 1994a) and local axon collaterals of STN neurons (Kita et al., 1983). In light of mRNA data and immunohistochemical findings from the striatum and other brain regions, cortical inputs can be distinguished from other sources based on their selective expression for vGluT1 and lack of vGluT2 immunoreactivity (Fremeau et al., 2001; Kaneko and Fujiyama, 2002; Fremeau et al., 2004; Raju et al., 2008). To confirm that this is also the case in the STN, we assessed the extent of vGluT1/vGluT2 co-localization in the monkey STN. Brain sections containing the STN from 3 normal and 3 parkinsonian monkeys (animals different from the ones used in LM studies) were selected. The sections were soaked in a cryoprotectant solution (PB 0.05 M, pH 7.4, 25% sucrose, and 10% glycerol) for 20 minutes before being frozen at -80 ºC for 20 minutes, thawed, and placed in a graded series of cryoprotectant (100, 70, 50 and 30% in PBS), and then washed in PBS. After completion of the cryoprotectant protocol, the sections were pre-incubated for 30 minutes at RT in PBS containing 5% dry milk. Sections were then rinsed with a TBS-gelatin buffer (0.02 M, 0.1% gelatin, pH 7.6). Following this, the sections were incubated for 24 hours at RT in TBS-gelatin buffer containing 1% dry milk and a cocktail of the primary antibodies, anti-vGluT1 (raised in guinea pig; 1:5000 dilution; EMD Millipore, Billerica,

MA, USA) and anti-human vGluT2 (raised in rabbit; 1:5000 dilution; Mab Technologies, Atlanta, GA, USA) (Raju et al., 2008). Additional control sections were incubated in solutions wherein either of the primary antibodies was omitted in turn to test the specificity of the immunoperoxidase and immunogold labeling. After 24 hours, sections were rinsed in TBS-gelatin buffer and incubated for 2 hours at RT in TBS-gelatin buffer containing 1% dry milk and a cocktail of the secondary antibodies, biotinylated anti-guinea pig IgGs (made in goat; 1:200 dilution; Vector) and gold-conjugated anti-rabbit IgGs (made in goat; 1:100 dilution; 1.4 nm particle size, Nanogold; Nanoprobes, Stony Brook, NY). After washing with TBS-gelatin buffer and then with 2% sodium acetate buffer, sections were incubated with the HQ Silver Kit (Nanoprobes) for 4-10 minutes at room temperature in the dark, to increase gold particle sizes to 30-50nm through silver intensification. After rinses with 2% sodium acetate buffer and then with TBS-gelatin buffer, the sections were incubated for 1.5 hours at RT in avidin-biotin peroxidase complex (ABC) solution (1:100; Vectastain standard ABC kit; Vector Laboratories) made in TBS-gelatin, followed by rinses in TBS-gelatin and then with Tris buffer (50 mM; pH 7.6). Sections were treated with a solution containing 0.025% 3,3'-diaminobenzidine tetrahydrochloride (DAB; Sigma-Aldrich), 10 mM imidazole, and 0.005% hydrogen peroxide in Tris buffer for 10 minutes at RT. Sections were then transferred to PB (0.1 M, pH 7.4) for 10 minutes and subjected to 1% $OsO_4$ for 10 minutes. Following subsequent rinses with PB, the sections were dehydrated through solutions containing an increasing gradient of ethanol (50, 70, 90 and 100%). The 70% ethanol solution also contained 1% uranyl acetate to increase tissue contrast under the EM. During this step, the sections were placed in the uranyl acetate solution for 10

minutes and kept in the dark. The sections were then immersed in propylene oxide before being embedded in epoxy resin (Durcupan ACM; Fluka, Buchs, Switzerland) overnight. Finally, the sections were mounted on microscope slides, dabbed with epoxy resin, coverslipped with oil-coated coverslips and placed in a 60 ºC oven for 48 h. After removing the slides from the oven, the coverslips were taken off the slides. Blocks of tissue from the dorsolateral STN (Fig. 2.2 A,B) were cut out from the slides, glued on top of resin blocks with cyanoacrylate glue, cut into 60-nm ultrathin sections with an ultramicrotome (Ultracut T2; Leica, Nussloch, Germany) and collected on single-slot Pioloform-coated copper grids. The sections were then stained with lead citrate for 5 minutes and viewed under an EM (JEM-1011; JEOL, Peabody, MA, USA). Digital micrographs were collected with a Gatan CCD camera (Model 785; Gatan Inc., Pleasanton, CA) controlled by Digital Micrograph 3.11.1 software (Gatan).

#### *2.2.4.6. Analysis of EM material*

##### *2.2.4.6.1. Co-localization of vGluT1 and vGluT2*

Superficial sections from the dorsolateral STN tissue were extensively sampled to assess whether vGluT1 and vGluT2 were co-expressed. Immunoperoxidase labeled boutons were tested for the presence of immunogold labeling in both normal and parkinsonian animals.

*2.2.4.6.2. Density of vGluT1-containing terminals*

To quantify the relative density of vGluT1-immunopositive terminals (revealed with immunoperoxidase) in tissue from normal and parkinsonian animals, we used the same double immunolabeled material which was used for the vGluT1&2 co-localization studies. We sequentially imaged viewing fields of ultrathin sections taken from the surface of STN tissue. In brief, we initially positioned the camera at the superficial edge of the tissue with a magnification of 25,000x (Fig. 2.3 A). Beginning at the edge, we imaged adjacent fields of view (39.6 $\mu m^2$) in the X direction, while moving towards the center of the tissue, until about 10 viewing fields were sampled. At that point, we progressed to a neighboring field in the Y direction, and from there on moved backwards in the negative X direction towards the edge. Then, we moved to the adjacent field in the same Y direction as before and repeated this pattern of sampling. Thus, we ensured that only superficial tissue layers where the antibody penetration was optimal were sampled. Once 100 viewing fields were imaged, the sampling was stopped. In each micrograph, vGluT1-immunopositive vesicle-filled neuronal profiles, with an ultrastructure reminiscent of axon terminals (Peters et al., 1991), were counted. The density of vGluT1-immunopositive terminals was calculated after dividing the total terminal count across the 100 micrographs by the total surface area sampled (3960 $\mu m^2$).

*2.2.4.6.3. Density of asymmetric synapses*

To quantify the density of asymmetric synapses in the STN, we used a technique previously used by Ingham and others to determine the prevalence of asymmetric synapses in the rat striatum (Ingham et al., 1998). First, serial ultrathin sections were

collected from the STN. Then, fifty viewing fields (total area 1980 $\mu m^2$) from one ultrathin section were sampled in the same manner as was done for quantifying the density of vGluT1-positive terminals (see above). Further, we imaged the overlapping fields of the formerly sampled viewing fields from the adjacent ultrathin section. Thus, we effectively sampled fifty overlapping pairs of viewing fields from adjacent ultrathin sections. Finally, we identified the asymmetric synapses that were clearly present in both the adjacent ultrathin sections in each pair (Fig. 2.3 B,C) (Ingham et al., 1998).

*2.2.4.6.4. Post-synaptic targets of vGluT1-positive terminals*

To assess possible changes in the synaptic microcircuitry of vGluT1-positive terminals in parkinsonian animals, we compared the distribution of post-synaptic targets contacted by vGluT1-immunopositive boutons between normal and MPTP-treated monkeys. To do so, we collected digital images of STN tissue at 60,000X, and sampled only those vGluT1-immunopositive terminals whose synapse could be clearly seen in the plane of section (Fig. 2.4 A,B). The post-synaptic targets of these glutamatergic terminals were identified based on their ultrastructural features (Peters et al., 1991). Dendritic spines were differentiated from dendritic shafts based on the absence of mitochondria and in some cases, the presence of spine apparatus. If a post-synaptic target was a dendritic shaft, it was further classified based on its width at the point where it received the synaptic innervation by the terminal. These diameters were measured using NIH's ImageJ software as the shortest diameter passing through the approximate center of its 2D representation on the EM image (Fig. 2.4 A).

### 2.2.5. TH immunostaining

To assess the degree of nigrostriatal dopamine denervation, series of tissue sections from the striatum or the ventral midbrain were immunostained with antibodies against tyrosine hydroxylase (mouse anti-TH; 1:1000 dilution; EMD Millipore) (Fig. 2.1). The intensity of TH immunoreactivity was then measured at the level of the postcommissural putamen from one section in each parkinsonian monkey that was used for the anatomical studies and 3 coronal sections from animals used in the electrophysiological studies, using NIH's Image-J software, as described in our previous studies (Galvan et al., 2011; Masilamoni et al., 2011; Villalba et al., 2013). The putamenal TH immunostaining of these parkinsonian monkeys were compared with controls from our laboratory's monkey brain tissue bank.

### 2.2.6. Electrophysiological Experiments

#### *2.2.6.1. Surgery*

Under aseptic conditions and isofluorane anesthesia (1-3%), stainless steel cylindrical recording chambers (16 mm i.d., Crist Instrument Co., Hagerstown, MD, USA) were fastened to the skull over trephine holes. Using stereotaxic coordinates (Paxinos et al., 1999), the chambers were targeted to the putamen/pallidum and STN regions with a 36º angle from the vertical in the coronal plane in one monkey, and with a 40º angle in the other. The chambers were affixed to the skull with dental acrylic and stainless steel screws. Metal head holding bolts (Crist Instrument) were also embedded in the acrylic. Post-surgery, the monkeys were given prophylactic antibiotic treatment, and were

allowed to recuperate for at least a week before the start of the electrophysiological experiments.

*2.2.6.2. Electrophysiological recordings*

All recording sessions were conducted with the monkeys awake and quietly seated in a primate chair with the head restrained. We first electrophysiologically mapped the locations of the internal capsule (IC), putamen, GPe, GPi and STN, with standard tungsten microelectrodes (impedance 0.5-1 MΩ at 1 kHz; Frederic Haer Co., Bowdoin, ME, USA). After conclusion of the electrophysiological mapping, a stimulation electrode (impedance 40-50 kΩ at 1 kHz; Rhodes Medical, Summerland, CA) was positioned in the posterior limb of the IC (Fig. 2.5 A), followed by insertion of a tungsten microelectrode into the ventrolateral region (i.e., sensorimotor territory) of the GPe and GPi (Fig. 2.5 A). Spiking activity of pallidal cells was accepted for recording if the signal to noise ratio was >= 3. Baseline signals were recorded for 60s, followed by recordings during internal capsule stimulation with 100 randomly spaced single biphasic square wave pulses (500 μA, 200 μs/phase, minimum spacing between consecutive pulses 250ms, monopolar stimulation). We estimate that stimulation with these parameters affected myelinated axons up to 1.7 mm away from the stimulation site (Ranck, 1975). The stimulation did not induce movements in the animals.

At the beginning of each experimental session, the dura was punctured with a guide tube, while the stimulation and recording electrodes were lowered into the brain, directed at pre-determined anteroposterior and mediolateral coordinates, using a multi-probe

microdrive (NAN Instruments Ltd., Nazareth, Israel). The depth of the tip of each electrode during its advancement was controlled by the microdrive's software. Extracellular neuronal activity was recorded from the tungsten microelectrode, filtered (Butterworth band-pass filter; 400Hz-6kHz) and amplified (DAM80 pre amplifier, WPI Inc., Sarasota, FL, USA, and model 3364 filter and amplifier, Krohn-Hite, Brockton, MA). The resulting signal was then digitized using an A-D interface (sampling rate, 50 kHz; Power1401/Spike2; Cambridge Electronic Design, Cambridge, UK) and stored to computer disk for off-line processing. The analog signal was also displayed on a digital oscilloscope (DL 1540; Yokogawa, Tokyo, Japan) and audio-amplified. The timing and size of stimuli was controlled via the Power1401 interface and stimuli generated by a constant-current stimulus isolation unit (A395R, WPI).

*2.2.6.3. Analysis of electrophysiological data*

The electrophysiological data were pre-processed with a Matlab (Mathworks, Natick, MA, USA) based stimulus artifact removal program (Fig. 2.5 B). Due to clipping of stimulation artifacts, the neuronal activity occurring during the initial 2 ms post-stimulation could not be recovered. The resulting records were subjected to waveform matching spike-sorting in Spike2. Inter-spike interval (ISI) distribution histograms were generated for each cell to examine the quality of recording and spike sorting.

All subsequent analysis steps were carried out in the Matlab environment. We generated peri-stimulus histograms (PSTHs) (bin size 1 ms; pre-stimulus period 100 ms; post-stimulus period 20 ms) (Fig. 2.5 B). The mean and standard deviation (SD) of the PSTH

bins of the pre-stimulus period were calculated, and a threshold (mean + 2SD) was established to identify excitation events. If at least 2 consecutive PSTH bins were above the threshold, with the first bin occurring no later than 12 ms after the stimulus, the neuron was identified as showing an early excitatory response (Fig. 2.5 B). This selection criterion was based on earlier studies of the responses of pallidal neurons to activation of the corticosubthalamic pathway (Nambu et al., 2000). The entire duration encompassed by the consecutive supra-threshold PSTH bins was considered as the period of the early excitatory response. If there were multiple excitatory responses (as defined) within the 12 ms window, only the first one was considered. Finally, we compared the proportion of pallidal neurons showing a characteristic early excitatory response to IC stimulation between normal and parkinsonian states (Fig. 2.6 A).

We also calculated Z-scores of each PSTH bin with respect to the pre-stimulus period mean and SD. For neurons with early excitatory responses, the mean Z-score of all bins constituting the excitation response was calculated as a measure of the strength of excitation (Fig. 2.6 B).

*2.2.6.4. Post-mortem identification of electrode tracks*

After conclusion of the recording experiments, the monkeys were killed, and their brains perfused, fixed and processed, as stated previously. In this case, brain sections were cut into 50 µm thick coronal sections using a freezing microtome. Out of every 12 sections, one was Nissl-stained and another was immunolabeled for LM observations to reveal the neuronal marker microtubule associated protein 2 (mouse anti-MAP2; 1:1000 dilution;

EMD Millipore), using protocols described earlier (Galvan et al., 2010, 2011). The slides were scanned with a ScanScope CS scanning light microscope system (Aperio Technologies, Vista, CA, USA) at 20x magnification, and their digital representations were analyzed. Appropriate interaural co-ordinates were ascribed to the sections after confirming their anteroposterior locations by comparing the images with standard monkey atlas coronal plates (Paxinos et al., 1999). The relatively thick stimulation electrode tracks were easily reconstructed. The recording sites were within the ventrolateral two-thirds of the GPe and GPi. Most of the recording electrode tracks which were formed by the electrodes traversing towards the recording sites were identified.

## 2.3. Results

### 2.3.1. State of Parkinsonian Motor Symptoms and Nigrostriatal Dopaminergic Pathology in MPTP-treated Monkeys

All MPTP-treated monkeys used in the anatomical and electrophysiological experiments presented in this study displayed moderate to severe parkinsonian motor symptoms, as assessed using beam break counts in a behavioral cage and the PRS described in the Methods section, and used in many of our previous studies (Kliem et al., 2010; Hadipour-Niktarash et al., 2012; Bogenpohl et al., 2013). Consistent with these behavioral observations, all parkinsonian animals displayed more than 80% dopaminergic denervation of the postcommissural putamen, based on reduced densitometry measurements of TH immunoreactivity (Fig. 2.1).

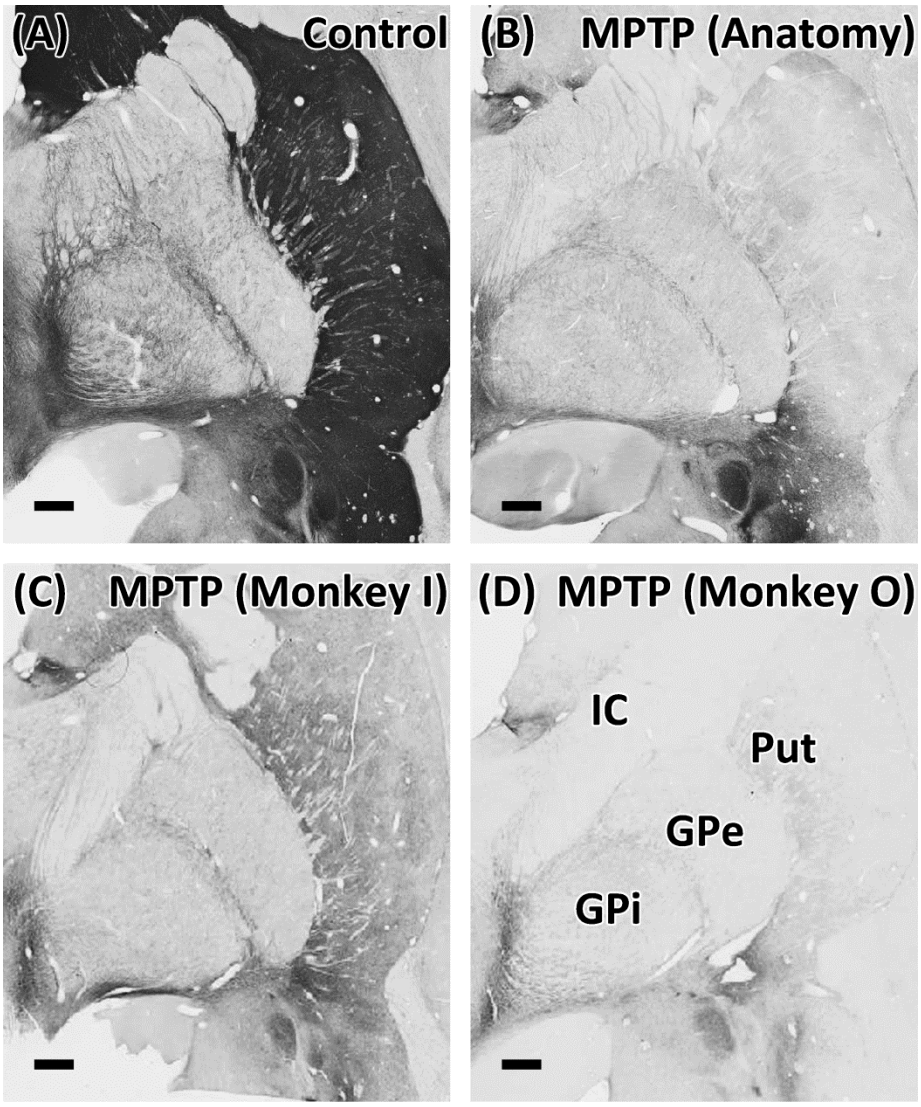


**Figure 2.1: Nigrostriatal dopaminergic innervation of the monkeys used in the anatomical and electrophysiological studies**

(A-D) Light micrographs of coronal monkey brain sections showing immunostaining for tyrosine hydroxylase (TH) in the post-commissural putamen. Examples of control and MPTP-treated parkinsonian monkeys used in the anatomical experiments are depicted in A and B, respectively. C and D depict the dopaminergic innervation of monkeys used for

electrophysiologic experiments at the conclusion of the studies. Abbreviations: Put – putamen, IC – internal capsule, GPe – external globus pallidus, GPi – internal globus pallidus. Scale bar: 1mm.

2.3.2. Lack of vGluT1 and vGluT2 co-localization in the Monkey STN

In order to examine whether the segregation of vGluT1 and vGluT2 described in the striatum (Fujiyama et al., 2004; Fujiyama et al., 2006; Raju et al., 2006; Raju et al., 2008) and other forebrain regions (Hur and Zaborszky, 2005; Kubota et al., 2007; Liguz-Lecznar and Skangiel-Kramska, 2007) also applies to the STN, we carried out co-localization EM studies of vGluT1 and vGluT2 at the single terminal level using immunoperoxidase or immunogold labeling for either vGluTs (Fig. 2.3 A). Of 255 vGluT1-immunoreactive terminals, none displayed vGluT2 immunostaining. Together with the known localization of vGluT1 and vGluT2 mRNA (and protein) in the various sources of glutamatergic afferents to the STN (i.e., thalamus, brainstem, STN collaterals and cortex), these data show that vGluT1 is a reliable marker of corticosubthalamic terminals in monkeys.

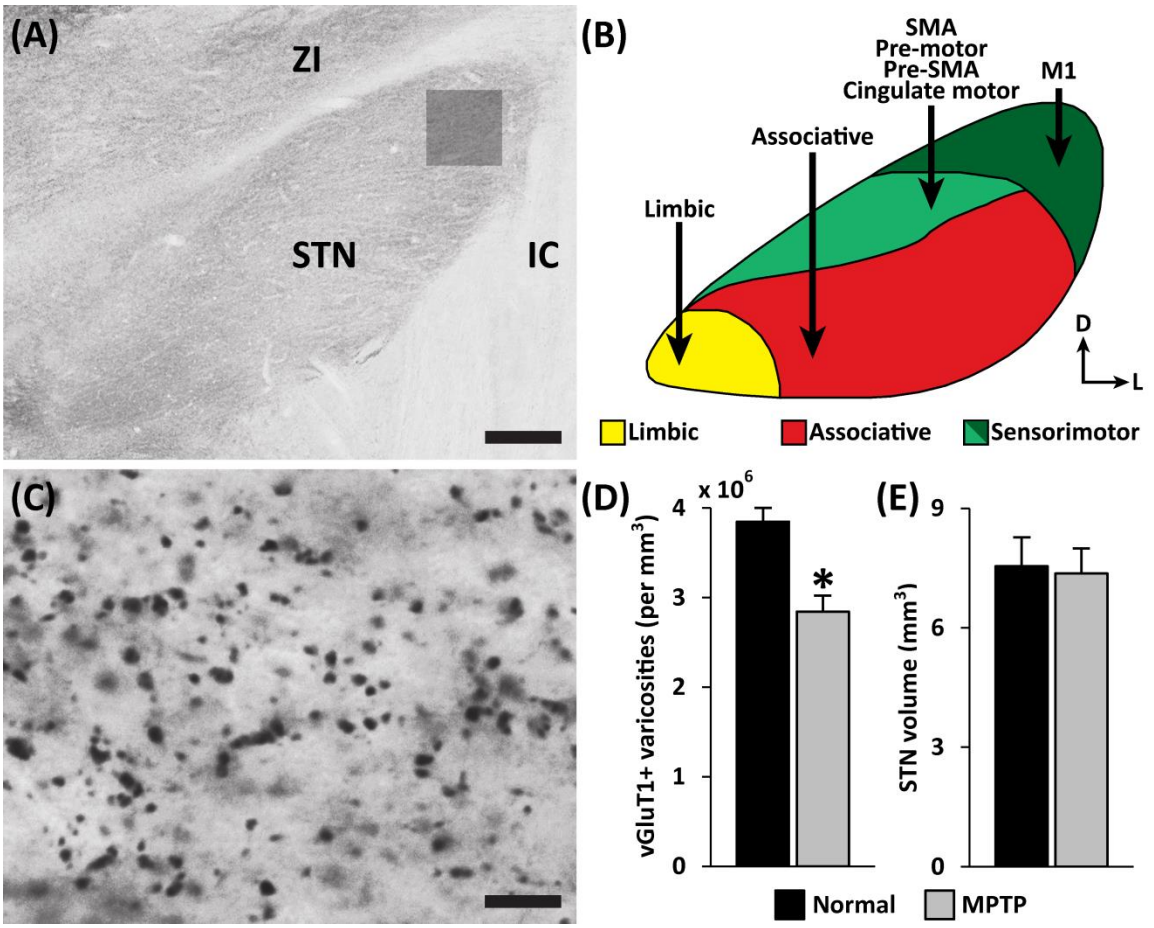


**Figure 2.2: VGluT1-immunostained varicosities in the STN.**

(A) Light micrograph of the monkey STN in coronal plane showing immunostaining for vGluT1. The gray square indicates the size and approximate position of the region of interest placed in the dorsolateral territory of the STN to quantify the density of vGluT1-positive pleomorphic varicose processes. Scale bar: 0.5 mm. Abbreviations: ZI – zona incerta, IC – internal capsule. (B) Schematic coronal view depicting the topographical organization of functionally segregated cortical afferents to various domains in the STN [Adapted from (Mathai and Smith, 2011; Smith, 2011)]. The dorsolateral sector

corresponds to the sensorimotor region of the STN. Abbreviations: SMA – supplementary motor area, M1 – primary motor cortex, D – dorsal, L – lateral (C) Light micrograph showing vGluT1-immunopositive pleomorphic varicose processes in the dorsolateral STN of a normal monkey. Scale bar: 10 µm. (D) Density of vGluT1-immunoreactive varicosities in the dorsolateral STN of normal versus parkinsonian monkeys. The density of vGluT1-positive varicosities in the dorsolateral STN is significantly lower in parkinsonian monkeys compared with normal animals (*$p = 0.012$, Student's t-test). (E) No significant difference was found in the STN volume between normal and parkinsonian animals. Columns (D & E) represent means ± standard error of the mean across 3 normal and 3 parkinsonian monkeys.

### 2.3.3. Changes in vGluT1-immunopositive innervation of the dorsolateral STN in MPTP-treated monkeys

#### *2.3.3.1. Light microscopic observations*

At the LM level, the whole extent of the STN in normal and MPTP-treated monkeys contained a moderate level of vGluT1 immunoreactivity (Fig. 2.2 A) which, at higher power, was found to be confined to pleomorphic varicose processes of different sizes (Fig. 2.2 C). To determine if there was a significant change in the prevalence of vGluT1-positive elements between normal and parkinsonian monkeys, we generated unbiased quantitative estimates of the relative density of vGluT1-positive profiles in the dorsolateral 'motor' territory of the STN (Fig. 2.2 A,B) in normal and MPTP-treated monkeys. In normal monkeys, we found that the dorsolateral STN contained approximately 3.85 ± 0.15 million vGluT1-immunopositive varicosities per cubic mm, while this density was reduced by 26.1% (Student's t- test; $p = 0.012$), to about 2.84 ± 0.18 million vGluT1-immunoreactive varicose profiles per cubic mm, in parkinsonian animals (Fig. 2.2 D).

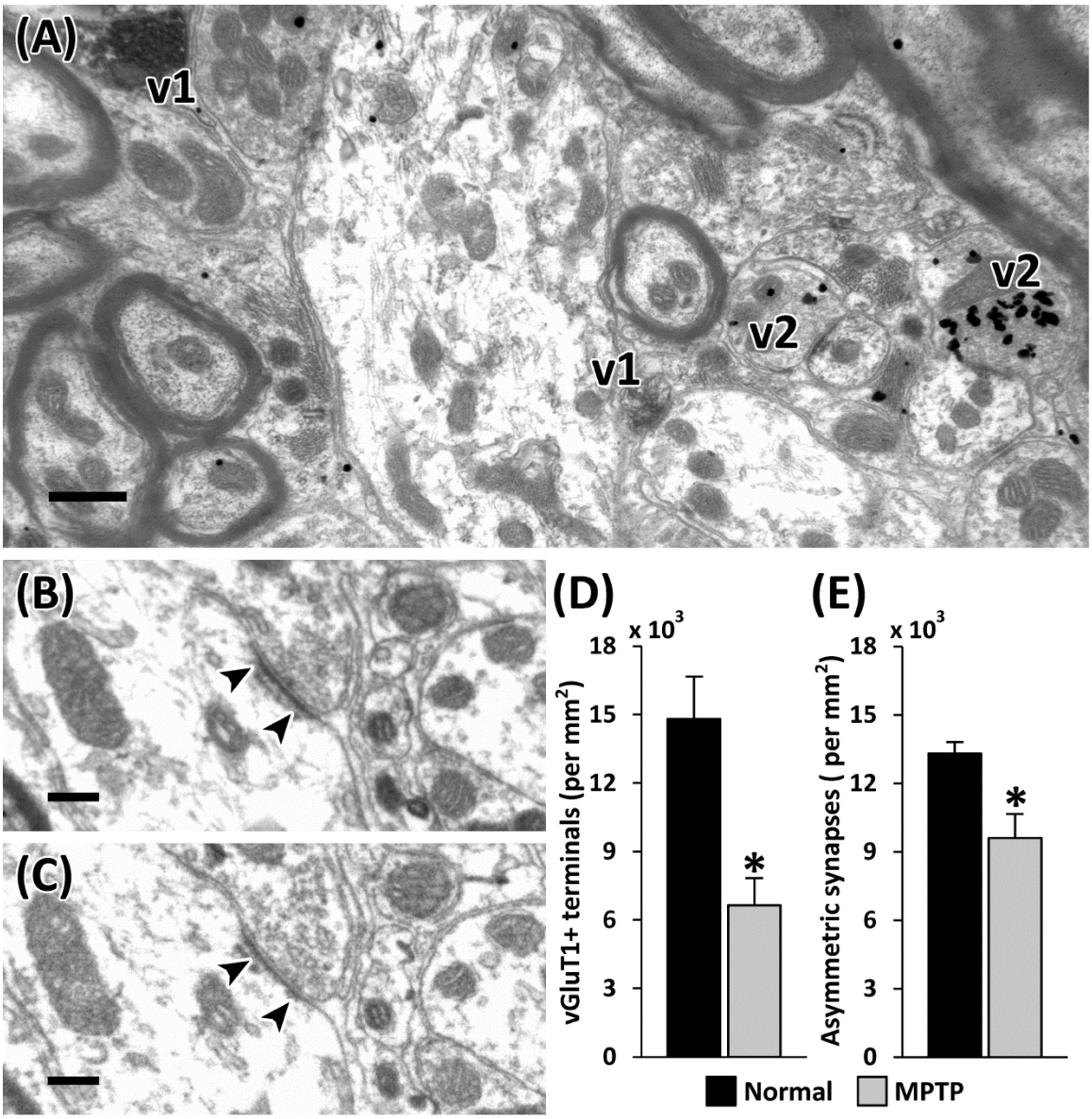


**Figure 2.3: Electron microscopic observations: Density of vGluT1-positive terminals in the dorsolateral STN**

(A) Electron micrographs showing vGluT1-positive (V1-immunoperoxidase) and vGluT2-labeled (V2-immunogold) terminals in the dorsolateral STN. Scale bar: 0.5 µm. (B & C) Electron micrographs depicting an asymmetric synapse (putatively

glutamatergic) in consecutive serial ultrathin sections of the dorsolateral STN in monkeys. The asymmetric synapse is indicated by arrowheads. Scale bar: 0.2 µm. (D) Density of vGluT1-immunopositive terminals in the dorsolateral STN of normal versus parkinsonian monkeys. The density of vGluT1-containing terminals is significantly lower in parkinsonian monkeys than in healthy controls (*p = 0.02, Student's t-test). Total surface area analyzed: 3960 $\mu m^2$/animal. (E) Density of asymmetric synapses in the dorsolateral STN of normal and parkinsonian monkeys. The number of asymmetric synapses per square mm is significantly lower in parkinsonian monkeys than in normal animals (*p = 0.029, Student's t-test). Total surface area analyzed: 1980 $\mu m^2$/animal. Columns (D & E) represent means ± standard error of the mean across 3 normal and 3 parkinsonian monkeys.

*2.3.3.2. Electron microscopic Observations: Density of vGluT1-positive Terminals*

To confirm and extend these light microscopic observations, we compared the density of vGluT1-positive terminal profiles between the dorsolateral STN of normal and MPTP-treated monkeys (Fig. 2.3 A). At the light microscopic level, it is not possible to ascertain whether a vGluT1-immunolabeled varicosity is a vGluT1-containing terminal. Hence, we analyzed the tissue under the electron microscope to ultrastructurally identify only those elements which were vGluT1-immunopositive terminals. In line with the light microscopic data, our EM studies showed a 55.1% (Student's t- test; $p = 0.02$) reduction in the density of vGluT1-positive terminals in parkinsonian monkeys compared with controls (compare 14,814 ± 1,846 vGluT1-containing terminals per square mm in normal monkeys to 6,649 ± 1,178 in parkinsonian animals) (Fig. 2.3 D).

*2.3.3.3. Electron Microscopic Observations: Loss of Asymmetric Synapses*

The reduced density of vGluT1-immunopositive terminals in the STN of parkinsonian monkeys shown in Fig. 2.3 D may not be due to the loss of glutamatergic terminals, but could be the result of reduced expression of vGluT1 immunoreactivity in corticosubthalamic boutons. To determine if the STN of parkinsonian monkeys displayed genuine glutamatergic synaptic loss, we quantified the density of asymmetric synapses in the dorsolateral STN of normal and parkinsonian animals (Fig. 2.3 B,C). These data showed a 27.9% reduction (Student's t-test; $p = 0.029$) in the density of asymmetric synapses between parkinsonian monkeys and controls (i.e., a reduction from

13,323 ± 446 asymmetric synapses per square mm in normal monkeys to 9,613 ± 1,012 in parkinsonian animals) (Fig. 2.3 E).

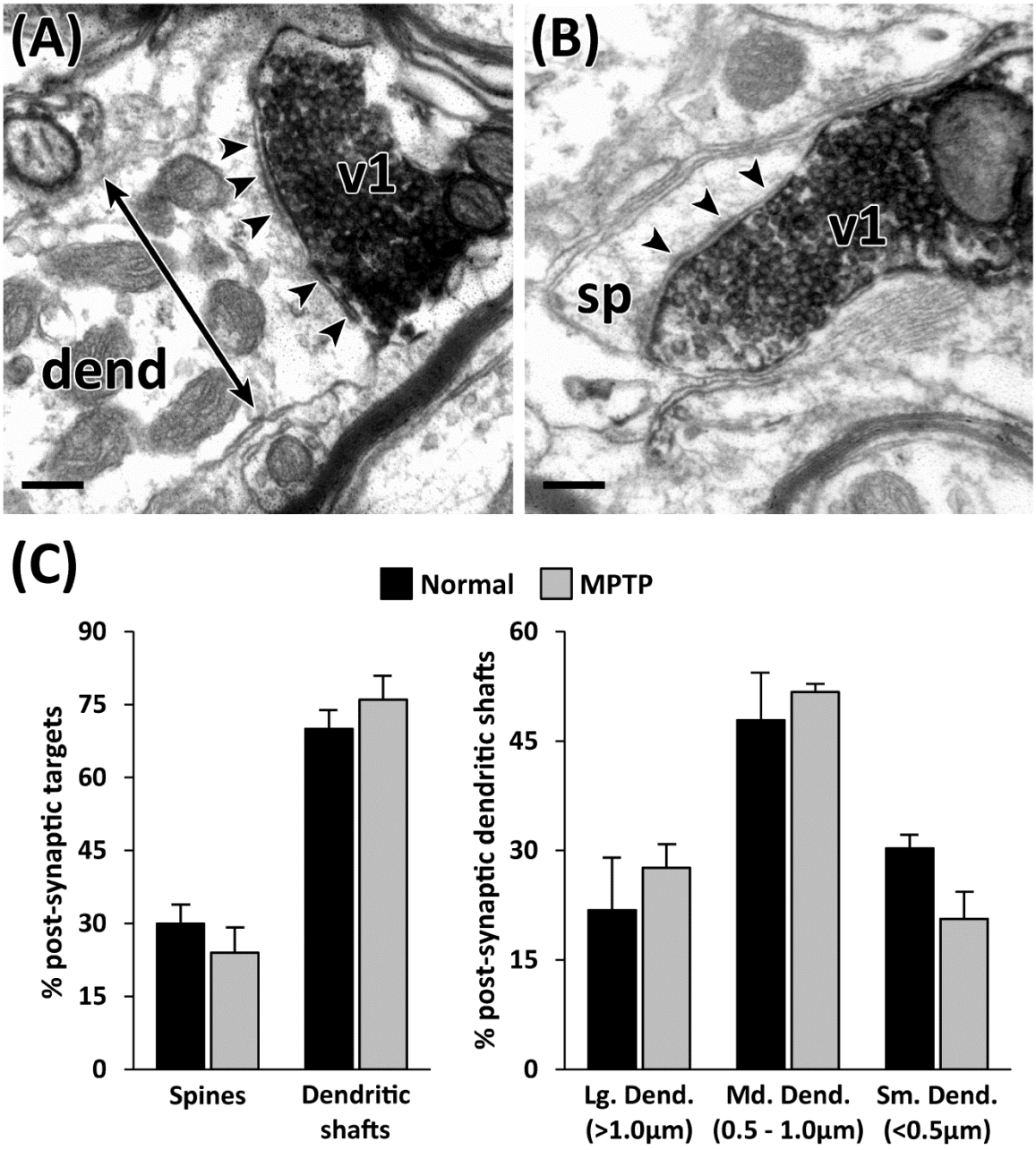


**Figure 2.4: Electron microscopic observations: Post-synaptic targets of vGluT1-immunopositive terminals in the dorsolateral STN**

(A & B) Electron micrographs showing vGluT1-containing terminals (V1) forming asymmetric synapses (indicated by arrowheads) with a dendritic shaft (dend) (A) and a dendritic spine (sp) (B). The black line with double ended arrows on the dendritic shaft

(A), illustrates the measurement of its cross-sectional diameter, defined as the shortest diameter passing through the approximate center of its 2D representation on the EM image. Scale bar: 0.2 µm. (C) Post-synaptic targets of vGluT1- immunopositive terminals in the dorsolateral STN. No significant difference was found in the proportion of vGluT1-immunoreactive terminals forming asymmetric synapses with dendritic shafts and spines in normal versus parkinsonian monkeys (Left panel). Right panel shows the size distribution of all the post-synaptic dendritic shafts which were contacted by vGluT1-immunoreactive terminals, which is not significantly different between normal and parkinsonian animals. Abbreviations: Lg – large, Md – medium, Sm – small, Dend – dendritic shafts. Columns represent means ± standard error of the mean across 3 normal and 3 parkinsonian monkeys.

*2.3.3.4. Lack of Volumetric Changes of the STN in Parkinsonian Animals*

To ensure that the density values presented above for vGluT1-positive terminals and asymmetric synapses between normal and parkinsonian animals were collected from STN of comparable sizes, we measured the volume of the nucleus from 3D reconstructed images of the STN built from equally spaced coronal LM sections in 3 control and 3 MPTP-treated monkeys, and found no significant STN volume difference between normal and MPTP-treated monkeys (Student's t- test; $p = 0.858$) (Fig. 2.2 E).

2.3.4. The pattern of innervation of STN neurons by vGluT1-positive terminals is unchanged between normal and parkinsonian monkeys

In order to determine if the remaining vGluT1-positive terminals in the STN of parkinsonian monkeys displayed changes in their overall pattern of synaptic connectivity, we compared the distribution of postsynaptic targets in contact with vGluT1-positive terminals (N=50 terminals per animal) in the dorsolateral STN between normal and MPTP-treated monkeys. In both groups of animals, vGluT1-immunopositive terminals formed asymmetric synapses, primarily with dendritic shafts (70 ± 4% in normal and 76 ± 5% in parkinsonian animals) and, to a lesser extent, dendritic spines (30 ± 4% in normal and 24 ± 5% in parkinsonian animals) of STN neurons (Fig. 2.4 A,B), without any significant difference between normal and MPTP-treated monkeys (two-way ANOVA; $p = 0.223$).

The axo-dendritic synapses were further categorized as distal or proximal based on the sizes of the dendritic shafts being contacted. This was done by measuring the diameter of dendritic shafts at their vGluT1 terminal innervation site (Fig. 2.4 A), and classifying these dendrites as large (>1.0 μm), medium (0.5-1.0 μm) or small (<0.5 μm). In normal monkeys, 21.8 ± 7.0%, 47.9 ± 6.5% and 30.3 ± 1.7%, of axo-dendritic synapses formed by vGluT1-immunoreactive terminals targeted large, medium and small dendrites, respectively; a pattern that was not significantly different (two-way ANOVA; $p = 0.173$) from that seen in parkinsonian monkeys (i.e., 27.6 ± 3.3%, 51.7 ± 1.1% and 20.6 ± 3.7% onto large, medium and small sized dendritic shafts, respectively).

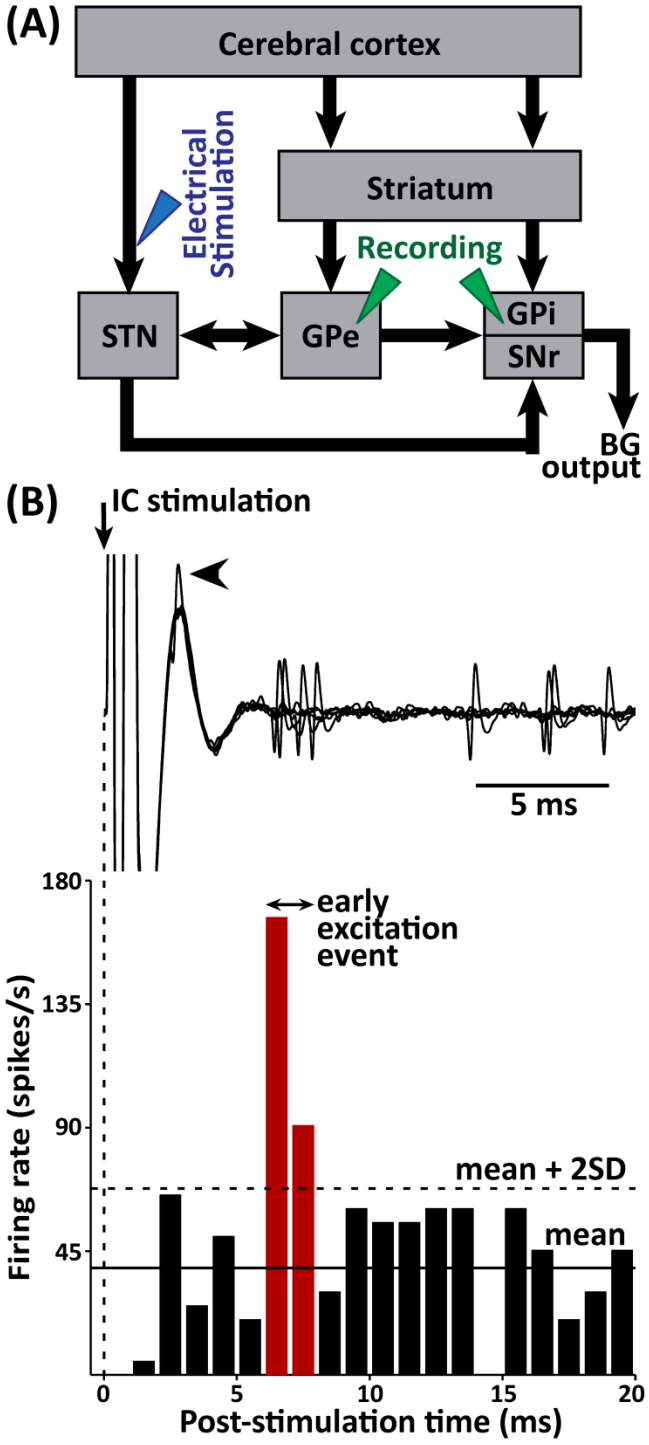


**Figure 2.5: Effects of corticosubthalamic system activation upon pallidal neurons.**

(A) Schematic showing the electrophysiological study design with respect to basal ganglia circuitry. Electrical stimulation (blue) is applied in the internal capsule (IC) to

activate corticosubthalamic axons. Extracellular single neuron activity in response to the IC stimulation is recorded (green) in the internal and external segments of the globus pallidus. (B) Response of a pallidal neuron to IC stimulation. Six overlaid traces of neuronal activity (top panel) shows that the neuron often fires around 6-8 ms post-stimulation. Arrowhead directed towards the left points to a neuronal spike occurring along with the stimulation artifact, which was successfully recovered after processing by the stimulus artifact removal program. Peri-stimulus histogram (PSTH) depicting the firing rate of the neuron during the first 20ms post-stimulation (bottom panel) shows an early excitation response (red) to IC stimulation. PSTH generated from 100 consecutive stimuli. Bin size – 1ms. Mean and standard deviation (SD) calculated from the -100ms to 0ms pre-stimulation period firing rate. Early excitation event of the neuron is defined as the time period when at least 2 consecutive bars cross the mean + 2SD threshold, with the first bar occurring within 12ms post-stimulation. Overlaid neuronal traces and peri-stimulus histograms are aligned on identical time axes. Vertical dotted line indicates the stimulation instance. Abbreviations: STN – subthalamic nucleus, GPe – external globus pallidus, GPi – internal globus pallidus, SNr – substantia nigra pars reticulata, BG – basal ganglia, IC – internal capsule, SD – standard deviation.

2.3.5. Physiological impact of corticosubthalamic activation on pallidal neurons between normal and parkinsonian monkeys

Because most vGluT1-positive terminals in the STN originate from the cerebral cortex (see above), we assessed the functional consequences of the loss of vGluT1-positive terminals in the dorsolateral STN on the electrophysiological effects of electrical stimulation of corticosubthalamic fibers upon pallidal neurons between normal and MPTP-treated monkeys, using extracellular single unit recordings in two monkeys (Fig. 2.5 A,B). IC stimulation was done in similar portions of the IC before and after induction of parkinsonism, and pallidal neurons were sampled from (roughly) equivalent portions of the ventrolateral (ie sensorimotor) globus pallidus. Preliminary results of these experiments are presented below.

Based on previous studies, early excitatory responses of pallidal neurons with latencies of up to 12 ms were considered to be likely due to activation of the cortico-subthalamo-pallidal sequence of connections (Nambu et al., 2000) (Fig. 2.5 B). In monkey I, such short-latency excitatory responses were recorded in 26.5% (total – 9/34; GPe – 8/23; GPi – 1/11) and 7.7% (total – 2/26; GPe – 2/20; GPi – 0/6) of pallidal neurons, in the normal and parkinsonian states, respectively (Fig. 2.6 A), while in monkey O, the corresponding proportions of responding pallidal neurons were 35.3% (total – 12/34; GPe – 7/21; GPi – 5/13) in normal animals compared with 28.6% (total – 6/21; GPe – 5/13; GPi – 1/8) in parkinsonian monkeys (Fig. 2.6 A).

In monkey I, the latencies of the early excitatory responses were 4.89 ± 0.35 ms and 5.50 ± 0.50 ms in the normal and parkinsonian states, respectively, while in monkey O, the corresponding latencies were 6.00 ± 0.69 ms in normal conditions and 7.33 ± 1.26 ms in parkinsonian conditions.

We also measured the intensity of the early excitation responses by calculating the average Z-score of the PSTH bins constituting the excitation response, and found no significant difference between the normal and parkinsonian state in either monkey (Fig. 2.6B). Thus, the proportion of neurons responding to the internal capsule stimulation was reduced, but the average amplitude of the physiological responses remained the same between normal and parkinsonian animals.

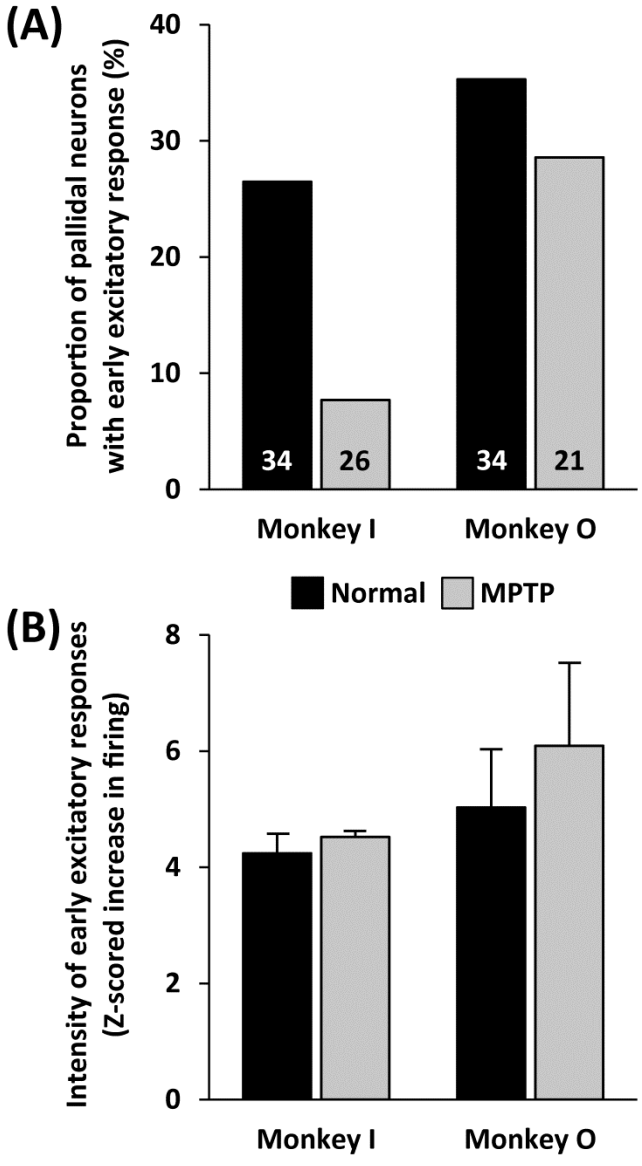


**Figure 2.6: Physiological responses of pallidal neurons to corticosubthalamic system activation.**

(A) Proportion of pallidal neurons responding with early excitation (occurring within 12ms of stimulation) to internal capsule stimulation in normal and parkinsonian states. Total number of neurons recorded in each condition in both monkeys depicted by the

numbers within the columns. (B) Intensity of early excitatory events in pallidal neurons showing an early excitatory response (occurring within 12ms of stimulation), in normal and parkinsonian states. No significant difference was found between the intensity of the early excitatory response between normal and parkinsonian states. Intensity of response defined as the average Z-score of peri-stimulus histogram bars constituting the early excitation event, with respect to the -100ms to 0ms pre-stimulation mean and standard deviation. Columns represent means ± SEM across the neurons with an early excitatory response.

## 2.4. Discussion

Our results demonstrate pathological changes of the glutamatergic corticosubthalamic system in MPTP-treated parkinsonian monkeys. These changes are characterized by a significant reduction in the prevalence of vGluT1-containing cortical terminals and total asymmetric synapses in the STN of parkinsonian monkeys. Preliminary electrophysiology data showed a trend towards a decrease in the number of pallidal neurons responding to corticosubthalamic activation in these monkeys. Together with previous data showing profound pathological and functional alterations of the corticostriatal system in parkinsonism (see Introduction), our findings provide evidence that the "hyperdirect" corticosubthalamic system is also significantly affected in parkinsonism.

### *Decreased Prevalence of Corticosubthalamic Terminals in Parkinsonian Monk*eys

One of the main observations of our study is that the density of vGluT1-positive terminals is significantly decreased in the sensorimotor territory of the STN in parkinsonian monkeys. Because of potential changes in the expression level of the vGluT1 protein, we must consider the possibility that the changes seen in the relative density of vGluT1-positive profiles might have been the result of a reduced sensitivity of the antibodies to detect subthreshold levels of vGluT1 in putative cortical terminals. However, although this cannot be completely ruled out, the fact that such loss was found using both light and electron microscopy unbiased counting methods, and that the intensity of immunostaining in positive terminals was relatively strong and comparable

between control and parkinsonian monkeys suggest that the decreased density of vGluT1-positive terminals reported in our study indicates genuine loss of putative corticosubthalamic terminals. Furthermore, the fact that a smaller number of asymmetric synapses were also found in the dorsolateral STN of parkinsonian monkeys adds credence to the possible loss of vGluT1-immunoreactive cortical terminals in parkinsonian animals. Another important point to consider is that the values of the reduced density of vGluT1-positive terminals in parkinsonian monkeys compared with controls is different between EM (55.1%) and LM (26.1%) observations. It is noteworthy that the EM data were collected from counts of terminals with clearly defined ultrastructural features; while such was not the case in the LM studies, which might have resulted in the quantification of immunoreactive axonal profiles in addition to immunopositive terminals. Despite this difference in the data collection, both LM and EM observations strongly suggest a significant degeneration of the sensorimotor hyperdirect corticosubthalamic projection in MPTP-treated monkeys.

The corticostriatal system also undergoes complex morphological and functional changes in animal models of Parkinson's disease (Calabresi et al., 1993; Onn and Grace, 1999; Calabresi et al., 2000; Onn et al., 2000; Calabresi et al., 2007; Villalba et al., 2009; Villalba and Smith, 2011). However, in contrast to the STN, the prevalence of vGluT1-immunoreactive cortical terminals is increased in the striatum of MPTP-treated parkinsonian monkeys (Raju et al., 2008), and the amount of striatal vGluT1 protein is significantly increased in postmortem brains of PD patients (Kashani et al., 2007). Consistent with these changes at the terminal level, the amount of extracellular glutamate is increased, and there is strengthening of cortical synapses in the striatum of rodent

models of PD (Lindefors and Ungerstedt, 1990; Calabresi et al., 1993; Meshul et al., 2000). Based on our data, it appears that opposite changes may occur at the corticosubthalamic synapse, ie a decreased number of cortical terminals may lead to a reduced cortical glutamatergic drive of STN neurons in parkinsonism (Ingham et al., 1989; Zaja-Milatovic et al., 2005; Raju et al., 2008; Villalba et al., 2009; Mathai and Smith, 2011). However, this remains to be directly tested. It is also not known whether there are any changes in the synaptic transmission, long term plasticity, and functional specificity of the corticosubthalamic pathway similar to those described regarding the corticostriatal pathway. A recent study in rats has shown that some of the corticosubthalamic inputs are collaterals of corticofugal systems (Kita and Kita, 2012). With changes occurring to both the major cortical input systems to the basal ganglia, it is worth considering if the denervation of the corticosubthalamic system is a corollary of pathological insult to cortical projection neurons innervating both the striatum and STN. However, as of now there is no clear evidence for single cortical projection neurons innervating both the striatum and STN in primates (Parent and Parent, 2006). Furthermore, although it is well known that dopamine and dopamine receptor agonists can elicit physiological effects on STN neuronal firing (Campbell et al., 1985; Hassani and Feger, 1999; Shen and Johnson, 2000), the functional link between the nigrosubthalamic dopaminergic inputs and the corticosubthalamic afferents is not clear. In light of the loss of corticosubthalamic inputs in dopamine-denervated conditions, the influence of dopamine on the integrity and functioning of individual corticosubthalamic inputs needs to be explored. Also, it is not clear if there are any associated morphological changes occurring to the remaining corticosubthalamic terminals in parkinsonism.

*Changes in the proportion of pallidal neurons activated by cortico-subthalamo-pallidal axons in parkinsonian animals*

Our preliminary electrophysiology data suggest that a lower proportion of pallidal neurons respond to internal capsule stimulation in MPTP-treated parkinsonian monkeys than in controls. Although we cannot fully rule out that this decreased responsiveness of pallidal neurons to corticosubthalamic activation might be due to changes affecting transmission along the subthalamopallidal projection, when considered jointly with our anatomical findings, these functional data suggest that there is a functionally relevant denervation of the corticosubthalamic system in MPTP-induced parkinsonism in primates. While understanding the electrophysiological results, we must consider the possibility that the stimulation could have influenced other non-corticosubthalamic projections (see section 4.1.4.). However, we believe that the placement of the stimulation electrodes and the criteria we used to identify the early excitatory responses caused by activation of the corticosubthalamic pathway limit the possibility of such an occurrence.

Another point to consider is that the reduction in the proportion of pallidal neurons with characteristic early excitatory responses seen in the parkinsonian state is starkly different between the two monkeys used in this study. Although the proportion of pallidal neurons showing an early excitatory response was comparable between monkeys I (26.5%) and O (35.3%) in the normal state, these values in the parkinsonian state were clearly different between monkeys I (7.7%) and O (28.6%). From these values, one might

deduce that monkey I was significantly more parkinsonian than monkey O. Surprisingly, it was monkey O which was significantly more parkinsonian than monkey I. Another reason why these differences are so remarkable could be due to the inherent inter-animal variability. Even in the normal state, monkey I was clearly more active than monkey O; and it took a significantly longer time and amount of MPTP to render monkey I parkinsonian than monkey O. Also, even after a higher cumulative dosage of MPTP, monkey I did not reach the same degree of parkinsonism. While it is not clear as to why some monkeys are more susceptible to develop parkinsonian symptoms after MPTP intoxication, anecdotal evidence (from personal communications with Dr. Gunasingh Masilamoni, Emory University) suggest that factors such as age, gender and body weight may contribute to MPTP susceptibility in rhesus macaques. Additional experiments with more monkeys would give us a clear picture whether indeed there are fewer pallidal neurons which respond with an early excitatory response to corticosubthalamic activation in parkinsonian conditions.

*Degeneration of vGluT1-containing terminals in the STN of parkinsonian monkeys: How does it compare to the vGluT1-positive corticostriatal system?*

Taking into account that pallidal inputs to the STN are strengthened in rodent models of parkinsonism (Fan et al., 2012) and our observations about the loss of the corticosubthalamic system in parkinsonian animals, an investigation about the status of other input systems to the STN, like the glutamatergic afferents from the thalamus and PPN, is warranted. Both the corticosubthalamic and corticostriatal system seem to be

pathologically affected in parkinsonism, although the number of vGluT1-immunopositive terminals seem to be reduced in the STN compared to their increase in the striatum (Raju et al., 2008; Villalba and Smith, 2013). Remarkably, though there is a pathological increase in the number of vGluT1-immunoreactive terminals within the striatum in parkinsonism, there is also a significant loss of the putatively glutamatergic asymmetric synapses in the striatum occurring concomitantly (Ingham et al., 1989; Zaja-Milatovic et al., 2005). Though there are clearly some differences in the way the corticosubthalamic system responds in pathological conditions compared with the corticostriatal system, it would be important to assess whether the corticosubthalamic system also undergoes any changes in the synaptic transmission, long term plasticity, and functional specificity, as is seen in the corticostriatal pathway (Lindefors and Ungerstedt, 1990; Calabresi et al., 1993; Onn and Grace, 1999; Calabresi et al., 2000; Onn et al., 2000). A recent study in rats has shown that some of the corticosubthalamic inputs are collaterals of corticofugal systems (Kita and Kita, 2012). With changes occurring to both the major cortical input systems to the basal ganglia, it is worth considering if the denervation of the corticosubthalamic system is a corollary of pathological insult to cortical projection neurons innervating both the striatum and STN. However, as of now there is no clear evidence for single cortical projection neurons innervating both the striatum and STN in primates, as was shown in a single axon tracing study done in monkeys (Parent and Parent, 2006). However, as is seen with single axon tracing studies, the study done by Parent and Parent did not have a large number of neurons which were traced. Hence, it would be worth doing some more studies to clearly establish whether there are any cortical neurons which project to both the striatum and STN.

Furthermore, although it is well known that infusion of dopamine and dopamine receptor agonists can physiologically affect STN neuronal firing (Campbell et al., 1985; Hassani and Feger, 1999; Shen and Johnson, 2000), the role of nigrosubthalamic dopaminergic inputs in maintaining the integrity and functioning of individual corticosubthalamic inputs is not known. 3D reconstruction studies of the morphology of individual corticosubthalamic terminals and their post-synaptic targets, in particular the post-synaptic dendritic spines, could help us detect any morphological plastic changes occurring to the corticosubthalamic terminal – postsynaptic target complexes in parkinsonism (Villalba and Smith, 2011). It is not clear whether the reduction of corticosubthalamic inputs in parkinsonism is also accompanied by changes in the expression of glutamate receptors within the surviving corticosubthalamic synapses, whose synaptic activity may be impacted by such underlying changes. Ultra-high resolution freeze substitution or freeze fracture EM studies of corticosubthalamic synapses could help ascertain whether such changes are endemic in parkinsonism (Nusser et al., 1998; Masugi-Tokita et al., 2007). Moreover, whether corticosubthalamic denervation occurs in patients with Parkinson's disease is unclear.

*Cortico-subthalamic degeneration: Potential impact upon basal ganglia functions?*

The temporal interplay of the corticosubthalamic and corticostriatal pathways is a critical element in 'action selection' models of basal ganglia function (Nambu et al., 2002) or in models that ascribe response inhibition to the hyperdirect pathway (Jahfari et al., 2011) (see section 4.1.4. for more details). Central to arguments in favor of these

models is the apparent restriction of action selection in PD patients (Mink and Thach, 1993; Nambu et al., 2000; Nambu et al., 2002; Helmich et al., 2009; Wylie et al., 2010). It will be important to consider the prominent reduction of the 'hyperdirect' pathway when modeling action selection mediated by the basal ganglia in parkinsonism.

Knowing that STN neurons pathologically increase their firing rate in parkinsonism (Bergman et al., 1994; Wichmann and DeLong, 2003), the potential impact of a partly degenerated corticosubthalamic system on these STN firing changes is an interesting question to address. Increased motor cortex-STN functional connectivity (Baudrexel et al., 2011) and greater entrainment of STN neurons to cortical activity (Mallet et al., 2008; Shimamoto et al., 2013) occur in the parkinsonian state. Whether the degeneration of the corticosubthalamic system in parkinsonism is independent of, or compensatory to these pathological changes is not known. Another important problem to evaluate is the effect of corticosubthalamic denervation in parkinsonism on the probability of antidromic cortical activation during STN-DBS. Also, it would be interesting to know whether the corticosubthalamic degenerative process in parkinsonism is restricted only to the motor cortical afferents, or if it likewise affects associative and limbic cortical inputs to the STN.

In summary, we have shown that the corticosubthalamic pathway partly degenerates in parkinsonism, which could have a major impact on the current understanding of basal ganglia functioning in pathological conditions.

# 3. Loss of Motor and Non-motor Glutamatergic Inputs to the Subthalamic Nucleus in MPTP-treated parkinsonian monkeys

## 3.1. Introduction

In addition to its main GABAergic input from the external globus pallidus (GPe), the subthalamic nucleus (STN) also receives a significant contingent of glutamatergic inputs from the cerebral cortex, thalamus and pedunculopontine nucleus (PPN) (Wichmann and DeLong, 1996, 2003). Cortical glutamatergic afferents arise from the motor, associative and limbic cortical areas and mainly target their respective functional territories within the STN (Nambu et al., 1996; Haynes and Haber, 2013), as defined on the basis of STN's reciprocal connections with different functional regions of the GPe (Shink et al., 1996; Smith, 2011). Inputs from the centromedian nucleus of the thalamus (CM) innervate the dorsolateral 'motor' sector of the nucleus; whereas the parafascicular nucleus of the thalamus (PF) projects to the ventral 'associative' part of the nucleus (Sadikot et al., 1992). While the sources of glutamatergic afferents to the STN are well known, the relative abundance of cortical versus sub-cortical glutamatergic inputs to the motor and non-motor regions of the STN is unknown. In rodents, corticosubthalamic terminals mainly target distal dendrites and dendritic spines on STN neurons; whereas thalamosubthalamic terminals innervate proximal dendrites and dendritic spines on STN

neurons (Bevan et al., 1995). In primates, the innervation pattern of the cortical and sub-cortical glutamatergic afferents to the dendritic trees of STN neurons is not known.

STN neurons show increased spiking activity and fire in correlated, rhythmic and synchronous mode with GPe neurons in parkinsonism (Bergman et al., 1994; Bevan et al., 2002; Wichmann and DeLong, 2003). Though this abnormal pattern of STN neuronal activity is considered a key pathophysiological feature of parkinsonism, its origin(s) is/are not completely known. It is thought that both intrinsic factors (Wilson and Bevan, 2011) and extrinsic inputs (Fan et al., 2012) could influence the activity of STN neurons. In fact, a recent study showed that the pallidosubthalamic GABAergic projection, a prominent, and most likely sole, source of GABAergic inputs to STN neurons, is strengthened in parkinsonism (Fan et al., 2012). There is mounting evidence suggesting that activity of corticosubthalamic inputs is affected in parkinsonism (Orieux et al., 2002; Mallet et al., 2008; Baudrexel et al., 2011; Shimamoto et al., 2013). In the 6-OHDA rodent model of Parkinson's disease (PD), neurons within the PF and PPN, which project to the STN are metabolically hyperactive compared to controls (Orieux et al., 2000). However, the underlying anatomical changes occurring to these glutamatergic inputs to the STN in parkinsonism are not known.

To determine whether functional changes in the glutamatergic afferents to the STN activity could be attributed to underlying anatomical alterations, we used electron microscopy immunocytochemistry procedures to determine the relative abundance and dendritic innervation pattern of cortical (vGluT1-positive) and sub-cortical (vGluT2-positive) glutamatergic terminals in the motor and non-motor regions of the STN between normal and parkinsonian monkeys.

Preliminary results of this study have been presented in abstract form (Mathai et al., 2009; Mathai et al., 2010; Mathai et al., 2011).

## 3.2. Methods

### 3.2.1. Animals

Twelve adult rhesus monkeys (Macaca Mulatta, 4.4-15.0 kg, 2-11 years old, 7 males & 5 females) were used. The monkeys were raised in the breeding colony of the Yerkes National Primate Research Center. The animals had ad libitum access to food and water.

### 3.2.2. Induction of Parkinsonism

Six monkeys were rendered parkinsonian following chronic administration of MPTP as described in section 2.2.2. The extent of MPTP-induced nigrostriatal denervation was assessed anatomically as illustrated in Fig. 2.1 A,B.

### 3.2.3. Animal euthanasia and tissue fixation

The euthanasia method and tissue fixation procedures used in this study are the same as those described in detail in section 2.2.3.

### 3.2.4. Tissue processing

The tissue processing procedures used in this study are the same as those described in detail in section 2.2.4.1.

### 3.2.5. STN volume measurements

The procedures to measure the STN volume used in this study are the same as those described in detail in section 2.2.4.2.

### 3.2.6. Double Immuno EM for vGluT1 and vGluT2

Pairs of adjacent brain sections containing the STN from 3 normal and 3 parkinsonian monkeys (animals different from the ones used to assess STN volume) were processed for double immuno EM for vGluT1 and vGluT2 as described in section 2.2.4.5., except that a cocktail of secondary antibodies were used to reveal each vGluT. One section from each pair was treated with a cocktail of secondary antibodies such that vGluT1 was revealed using immunogold and vGluT2 was visualized with immunoperoxidase (See table 3.1). Then, the adjacent sections were processed using an inversed cocktail of secondary antibodies such that vGluT1 was revealed with immunoperoxidase and vGluT2 was labeled with immunogold (See table 3.1). This approach was employed to avoid any potential bias in the quantification of vGluT1 versus vGluT2 terminals due to differences in the tissue penetration of secondary antibodies used for immunogold versus immunoperoxidase histochemical methods.

Blocks of tissue from both the dorsolateral (DL) ‘motor’ and ventromedial (VM) ‘non-motor’ sectors of the STN (Shink et al., 1996; Smith, 2011) (Fig. 1.2) were analyzed.

Table 3.1: Primary and secondary antibodies used to detect vGluT1 and vGluT2

| Type | Reactions Set 1 (vGluT1 – immunogold; vGluT2 – immunoperoxidase) | |
|---|---|---|
| Primary Antibody | anti-vGluT1 (raised in guinea pig) [1:5000 dilution; EMD Millipore, Billerica, MA, USA] | anti-human vGluT2 (raised in rabbit) [1:5000 dilution; Mab Technologies, Atlanta, GA, USA] |
| Secondary Antibody | gold-conj. anti-guinea pig IgGs [raised in goat; 1:100 dilution; 1.4nm particle size; Nanogold; Nanoprobes, Stony Brook, NY, USA] | biotinylated anti-rabbit IgGs [raised in goat; 1:200 dilution; Vector Laboratories, Burlingame, CA, USA] |
| Type | Reactions Set 2 (vGluT1 – immunoperoxidase; vGluT2 – immunogold) | |
| Primary Antibody | anti-vGluT1 (raised in guinea pig) [1:5000 dilution; EMD Millipore, Billerica, MA, USA] | anti-human vGluT2 (raised in rabbit) [1:5000 dilution; Mab Technologies, Atlanta, GA, USA] |
| Secondary Antibody | biotinylated anti-guinea pig IgGs [raised in goat; 1:200 dilution; Vector Laboratories, Burlingame, CA, USA] | gold-conj. anti-rabbit IgGs [raised in goat; 1:100 dilution; 1.4nm particle size; Nanogold; Nanoprobes, Stony Brook, NY, USA] |

Abbreviations: conj. - conjugated

### 3.2.7. Analysis of EM material

#### *3.2.7.1. Co-localization of vGluT1 and vGluT2*

Ultrathin STN sections were sampled under the EM to assess whether vGluT1 and vGluT2 were co-expressed, as described in detail in section 2.2.4.6.1.

#### *3.2.7.2. Density of vGluT1- and vGluT2-containing terminals*

Using the sampling procedure described in section 2.2.4.6.2., both series of sections double-labeled for vGluT1&2 (ie set 1: vGluT1-immunogold, vGluT2-immunoperoxidase and set 2: vGluT1-immunoperoxidase, vGluT2-immunogold) were sampled. Then, the number of terminals immunopositive exclusively for either of the vGluTs was quantified from both sets of sections. Using the resulting two values from both sets of tissue sections, the average number of terminals was calculated for each vGluT. To illustrate further, if we were to sample the number of vGluT1 terminals in a given area of the STN, first the number of vGluT1 terminals (immunogold-labeled) in that area would be determined from tissue set 1 (vGluT1-immunogold, vGluT2-immunoperoxidase). Then the number of vGluT1 terminals (immunoperoxidase-labeled) would be quantified in the same area from tissue set 2 (vGluT1-immunoperoxidase, vGluT2-immunogold). An average value would then be calculated from these two values (area sampled: each set – 3960 $\mu m^2$; total area – 7920 $\mu m^2$/STN region/animal). Finally, the density of the terminals immunoreactive for vGluT1 would be calculated. A similar approach would be repeated for vGluT2.

It must be noted that all the antibody solutions used to reveal vGluT1 and vGluT2 produced robust immunolabeling of the transporters, thereby allowing us to unambiguously identify labeled elements (Figs. 3.1, 3.2).

*3.2.7.3. Post-synaptic targets of vGluT1- and vGluT2-positive terminals*

In order to characterize the synaptic microcircuits that underlie glutamatergic transmission from vGluT1 and vGluT2 afferents to the STN, we quantified the distribution of the postsynaptic targets of vGluT1- and vGluT2-containing terminals in different functional regions of the STN in normal and parkinsonian monkeys using the procedure described in section 2.2.4.6.4.

3.2.8. TH immunostaining

The TH immunostaining procedures used in this study are the same as those described in detail in section 2.2.5.

## 3.3. Results

3.3.1. vGluT1 and vGluT2 co-localization in the monkey STN

In order to examine whether the segregation of vGluT1 and vGluT2 described in the striatum (Fujiyama et al., 2004; Fujiyama et al., 2006; Raju et al., 2006; Raju et al., 2008) and other forebrain regions (Hur and Zaborszky, 2005; Kubota et al., 2007; Liguz-Lecznar and Skangiel-Kramska, 2007) also applies to the STN, we carried out co-localization EM studies of vGluT1 and vGluT2 at the single terminal level using immunoperoxidase or immunogold labeling for either vGluTs (Fig. 3.1 A,B). In normal

monkeys, only 0.58% (3/529) of vGluT1/2-immunoreactive terminals co-expressed both transporters in DL STN; whereas this value was 0.48% (3/621) in the VM STN. There was no major change in the terminal co-expression of vGluT1/2 within the STN in the parkinsonian state [0.38% (1/264) of terminals in DL STN, 0.00% (0/297) of terminals in VM STN]. Together with the known localization of vGluT1 and vGluT2 mRNA (and protein) in the various sources of glutamatergic afferents to the STN (i.e., thalamus, brainstem, STN collaterals and cortex), these data show that vGluT1 and vGluT2 are specific markers of glutamatergic inputs to the STN from cortical and sub-cortical sources, respectively in monkeys.

### 3.3.2. Relative abundance of vGluT1- and vGluT2-containing terminals in the 'motor' and 'non-motor' territories of the STN

Both vGluT1- and vGluT2-containing terminals were found in varying sizes with some terminals packed with mitochondria (Fig. 3.2 C,F) and others having few mitochondria (Fig. 3.2 A,D). The density of both vGluT1- and vGluT2-immunopositive terminals was not significantly different between the DL STN and the VM STN in in normal monkeys (Fig. 3.1C, 3.1D). The density of vGluT2-containing terminals was significantly lower than that of vGluT1-containing terminals in the DL STN (Student's t-test, $p = 0.002$) (Fig. 3.1 C,D), whereas there was no significant difference in the corresponding values in the VM STN (Student's t-test, $p = 0.565$) (Fig. 3.1 C,D).

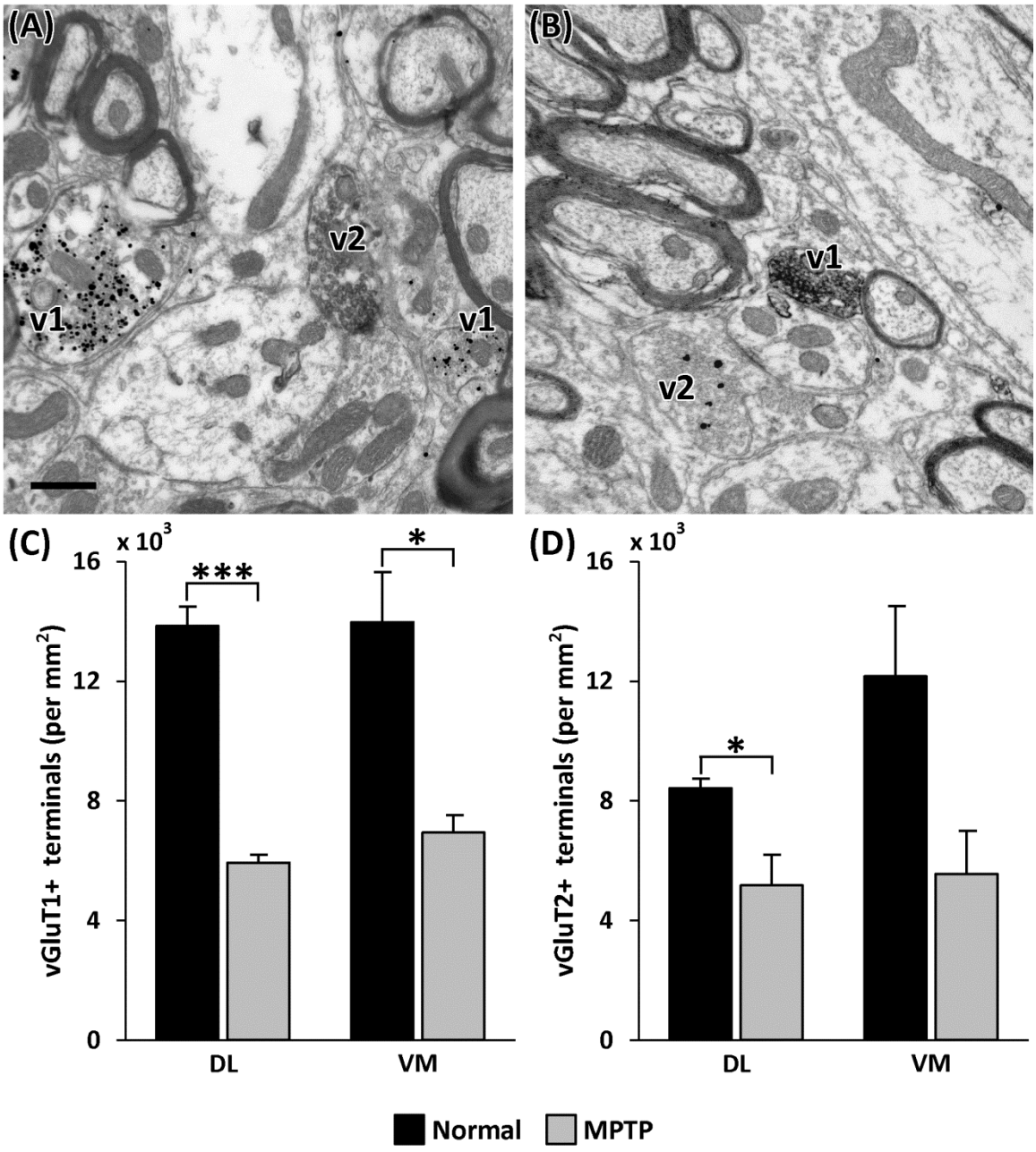


**Figure 3.1: Electron microscopic observations: Density of vGluT1- and vGluT2-immunopositive terminals in the STN**

(A) Electron micrograph showing vGluT1-positive (v1-immunogold) and vGluT2-labeled (v2-immunoperoxidase) terminals in the STN. (B) Electron micrograph showing vGluT1-positive (v1-immunoperoxidase) and vGluT2-labeled (v2-immunogold)

terminals in the STN. Scale bar: 0.5 μm (applies to both A & B). (C) Density of vGluT1-immunopositive terminals in the dorsolateral (DL) and ventromedial (VM) STN of normal versus parkinsonian monkeys. The density of vGluT1-containing terminals was significantly lower in the DL STN (***$p < 0.001$, Student's t-test) and VM STN (*$p < 0.05$, Student's t-test) of parkinsonian monkeys compared to healthy controls. Total surface area analyzed: 7920 $\mu m^2$/region/animal. Number of terminals sampled: DL STN (normal – 329, MPTP – 141), VM STN (normal – 332, MPTP – 162). (D) Density of vGluT2-immunoreactive terminals in the dorsolateral (DL) and ventromedial (VM) STN of normal versus parkinsonian monkeys. The density of vGluT2-containing terminals was significantly lower in the DL STN (*$p < 0.05$, Student's t-test) of parkinsonian monkeys compared to healthy controls. Total surface area analyzed: 7920 $\mu m^2$/region/animal. Number of terminals sampled: DL STN (normal – 200, MPTP – 123), VM STN (normal – 289, MPTP – 132). Columns (C & D) represent means ± standard error of the mean across 3 normal and 3 parkinsonian monkeys.

3.3.3. Dendritic innervation patterns of vGluT1- and vGluT2-containing terminals in the monkey STN

vGluT1- and vGluT2-containing terminals innervated dendritic shafts and spines in the STN (Fig. 3.2). In the DL STN, 70 ± 4% and 30 ± 4% of the vGluT1-immunoreactive terminals innervated dendritic shafts and spines, respectively (n = 150) (Fig. 3.3 A1), whereas in the VM STN, they contacted dendritic shafts and spines in 71.3 ± 3.7% and 28.7 ± 3.7% of the instances (n = 150), respectively (Fig. 3.3 B1). On the other hand, 90 ± 3.1% and 10 ± 3.1% of the targets of vGluT2-immunopositive terminals in the DL STN (n = 150) were dendritic shafts and spines, respectively (Fig. 3.3 A1), whereas in the VM STN, vGluT2-immunoreactive terminals were found appositioned to dendritic shafts and spines in 96 ± 1.2% and 4 ± 1.2% of the occasions (n = 150), respectively (Fig. 3.3 B1).

We found a significant difference between the dendritic innervation patterns of vGluT1- and vGluT2-containing terminals in both the DL STN (two way ANOVA, vGluT-type × post-synaptic target, $F_1 = 31.6$, $p < 0.001$) and VM STN (two way ANOVA, vGluT-type × post-synaptic target, $F_1 = 80.5$, $p < 0.001$). Pairwise Bonferroni multiple comparisons test revealed that dendritic spines constituted a significantly greater proportion of the post-synaptic targets of vGluT1-positive terminals compared with that of vGluT2-positive terminals (DL STN: $p = 0.004$, VM STN: $p < 0.001$), and that dendritic shafts were significantly less frequent post-synaptic targets of vGluT1-positive terminals compared with that of vGluT2-positive terminals (DL STN: $p = 0.004$, VM STN: $p < 0.001$) in both STN regions.

Furthermore, the axo-dendritic synapses were categorized as distal or proximal based on the sizes of the dendritic shafts being contacted. This was done by measuring the diameter of dendritic shafts at their vGluT1 terminal innervation site, and classifying these dendrites as large (>1.0 μm), medium (0.5-1.0 μm) or small (<0.5 μm). Of the axo-dendritic synapses formed by vGluT1-immunopositive terminals, 21.8 ± 7.0%, 47.9 ± 6.5% and 30.3 ± 1.7%, targeted large, medium and small dendrites, respectively in the DL STN (Fig. 3.3 A2); while 10.0 ± 5.6%, 44.4 ± 4.7% and 45.6 ± 4.3% of them innervated large, medium and small dendrites, respectively in the VM STN (Fig. 3.3 B2). With respect to the axo-dendritic synapses formed by vGluT2-immunoreactive terminals, 18.3 ± 3.4%, 60.0 ± 4.2% and 23.8 ± 3.9% of them contacted large, medium and small dendrites, respectively in the DL STN (Fig. 3.3 A2); whereas in the VM STN 26.4 ± 7.7%, 52.8 ± 5.9% and 20.8 ± 2.3% of them terminated onto large, medium and small dendrites, respectively (Fig. 3.3 B2).

The size distributions of the post-synaptic dendritic shafts contacted by vGluT1- versus vGluT2-containing terminals forming axo-dendritic synapses in the DL STN is significantly different (two way ANOVA, vGluT-type × post-synaptic dendritic shaft-size, $F_2 = 4.1$, $p = 0.044$). Pairwise Bonferroni multiple comparisons test showed that amongst the various size classifications of post-synaptic dendritic shafts formed by axo-dendritic synapses: the medium-sized dendrites represented a significantly lower proportion of the post-synaptic dendritic shaft population of vGluT1-positive terminals compared to that of vGluT2-positive terminals ($p = 0.003$), but not the corresponding large-sized ($p = 0.800$) and small-sized ($p = 1.000$) dendritic proportions. Similarly, in the VM STN, the size distributions of the post-synaptic dendrites contacted by vGluT1-

versus vGluT2-containing terminals forming axo-dendritic synapses was significantly different (two way ANOVA, vGluT-type × post-synaptic dendritic shaft-size, $F_2 = 7.6$, $p = 0.007$). Pairwise Bonferroni multiple comparisons test showed that amongst the various sizes of post-synaptic dendritic shafts formed by axo-dendritic synapses: both the large-sized ($p = 0.018$) and medium-sized ($p = 0.012$) dendrites constituted significantly lesser proportions of the post-synaptic dendritic shaft population of vGluT1-positive terminals compared to that of vGluT2-positive terminals, but not the corresponding small-sized dendritic proportion ($p = 0.077$).

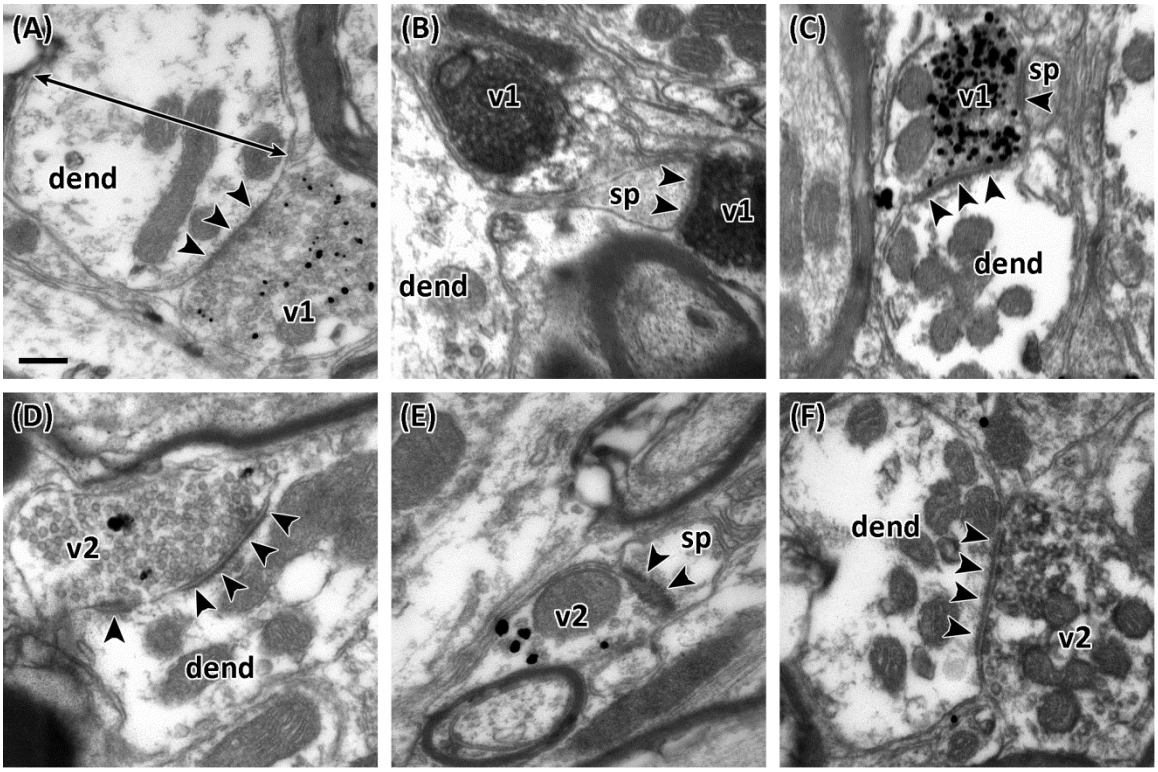


**Figure 3.2: Electron micrographs showing the post-synaptic targets of vGluT1- and vGluT2-containing terminals in the STN**

(A-C) vGluT1 (v1) containing terminals forming asymmetric synapses (indicated by arrowheads) with dendritic shafts (dend) (A,C) and dendritic spine (sp) (B,C). vGluT1 revealed with immunogold in panels A & C and immunoperoxidase in panel B. The black line with double ended arrows on the dendritic shaft (A), illustrates the measurement of its cross-sectional diameter, defined as the shortest diameter passing through the approximate center of its 2D representation on the EM image. (D-F) vGluT2 (v2) containing terminals forming asymmetric synapses (indicated by arrowheads) with dendritic shafts (dend) (D,F) and a dendritic spine (sp) (E). vGluT2 revealed with immunogold in panels D & E and immunoperoxidase in panel F.

Scale bar: 0.2 μm (applies to all panels A-F).

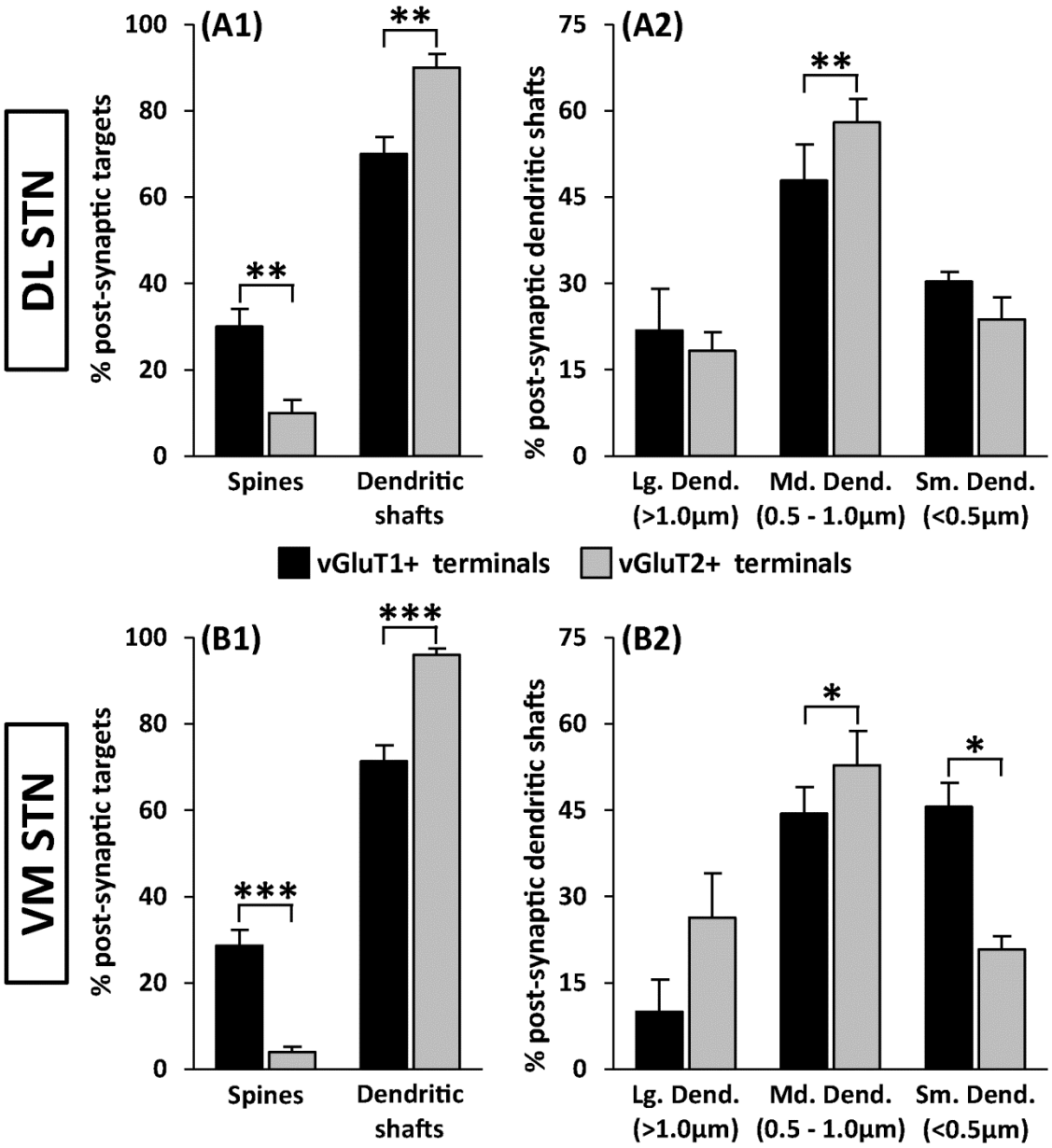


**Figure 3.3: Post-synaptic targets of vGluT1- and vGluT2-immunopositive terminals in the DL STN and VM STN of normal monkeys**

Significant differences were seen the proportions of the post-synaptic targets of vGluT1- versus vGluT2-immunoreactive terminals in both the DL STN (A1) and VM STN (B1). Also, in both the DL STN (A2) and VM STN (B2), significant differences were found between the size distributions of all the post-synaptic dendritic shafts which were

contacted by vGluT1- and vGluT2-immunoreactive terminals. Abbreviations: Lg – large, Md – medium, Sm – small, Dend – dendritic shafts. Columns represent means ± standard error of the mean across 3 normal and 3 parkinsonian monkeys. Significance levels: *$p < 0.05$; **$p < 0.01$; ***$p < 0.001$.

### 3.3.4. Relative abundance and synaptology of vGluT1- and vGluT2-containing terminals in normal versus parkinsonian monkeys

#### *3.3.4.1. State of parkinsonian motor symptoms and nigrostriatal dopaminergic pathology in MPTP-treated monkeys*

All MPTP-treated monkeys used in this study displayed moderate to severe parkinsonian motor symptoms at the time of euthanasia, as assessed using beam break counts in a behavioral cage and the PRS described in the Methods section, and used in many of our previous studies (Kliem et al., 2010; Hadipour-Niktarash et al., 2012; Bogenpohl et al., 2013). Consistent with these behavioral observations, all parkinsonian animals displayed more than 80% dopaminergic denervation of the postcommissural putamen, based on reduced densitometry measurements of TH immunoreactivity (Fig. 2.1 A,B).

#### *3.3.4.2. Loss of both vGluT1- and vGluT2-containing terminals in the STN of parkinsonian animals*

We compared the density of vGluT1-positive terminal profiles in the DL STN and VM STN of normal versus MPTP-treated monkeys (Fig. 3.1 A,B). In the DL STN, there was a 57.1% (Student's t- test; $p < 0.001$) reduction in the density of vGluT1-positive terminals in parkinsonian monkeys (5,934 ± 263 per $mm^2$, n = 141 terminals) compared with controls (13,846 ± 653 per $mm^2$, n = 329 terminals) (Fig. 3.1 C). Similarly, in the VM STN, the density of vGluT1-containing terminals decreased by 50.3% (Student's t-test; $p = 0.017$) in the parkinsonian state compared to normal conditions (normal

condition – 13,972 ± 1,688 per $mm^2$, n = 332 terminals; parkinsonian state – 6,944 ± 583 per $mm^2$, n = 165 terminals) (Fig. 3.1 C).

Moreover, the density of innervation of vGluT2-positive inputs to the STN was lower in the parkinsonian state compared to normal conditions (Fig. 3.1 A,B). In the DL STN, there was a 38.5% (Student's t- test; p = 0.038) reduction in the density of vGluT1-positive terminals in parkinsonian monkeys (5,176 ± 1,020 per $mm^2$, n = 123 terminals) compared with normal animals (8,417 ± 303 per $mm^2$, n = 200 terminals) (Fig. 3.1 D). However, in the VM STN, the density of vGluT2-containing terminals was not significantly different (Student's t-test; p = 0.075) between the parkinsonian and normal states (normal condition – 12,162 ± 2,343 per $mm^2$, n = 289 terminals; parkinsonian state – 5,555 ± 1,456 per $mm^2$, n = 132 terminals) (Fig. 3.1 D).

*3.3.4.3. Lack of volumetric changes of the STN in parkinsonian animals*

To ensure that the density values presented above for vGluT1- and vGluT2-positive terminals between normal and parkinsonian animals were collected from STNs of comparable sizes, we reconstructed, in 3D, the volume of the STN, from equally spaced coronal LM representations of the nucleus from 3 control and 3 MPTP-treated monkeys. There was no significant difference (Student's t- test; p = 0.858) in the volume of the STN between these animals (Fig. 2.2 E).

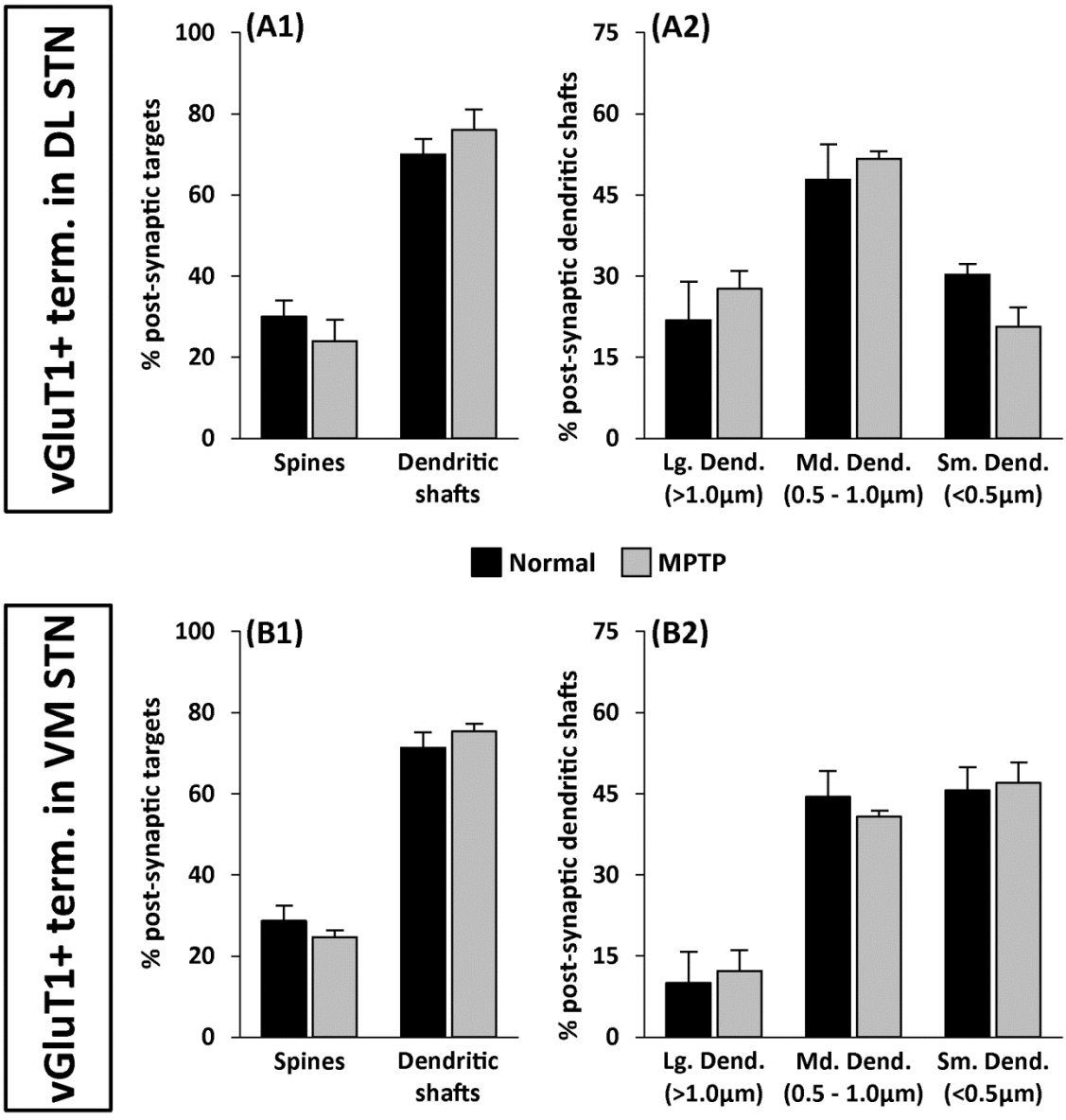


**Figure 3.4: Post-synaptic targets of vGluT1 immunopositive terminals in the DL STN and VM STN of normal versus parkinsonian monkeys**

No significant differences were seen the proportions of the post-synaptic targets of vGluT1 immunoreactive terminals between normal and parkinsonian monkeys, in both the DL STN (A1) and VM STN (B1). Also, in both the DL STN (A2) and VM STN (B2), no significant differences were found in the size distributions of all the post-synaptic

dendritic shafts which were contacted by vGluT1 containing terminals between normal and parkinsonian conditions. Abbreviations: Lg – large, Md – medium, Sm – small, Dend – dendritic shafts. Columns represent means ± standard error of the mean across 3 normal and 3 parkinsonian monkeys.

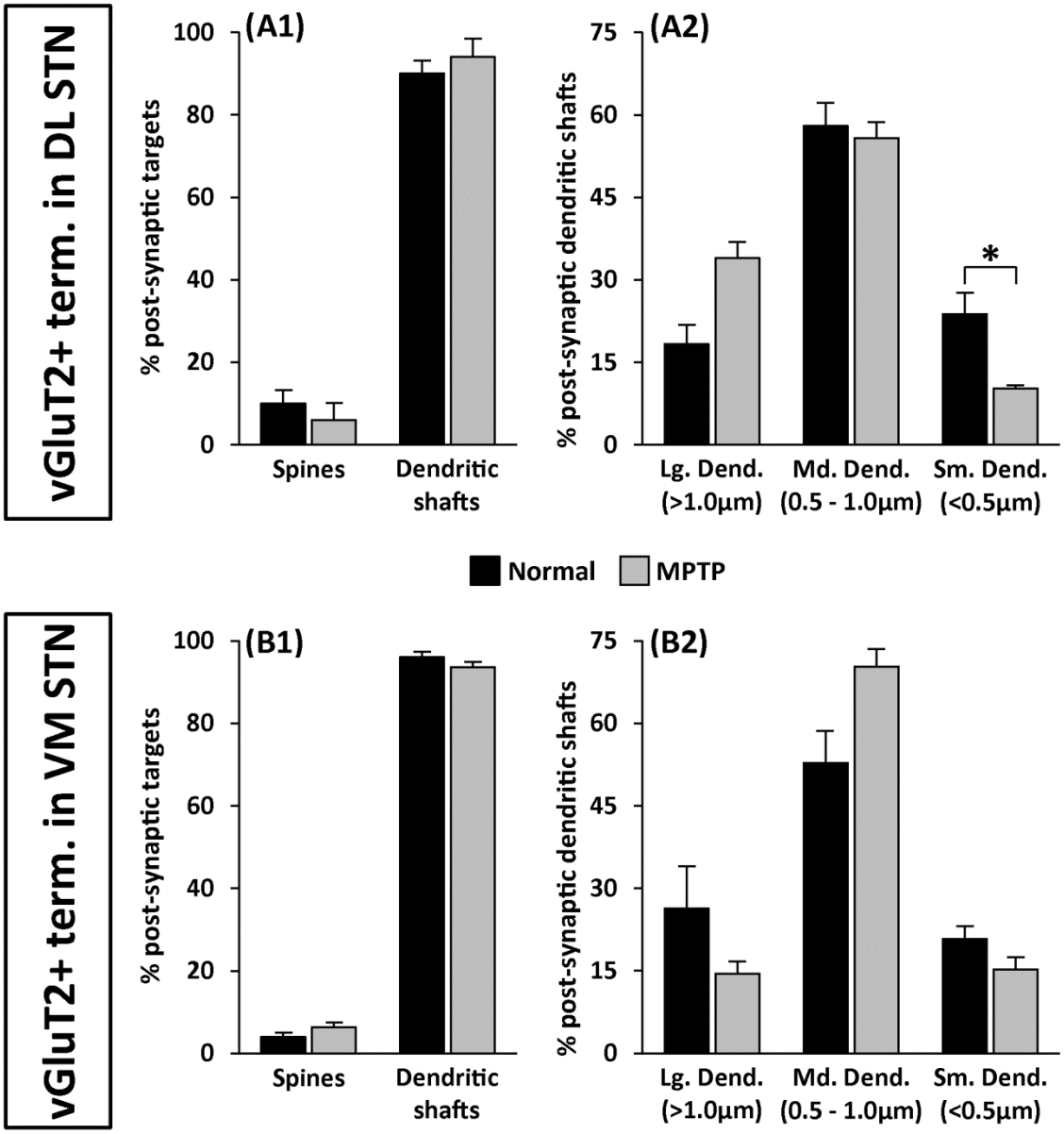


**Figure 3.5: Post-synaptic targets of vGluT2 immunopositive terminals in the DL STN and VM STN of normal versus parkinsonian monkeys**

No significant differences were seen the proportions of the post-synaptic targets of vGluT2-immunoreactive terminals between normal and parkinsonian monkeys, in both

the DL STN (A1) and VM STN (B1). Also, no significant differences were found in the size distributions of all the post-synaptic dendritic shafts which were contacted by vGluT2 containing terminals in the VM STN between normal and parkinsonian conditions (B2). However, in the DL STN, there was a significant difference in the size distributions of all the post-synaptic dendritic shafts which were contacted by vGluT2 containing terminals between normal and parkinsonian conditions (A2). Abbreviations: Lg – large, Md – medium, Sm – small, Dend – dendritic shafts. Columns represent means ± standard error of the mean across 3 normal and 3 parkinsonian monkeys. Significance levels: *$p < 0.05$.

*3.3.4.4. No change in the pattern of synaptic innervation of STN neurons by both vGluT1- and vGluT2- containing terminals between normal and parkinsonian monkeys*

To assess whether there were any changes in the pattern of synaptic innervation of vGluT1- and vGluT2-containing terminals in parkinsonism, we compared the post-synaptic targets of these two inputs between normal (data described earlier) and parkinsonian conditions. In the parkinsonian state, vGluT1-immunoreactive terminals innervated dendritic shafts and spines in 76.0 ± 5.0% and 24.0 ± 5.0% of the instances (n = 150), respectively in the DL STN (Fig. 3.4 A1); whereas, in the VM STN they contacted dendritic shafts and spines in 75.3 ± 1.8% and 24.7 ± 1.8% of the occasions (n = 150), respectively (Fig. 3.4 B1). On the other hand, in parkinsonian condition, vGluT2-immunopositive terminals targeted dendritic shafts and spines of the DL STN in 94.0 ± 4.2% and 6 ± 4.2% of the cases (n = 127), respectively (Fig. 3.5 A1); and they innervated dendritic shafts and spines of the VM STN in 93.6 ± 1.2% and 6.4 ± 1.2% of the instances (n = 128), respectively (Fig. 3.5 B1).

We found no significant difference in the dendritic innervation patterns of vGluT1-containing terminals in normal versus parkinsonian states in the DL STN (two way ANOVA, vGluT-type × post-synaptic target, $F_1 = 1.7$, $p = 0.223$) and VM STN (two way ANOVA, vGluT-type × post-synaptic target, $F_1 = 1.9$, $p = 0.206$). Similarly, there was no significant difference in the dendritic innervation patterns of vGluT2-containing terminals in normal versus parkinsonian states within the DL STN (two way ANOVA, vGluT-type × post-synaptic target, $F_1 = 0.3$, $p = 0.615$) and VM STN (two way ANOVA, vGluT-type × post-synaptic target, $F_1 = 1.5$, $p = 0.257$).

Additionally, we calculated the proportion of axo-dendritic synapses targeting large (>1.0 μm), medium (0.5-1.0 μm) or small (<0.5 μm) dendritic shafts (see description earlier). Of the axo-dendritic synapses contacted by vGluT1-immunopositive terminals in the parkinsonian state, 27.6 ± 3.3%, 51.7 ± 1.1% and 20.6 ± 3.7%, were located on large, medium and small dendrites, respectively in the DL STN (Fig. 3.4 A2); while 12.3 ± 3.7%, 40.7 ± 1.1% and 47.0 ± 3.9% of them were found on large, medium and small dendrites, respectively in the VM STN (Fig. 3.4 B2). With respect to the axo-dendritic synapses innervated by vGluT2-immunoreactive terminals in parkinsonian conditions, 33.9 ± 3.0%, 55.8 ± 2.9% and 10.3 ± 0.5% of them targeted large, medium and small dendrites, respectively in the DL STN (Fig. 3.5 A2); whereas in the VM STN 14.4 ± 2.2%, 70.3 ± 3.3% and 15.2 ± 2.3% of them were formed on large, medium and small dendrites, respectively (Fig. 3.5 B2).

The size distributions of the post-synaptic dendritic shafts contacted by vGluT1-containing terminals forming axo-dendritic synapses in the STN were not significantly different between normal and parkinsonian conditions (two way ANOVA, vGluT-type × post-synaptic dendritic shaft-size; DL STN, $F_2 = 2.0$, $p = 0.173$; VM STN, $F_2 = 0.2$, $p = 0.845$). Similarly, with respect to vGluT2-containing terminals forming axo-dendritic synapses in the VM STN, the size distributions of their post-synaptic dendritic shafts were not significantly different between normal and parkinsonian conditions (two way ANOVA, vGluT-type × post-synaptic dendritic shaft-size; $F_2 = 1.5$, $p = 0.273$). However, the size distributions of the post-synaptic dendritic shafts contacted by vGluT2-containing terminals forming axo-dendritic synapses in the DL STN were significantly different between normal and parkinsonian conditions (two way ANOVA, vGluT-type ×

post-synaptic dendritic shaft-size, $F_2 = 4.9$, $p = 0.035$). Pairwise Bonferroni multiple comparisons test showed that amongst the various size classifications of post-synaptic dendritic shafts contacted by vGluT2-containing terminals in the DL STN, the proportion of small-sized dendrites in the post-synaptic dendritic shaft population was significantly higher in normal animals compared with parkinsonian animals ($p = 0.047$); but there were no significant differences in the corresponding values for large-sized ($p = 0.101$) and medium-sized ($p = 0.175$) dendrites.

### 3.4. Discussion

Our results show that both cortical (ie vGluT1-positive) and sub-cortical (ie vGluT2-positive) glutamatergic afferents equally innervate the motor and non-motor territories of the monkey STN in normal and parkinsonian monkeys. Furthermore, in line with data presented in chapter 2, these findings confirm a significant loss of vGluT1-positive terminals in the DL sector of the monkey STN in parkinsonism. In addition, our data demonstrate that this loss of vGluT1 terminals also occurs in the VM STN, and that the prevalence of vGluT2-containing terminals is also significantly reduced throughout the STN in parkinsonian animals. Thus, both the motor and non-motor territories of the STN undergo a significant degeneration of their cortical and sub-cortical glutamatergic drive in MPTP-treated parkinsonian monkeys. This homogeneous glutamatergic denervation of the motor versus non-motor STN territories suggests that this pathology may have widespread effects upon STN activity. Considering the increased interest in the STN as a target for deep brain stimulation (DBS) for alleviating addiction (Pelloux and Baunez, 2013) and neuropsychiatric diseases (Bourne et al., 2012), the pathological changes in

glutamatergic inputs to the non-motor territory of the STN reported in our study certainly merit consideration.

We found that sub-cortical glutamatergic inputs almost exclusively targeted dendritic shafts, rarely contacting dendritic spines; whereas their cortical counterparts formed synapses with both dendritic shafts and spines in approximately 70% and 30% of the instances, respectively. Because dendritic spines are considered the most plastic elements of dendritic trees in the mature adult brain (Alvarez and Sabatini, 2007), it would be reasonable to conclude that cortical glutamatergic afferents to the STN are more amenable to plastic changes compared with those of sub-cortical origin. In cases where glutamatergic inputs terminated onto dendritic shafts of STN neurons, we estimated the proximity of the innervation site to the soma by measuring the approximate diameter of the 2D representation of the dendritic shaft. Since we know that STN dendrites taper off as they extend out away from the soma (Rafols and Fox, 1976), we can assume that the dendritic shaft would have a larger diameter when closer to the soma than it would when further away from the soma. We found that cortical and sub-cortical glutamatergic inputs target the dendritic shafts of STN neurons at different locations, with the sub-cortical inputs contacting dendritic shafts at sites closer to the soma than the cortical ones. This finding is in line with the previous report that anterogradely labeled thalamosubthalamic afferents innervate STN neurons at sites closer to the soma than corticosubthalamic inputs in rodents (Bevan et al., 1995). If all other factors governing the tendency of a neuron to respond to a target are similar, the relative proximity of a terminal to the soma of a target neuron determines the propensity of that neuron to respond to the input (Stuart and Spruston, 1998). Hence, it is reasonable to consider that the relative tendencies of

STN neurons to fire in response to cortical versus sub-cortical glutamatergic afferents might be different, on account of the differential pattern of STN dendritic innervation by these two inputs. It would be exciting to explore this question using electrophysiological techniques to measure the likelihood of activation of the post-synaptic STN neuron in response to cortical versus sub-cortical glutamatergic stimulation.

*Changes of the glutamatergic inputs to the STN in parkinsonism*

Our data demonstrate a significant loss of glutamatergic inputs of cortical and sub-cortical origin to the STN in MPTP-induced parkinsonian monkeys. Significant changes in the pattern of synaptic innervation, functional connectivity, synaptic transmission and long term plastic properties of other major glutamatergic inputs to the basal ganglia, such as the corticostriatal and thalamostriatal projections, have been extensively described in animal models of PD (Ingham et al., 1989; Stephens et al., 2005; Zaja-Milatovic et al., 2005; Raju et al., 2008; Smeal et al., 2008; Villalba et al., 2009; Galvan and Smith, 2011; Mathai and Smith, 2011; Shepherd, 2013; Villalba et al., 2013). Whether similar changes also affect the glutamatergic inputs to the STN is an important question to consider. It would be interesting to compare the common thread underlying the changes in the integrity of glutamatergic inputs to the basal ganglia in dopamine-denervated conditions.

It is necessary to understand whether the changes occurring to glutamatergic inputs to both the striatum and STN in parkinsonian condition can be ascribed to pathological insults of vGluT1- or vGluT2-positive neurons projecting concurrently to both of these nuclei or to different neuronal populations. Because there is no evidence that single

glutamatergic neurons in the cortex, thalamus or PPN, simultaneously project to both the striatum and STN in primates (Mathai and Smith, 2011; Smith et al., 2013), the likelihood that these changes are due to the pathology of a single neuronal population is limited. However, the situation may be different in rodents, at least for corticofugal neurons, which appear to be highly collateralized, thus giving rise to both corticostriatal and corticosubthalamic projections (Kita and Kita, 2012; Shepherd, 2013). Further characterization of the potential species differences in the degree of axonal collateralization of individual glutamatergic neurons projecting to both the striatum and the STN between primates and non-primates is essential. A clear map of the trajectories taken by afferents to the STN and their axon collaterals would help us better model the stimulation effects of an electrode placed within the STN, as usually done in STN-DBS. With this knowledge, we could probably understand some of the network-wide effects seen after STN-DBS, which is a major unresolved problem of the procedure (Humphries and Gurney, 2012). Finally, these anatomical maps could also help us understand better the functional significance of a dual gateway for glutamatergic inputs to reach the basal ganglia circuitry (Mathai and Smith, 2011).

Dopamine and dopamine receptor agonists are known to induce physiological changes in STN neuronal activity (Campbell et al., 1985; Hassani and Feger, 1999; Shen and Johnson, 2000). However, the precise functional effects of nigrosubthalamic dopaminergic projections onto STN glutamatergic afferents to the STN are not clear. The role of dopamine in maintaining the integrity of individual glutamatergic inputs to the STN is an important scientific problem to address especially since our data shows a major loss of these inputs to the STN in parkinsonism. Also, we could study the plastic changes

occurring to the remaining glutamatergic synapses in the parkinsonian STN. In this regard, one could study the expression of glutamate receptors in glutamatergic synapses within the parkinsonian STN using ultra-high resolution EM methods (Nusser et al., 1998; Masugi-Tokita et al., 2007).

Over the past few years, a dual target DBS approach of stimulating both the STN and PPN has been used in PD patients with major gait problems, where it is thought that STN-DBS and PPN-DBS work synergistically to deliver a much better therapeutic outcome than STN-DBS alone (Ferraye et al., 2011). In the case of the supposed synergistic effects of concurrent STN- and PPN-DBS, the connections between these two nuclei may play an important role. While we don't know whether the observed loss of sub-cortical glutamategic afferents to the STN also includes the ones originating in the PPN, it must be noted that the abundance of PPN afferents to the STN might determine in part the outcome of simultaneous STN- and PPN-DBS. Moreover, some of the effects of STN-DBS are thought to arise from antidromic activation of cortical afferents (Li et al., 2007), and hence, the density of these cortical inputs may underlie the efficacy of STN-DBS. In light of our data which shows that both the cortical and sub-cortical glutamatergic inputs are affected in parkinsonism, it is important to weigh this loss while modeling the effects of STN-DBS and PPN-DBS in PD patients.

Apart from their loss in parkinsonism, we did not detect any morphological changes occurring to individual glutamatergic terminals innervating the STN in parkinsonism. However, one cannot rule out the possibility of such changes. A thorough three-dimensional reconstruction study of these glutamatergic boutons in normal versus

parkinsonian states may give us more insight into possible structural plastic changes affecting them (Villalba and Smith, 2011).

The cortical and sub-cortical glutamatergic afferents to the STN undergo major functional changes in parkinsonism. Cortical and sub-cortical glutamatergic inputs show a lower and higher metabolic activity, respectively, in 6-OHDA treated rats (Orieux et al., 2000; Orieux et al., 2002). Also, beta oscillations in the corticosubthalamic connection are enhanced in 6-OHDA treated rats (Mallet et al., 2008). Moreover, the cortex and STN are functionally more connected and pathologically synchronized with each other in Parkinson's patients (Baudrexel et al., 2011; Shimamoto et al., 2013). It would be important to know if these functional changes occurring to the glutamatergic afferents of the STN are responsible for the more famous pathology of the STN in parkinsonism – increased oscillations. Another noteworthy point is that the CM/PF thalamic nuclei, which give rise to a major component of sub-cortical glutamatergic afferents to the STN, undergo a massive cell loss in MPTP-treated monkeys (Villalba et al., 2013), and in PD patients (Henderson et al., 2000). It is not known whether the CM/PF neurons which degenerate also include some which project to the STN, which could explain in part the loss of sub-cortical glutamatergic afferents to the STN.

# 4. Conclusions and Future Directions

The STN receives significant glutamatergic inputs from cortical and sub-cortical sources. However, much of our knowledge about these glutamatergic afferents to the primate STN is limited to anatomic and functional studies done in the normal state. Not much is known about changes occurring to these inputs in pathological conditions. Using anatomic techniques, I have studied the underlying structural changes occurring to these inputs in a primate model of PD. Further, I started exploring some aspects of the functional consequences of my anatomical findings on the functional integration of the corticosubthalamic pathway in the basal ganglia circuitry. The key conclusions of this thesis and future directions for exploration are summarized below:

## 4.1. Conclusions

### 4.1.1. Both the motor and non-motor territories of the STN receive significant cortical and sub-cortical glutamatergic afferents

There have been several anatomical tract-tracing studies and some functional connectivity studies which clearly demonstrate the innervation of both non-motor and motor STN regions by glutamatergic afferents arising from either cortical or sub-cortical sources (Monakow et al., 1978; Sadikot et al., 1992; Lavoie and Parent, 1994a; Bevan et al., 1995; Nambu et al., 1996; Chudasama et al., 2003; Haynes and Haber, 2013). However, there has been no study exploring whether both the non-motor and motor

territories of the STN are innervated to the same extent by these inputs. In fact, the existence of significant corticosubthalamic projections originating in non-motor cortical areas have only recently been shown conclusively in primates (Haynes and Haber, 2013). Also, until recently, conducting a study to compare the degree of innervation of the non-motor and motor STN by total glutamatergic inputs was technically challenging due to the limitations in applying neuronal tracers in huge regions such as the cerebral cortex. However, with the introduction of vGluT1 or vGluT2 as specific markers of glutamatergic inputs from cortical and sub-cortical sources, respectively (Fremeau et al., 2004; Liguz-Lecznar and Skangiel-Kramska, 2007), one can efficiently quantify the relative propensity of innervation of these inputs in both the non-motor and motor STN. Thus, taking advantage of these markers, we showed that cortical and sub-cortical glutamatergic afferents equally innervate motor and non-motor regions of the monkey STN.

*Technical considerations:* We have relied heavily on vGluT1 and vGluT2 as the markers to identify all the cortical and sub-cortical glutamatergic afferents, respectively. However, it must be noted that of all the putatively glutamatergic terminals forming asymmetric synapses in the monkey striatum about 15-20% do not express either vGluT1 or vGluT2 (Raju et al., 2008). A comparable finding was seen in the rat striatum with around 30% of terminals forming asymmetric synapses devoid of any immunolabeling for vGluT1 or vGluT2 (Lacey et al., 2005). While the exact reason for this discrepancy in the striatum is unclear, the same issue may also apply to the STN. Importantly, if this inconsistency occurs due to an inadequate immunolabeling of vGluT1/vGluT2 or due to weak immunohistochemical signals caused by the dynamics of vGluT1/vGluT2

expression in glutamatergic terminals, one could say that the estimates of the relative abundance of vGluT1 and vGluT2 terminals would be imprecise. However, we believe that even in such a situation where we cannot identify all the vGluT1- and vGluT2-containing terminals, the immunolabeling procedure will label these terminals in both the motor and non-motor areas to a similar extent. Thus, even with its imperfections, this procedure will yield results to adequately compare the abundance of vGluT1- and vGluT2-containing terminals between the non-motor and motor regions of the STN.

### 4.1.2. Cortical and sub-cortical glutamatergic inputs innervate different parts of the dendritic tree of STN neurons

If the post-synaptic target of a terminal is a dendritic spine, the likelihood of the terminal-target complex to undergo plastic changes under normal or pathological conditions is much higher than that if the post-synaptic target is a dendritic shaft (Alvarez and Sabatini, 2007; Villalba and Smith, 2013). Hence, we compared the post-synaptic targets (dendritic shafts or spines) of cortical and sub-cortical glutamatergic afferents in the STN to predict the plasticity of these two different input systems. We found that sub-cortical glutamatergic inputs almost exclusively targeted dendritic shafts, rarely contacting dendritic spines; whereas, their cortical counterparts were found in synaptic contact with both dendritic shafts and spines in approximately 70% and 30% of the instances, respectively. Because a higher degree of plasticity is ascribed to dendritic spines compared to dendritic shafts (Alvarez and Sabatini, 2007), it would be logical to conclude that glutamatergic afferents to the STN of cortical origin are more amenable to plastic changes compared to those of sub-cortical origin.

In addition to identifying whether the post-synaptic target was a dendritic shaft or a spine, we also assessed the relative proximity of the terminal to the soma on the dendritic tree. The proximity of the terminal to the soma is one of the anatomical estimates of the tendency of the post-synaptic neuron to respond to inputs arriving from that terminal. Assuming that all other aspects are similar, a more proximally placed input would more readily influence the activity of the post-synaptic neuron compared to a distal input (Stuart and Spruston, 1998). Hence, in cases where glutamatergic inputs terminated onto dendritic shafts of STN neurons, we estimated the proximity of the innervation site to the soma by measuring the approximate diameter of the 2D representation of the dendritic shaft. Since we know that STN dendrites taper off as they extend out away from the soma (Rafols and Fox, 1976), we can assume that the dendritic shaft would have a larger diameter when closer to the soma than it would when further away from the soma. We found that cortical and sub-cortical glutamatergic inputs target the dendritic shafts of STN neurons at different locations, with the sub-cortical inputs contacting dendritic shafts at sites closer to the soma than the cortical ones, an observation in line with a previous rodent study (Bevan et al., 1995). Therefore, if we assume that all the other factors which govern the response of the post-synaptic STN neuron to a synaptic input, such as post-synaptic receptor expression, dynamics of neurotransmitter release and reuptake, etc are similar, a sub-cortical glutamatergic input seems to have a higher connection weight than a cortical glutamatergic input (Stuart and Spruston, 1998). Another key point to consider is that the glutamatergic afferents originating from the cortical versus sub-cortical regions use a different vGluT isoform (vGluT1 versus vGluT2) for packaging glutamate. In fact, the dynamics of glutamate

release by glutamatergic neurons containing vGluT1 are different to those using vGluT2 (Weston et al., 2011). In fact, vGluT2-immunopositive glutamatergic neurons tend to readily release glutamate compared with vGluT1-immunoreactive ones. Although we cannot predict the exact difference in the influence and dynamics of the cortical versus sub-cortical glutamatergic inputs, computational modeling studies which take into account the dendritic innervation pattern and the dynamics of neurotransmitter release could shed some light on the interplay of these two inputs in regulating the physiology of the STN.

*Technical considerations:* The identification of the post-synaptic elements and the diameter measurements of the post-synaptic dendritic shafts were done using single ultrathin EM sections, which gave us only a 2D representation of the morphology. A precise way to perform these studies would be using 3D representations of the terminal-post synaptic element complex. Another important point to note is that the diameter of the post-synaptic dendritic shaft was used as an estimate of the proximity of the input to the soma. However, there are special situations where such an assumption would be incorrect. For example, if there are two equally thick dendrites emanating from the soma, such that one of them gives rise to multiple branches at a proximal location and the other one extends outwards without branching. Typically, dendritic branches tend to be thinner than the parent dendrite. Thus, it is very likely that a dendritic branch which may be thinner than an unbranched dendrite would actually be much closer to the soma than the other. Hence, the ideal way to estimate the proximity of an input to the soma would be using a high resolution 3D reconstruction of the entire dendritic arborization, which has

recently become possible using automated EM sampling methods (Helmstaedter and Mitra, 2012).

4.1.3. Both cortical and sub-cortical glutamatergic inputs to the STN are partially lost in MPTP-treated parkinsonian monkeys

Besides the STN, the striatum is a basal ganglia nucleus which receives major glutamatergic inputs from cortical and sub-cortical regions. It is known that there are significant changes occurring into the innervation, functional connectivity, synaptic transmission and plasticity of major glutamatergic inputs to the striatum in animal models of PD (Ingham et al., 1989; Stephens et al., 2005; Zaja-Milatovic et al., 2005; Raju et al., 2008; Smeal et al., 2008; Villalba et al., 2009; Galvan and Smith, 2011; Mathai and Smith, 2011; Shepherd, 2013; Villalba et al., 2013). Based on the major structural and functional reorganization of the glutamatergic inputs to the striatum in animal models of PD, we assessed whether similar changes occurred in the STN of parkinsonian monkeys. We, indeed, found a significant loss of both cortical (~50%) and sub-cortical (~40%) glutamatergic afferents to the STN in MPTP-treated parkinsonian monkeys. Jointly considering the impact of dopamine loss on the integrity of glutamatergic inputs in the striatum and STN in parkinsonism, one could speculate that common underlying mechanisms affect glutamatergic transmission to the basal ganglia in the dopamine-denervated state.

*Technical considerations:* As discussed in section 4.1.1., we assumed that vGluT1 and vGluT2 could be used as markers to adequately quantify cortical and sub-cortical

glutamatergic terminals, respectively. However, this technical aspect becomes more amplified when we consider that we used these markers to compare the abundance of these glutamatergic inputs between normal and parkinsonian conditions. Not knowing exactly what happens to the expression of these vGluT isoforms in the pathological state, it is possible to undersample or even oversample these glutamatergic afferents. For example, a lower expression of vGluT1 protein in corticosubthalamic terminals in parkinsonian conditions would lead us to wrongly conclude that there is a loss of cortical inputs to the STN in parkinsonism. To counter this limitation, we used a method independent of immunohistochemistry which would give us an estimate of the number of glutamatergic inputs in the STN. By quantifying the number of terminals forming asymmetric synapses, which are considered putatively glutamatergic, we were able to get an approximate number of the glutamatergic inputs. Hence, we are confident that the anatomical result which showed a loss of glutamatergic inputs to the STN is not merely an artifact of the sampling process. However, we would not be able to say with certainty that both the putatively cortical and sub-cortical glutamatergic afferents are lost in parkinsonism, since the immunolabeling independent count of asymmetric synapses samples both vGluT1- and vGluT2-containing terminals. An absolute method to answer this question would be by completing filling all the glutamatergic neurons originating from the cerebral cortex and sub-cortical regions with anterograde tracers and quantifying the terminals in the STN which are immunoreactive for the tracers. But it must be noted that such experiments are practically impossible to execute.

4.1.4. Potential changes in the functional impact of the hyperdirect corticosubthalamic pathway upon pallidal neurons in parkinsonism

To confirm whether our anatomic findings regarding the degeneration of the corticosubthalamic system in parkinsonism translate to any noticeable changes in the functional connectivity of the corticosubthalamic system, we recorded the activity of pallidal neurons downstream from the STN in response to electrical activation of the corticosubthalamic projection. In preliminary experiments in two monkeys, we found that a smaller proportion of pallidal neurons responded to electrical stimulation of the internal capsule with an early excitatory response (latency < 12ms), known to be generated activation of corticosubthalamic projection. Although it is not possible to fully rule out that this decrease in responding neurons in the pallidum was due to functional changes in the subthalamopallidal projection, the pilot electrophysiological studies tend to suggest that there is a functionally relevant denervation of the corticosubthalamic system in MPTP-induced parkinsonism in primates.

The temporal interplay between the corticosubthalamic and corticostriatal pathways has been suggested as a critical element in 'action selection' models of basal ganglia function (Nambu et al., 2002) or in models that ascribe response inhibition to the hyperdirect pathway (Jahfari et al., 2011). According to the action selection model, activation of the hyperdirect pathway causes a surround inhibition of thalamocortical neurons by providing a diffuse excitation of inhibitory pallidothalamic neurons in GPi. A subsequent focal activation of direct striatofugal GABAergic neurons by the corticostriatal system onto this surround inhibition activates a focal group of thalamocortical neurons in a center-surround manner. Later, the activation of the indirect

pathway results in a global inhibition of thalamocortical neurons. According to some authors, such an organization of the corticosubthalamic and corticostriatal pathways allows for a focused selection of motor programs within the basal ganglia (Mink and Thach, 1993; Nambu et al., 2000; Nambu et al., 2002; Helmich et al., 2009; Wylie et al., 2010). Thus, a pathological loss of the 'hyperdirect' pathway could hamper the ability of parkinsonian patients to generate the surround inhibition of thalamocortical neurons. If the proposed action selection mediated by the basal ganglia is important in the physiological selection of motor programs, an alteration of the basal ganglia temporal dynamics could affect the ability to select actions in parkinsonian states. In fact, this possibility is supported by the clinical observations that there is an apparent restriction of action selection in PD patients (Helmich et al., 2009; Wylie et al., 2010). The prominent reduction of the 'hyperdirect' pathway must be considered when modeling action selection mediated by the basal ganglia in parkinsonism. However, it must be noted that a recent study where the corticosubthalamic system of some monkeys was selectively eliminated did not produce any noticeable deficits in the animals (Inoue et al., 2012).

*Technical considerations:* To assess the physiological impact of this pathological change, responses of pallidal neurons to electrical stimulation of the internal capsule were recorded. Because previous STN inactivation studies have shown that "early excitatory" responses (ie below 10-12 msec) generated in the globus pallidus following stimulation of motor cortices, originate from activation of the corticosubthalamic system in rats and monkeys (Kita, 1992; Nambu et al., 2000), we used that approach to determine potential changes in the functional effects of corticosubthalamic activation upon pallidal neurons in MPTP-treated monkeys. Although recordings of STN neurons in response to cortical

stimulation might have been a more direct approach to assess the functional integrity of the corticosubthalamic system in parkinsonian animals, technical challenges in collecting a large and reliable data set from STN neurons in awake monkeys led us to consider the GPe and GPi recording sites for these experiments. To activate the corticosubthalamic system, stimulation electrodes were placed into the posterior limb of the internal capsule. While the placement was not identical across monkeys and stimulation sites, the strength of stimulation was adequate to stimulate a large portion of the internal capsule in all cases. The stimulation parameters were such that the current would stimulate myelinated axons up to 1.7 mm away from the stimulation site (Ranck, 1975). In all cases, a large portion of the internal capsule lay within the 1.7 mm radial distance, and we thus believe that the internal capsule was adequately stimulated. We were also very careful in mapping the borders and extent of GPe and GPi in each case to ensure that comparable recording sites into the ventrolateral part of the pallidal complex were sampled in each animal under normal and parkinsonian conditions. The ventrolateral GPe/GPi region was chosen as recording sites because it is the main target of the dorsolateral STN (ie the main site of pathological changes described in this study), represents the sensorimotor region of GPe/GPi and is located far enough from the internal capsule stimulation electrodes not to be affected by current spread. A possible caveat of our approach is the possibility that stimulation of fibers other than those being part of the cortico-subthalamo-pallidal system might have contributed to the early excitatory responses generated in GPe and GPi. For instance, orthodromic activation of pallidosubthalamic axons or antidromic activation of pallidothalamic pathways could both have also resulted in short latency responses in GPe and GPi neurons. However, such responses were

unlikely because of the dorsal placement of the stimulation electrode away from the trajectory of these fiber tracts (Smith et al., 1990). Also, we have recorded pallidal responses which are significantly longer than what would be expected for antidromic activation of pallidal cells. For almost 2ms after the onset of stimulation, it was not possible to reproduce any neuronal spikes completely due to clipping of the stimulus artifact upto this time. If we were to discount for any excitatory responses that may have occurred during the initial 2ms period post stimulation, the shortest latency of the early excitatory responses recorded in our electrophysiological studies was 3ms. Hence, we think that we have not measured any excitatory responses induced by antidromic stimulation of pallidal efferents. Another important point about antidromic stimulation induced responses is that their failure rate is almost zero. However, for all the early excitatory responses we recorded, there was a considerable failure rate, which is due to the synaptic dynamics. Hence, we know that most of the responses we recorded were likely to have occurred after at least one synaptic transmission event, thus eliminating the possibility of having recorded any antidromic activation events. The stimulation may have activated corticostriatal axons, but if this were the case, the latencies of the excitatory responses generated in GPe and GPi by this activation would have been longer than 12 msec, as shown in previous studies (Nambu et al., 2000). Our response selection criteria excluded this possibility. A similar argument applies to the possibility that the stimulation could have activated the thalamostriatal system. The only projections that might have been activated, and possibly contributed to some of the responses recorded in our study are the cortico-thalamic axons that innervate thalamo-subthalamic or thalamo-pallidal neurons. However, because it involves an additional synaptic delay, it is unlikely

that activation of the cortico-thalamo-subthalamo-pallidal tract was responsible for these effects. Although antidromic activation of thalamo-pallidal neurons cannot be ruled out, this projection is very sparse in primates (Sadikot et al., 1992), and unlikely to have significantly contributed to the electrophysiological responses described in this study. Also, it is likely that some thalamo-subthalamic projections may have axon collaterals which pass through the internal capsule en route to the striatum or cortex. If these axon collaterals are stimulated, there would be an antidromic activation of the CM/PF, in turn activating the STN which would further drive pallidal neurons. However, a single axon tracing study of CM/PF neurons in monkeys did not provide evidence for any such connections (Parent and Parent, 2005). Also, there is no major chance of direct activation of thalamo-subthalamic axons due to their general trajectory which generally steers clear of the internal capsule (Sadikot et al., 1992). Thus, the most likely source of the early excitatory responses generated in the globus pallidus following the internal capsule stimulation is the activation of the cortico-subthalamo-pallidal system (Nambu et al., 2000).

## 4.2. Future Directions

### 4.2.1. Role of the STN in non-motor functions of the basal ganglia

One of the key findings of this thesis is that glutamatergic inputs innervate both the motor and non-motor regions of the STN in similar degrees. Though the connectivity of the STN with non-motor cortical areas has only recently been established in primates (Haynes and Haber, 2013), the STN's non-motor functions are increasingly being

recognized (Teagarden and Rebec, 2007). Also, considering the growing interest in electrically stimulating the STN to alleviate addiction (Pelloux and Baunez, 2013) and neuropsychiatric diseases (Bourne et al., 2012), the non-motor functions of the STN in normal and diseased states warrant extensive examination.

### 4.2.2. Integration of functionally distinct information in the STN

STN neurons extend forth their dendrites to great distances, some as far as 750 μm away from the soma (Rafols and Fox, 1976). These stretches covered by STN dendrites from the soma are so far-reaching, that a single STN neuron can encompass about half, one-fifth, and one-ninth of the STN in the cat, monkey and human, respectively (Yelnik and Percheron, 1979). Reflected upon jointly with our finding that both the motor and non-motor STN regions are equally innervated by glutamatergic inputs, the anatomical composition of the STN seems conducive for greater levels of integration of functionally distinct information. In the striatum, which is the other major input station for glutamatergic inputs to the basal ganglia, the dendritic tree of medium spiny neurons is more restricted (Graveland et al., 1985) compared to that of STN neurons. Considering that functionally distinct information flows in the striatum along highly topographical maps in a segregated manner, it is reasonable to contemplate the possibility that the STN is the basal ganglia input station where external glutamatergic inputs can integrate across functional domains (Smith et al., 1998; Mathai and Smith, 2011). In fact, an important point to note is that in the dopamine denervated state, STN neurons lose their specificity. This question certainly needs further investigation since it will build a much more dynamic model of basal ganglia function.

### 4.2.3. Influences of cortical versus sub-cortical glutamatergic afferents on activity of STN neurons

One can posit from the differential innervation pattern of cortical versus sub-cortical glutamatergic afferents on STN neurons, that these two different sets of glutamatergic inputs have different effects on the activity of STN neurons. Using a combination of behavioral, electrophysiologic and optogenetic approaches, studies could be designed to dissect the control of STN activity by the cortical and sub-cortical glutamatergic input systems, which would be exciting avenues to pursue.

### 4.2.4. Functions of the STN in basal ganglia mediated action selection programs

The action selection model hypothesized by Nambu and others suggests that the sequential activation of pallidal neurons by the hyperdirect, direct and indirect pathways, respectively, could generate a center-surround method to select appropriate motor programs (Nambu et al., 2002). However, it must be noted that the experiments done in support of this model have been done in non-physiological conditions by electrically stimulating the cerebral cortex, whereby large numbers of cortical neurons and passing fibers are electrically stimulated simultaneously. To evaluate the impact of the loss of the hyperdirect pathway in parkinsonism on basal ganglia mediated action selection programs, one has to first recognize whether this pathway is necessary for action selection in normal physiological conditions.

4.2.5. Do glutamatergic inputs to the striatum and STN arise from single neurons within the cortex and/or thalamus in primates?

Some of the corticostriatal and corticosubthalamic inputs originate from single neurons within the cortex in rodents (Kita and Kita, 2012). Whereas, in case of the thalamostriatal and thalamosubthalamic projections, they arise from distinct sets of neurons in the PF of rats (Feger et al., 1994). We need to explore whether the corresponding projection patterns are similar in primates. When we consider that STN-DBS has network wide effects, it is worth considering whether glutamatergic inputs to the STN are collaterals of striatal afferents. Anatomical studies finely characterizing these connections would help us better model the effects of STN-DBS. In fact, when we consider that the cortical and sub-cortical glutamatergic afferents to both the striatum and STN are affected in parkinsonism, it is reasonable to suggest that probably some of them are common neurons which project to both the STN and striatum. However, it must be noted that single-axon tracing studies in primates have not been able to identify cortical or sub-cortical inputs which project to both these regions (Parent and Parent, 2005, 2006). It must be noted that these studies are very labor intensive and have a very small sample set of neurons. Hence, one can hope that automated methods to map the connectivity of the brain may yield faster and efficient results in answering this problem.

4.2.6. Functional changes to corticosubthalamic and subcorticosubthalamic excitatory inputs in parkinsonism

Because glutamatergic inputs to the STN are reduced in parkinsonism, we need to explore whether there are associated changes in the functional connectivity, synaptic

transmission and plasticity, similar to those seen in the glutamatergic afferents to the striatum (Ingham et al., 1989; Ingham et al., 1998; Stephens et al., 2005; Zaja-Milatovic et al., 2005; Raju et al., 2008; Smeal et al., 2008; Villalba et al., 2009; Galvan and Smith, 2011; Mathai and Smith, 2011; Villalba and Smith, 2011; Shepherd, 2013; Villalba et al., 2013). There is some evidence in the literature which points to significant functional changes occurring to the cortical and sub-cortical glutamatergic inputs, including changes in the metabolic activity of these neurons, exaggerated beta oscillations and entrainment between the STN and the brain regions from where the neurons arise (Orieux et al., 2000; Orieux et al., 2002; Mallet et al., 2008; Baudrexel et al., 2011; Shimamoto et al., 2013). Further investigations studying these functional changes are warranted in light of our findings. Moreover, neurons within the CM/PF thalamic nuclei, which are prominent sources of sub-cortical glutamatergic afferents to the STN, degenerate in parkinsonism (Henderson et al., 2000; Villalba et al., 2013). Whether the CM/PF neurons which directly project to the STN are affected in parkinsonism, thereby contributing to the loss of sub-cortical glutamatergic afferents to the STN, is not known.

In fact, the possibility of a decreased activity of the corticosubthalamic system suggested by its partial degeneration in our study is at odds with recording data suggesting that the STN firing rate is pathologically increased in parkinsonism (Bergman et al., 1994; Wichmann and DeLong, 2003) These observations are also difficult to reconcile with data showing an increased motor cortex-STN functional connectivity (Baudrexel et al., 2011) and a greater entrainment of STN neurons to cortical activity (Mallet et al., 2008; Shimamoto et al., 2013) in the parkinsonian state. Although our morphological data may appear in contradiction with these functional studies, it is

noteworthy that increased corticostriatal glutamatergic transmission has been reported in parkinsonism despite a significant loss of glutamatergic synapses in 6-OHDA-treated rats. Whether the degeneration of the corticosubthalamic system in parkinsonism is independent of, or compensatory to these pathological changes is not known.

Thus, a deeper knowledge of the physiological changes of the corticosubthalamic and subcorticosubthalamic synapses in dopamine depleted animals is needed.

### 4.2.7. Plastic changes in response to the functional loss of glutamatergic inputs to the STN: Quantification of glutamate receptors on cortical and sub-cortical glutamatergic afferents to the STN

Although it is well known that dopamine and dopamine receptor agonists can induce physiological changes in STN neuronal activity (Campbell et al., 1985; Hassani and Feger, 1999; Shen and Johnson, 2000), the functional link between the nigrosubthalamic dopaminergic inputs and the glutamatergic inputs to the STN is unclear. In light of the loss of glutamatergic inputs in dopamine denervated conditions, the role of dopamine in maintaining the integrity of individual glutamatergic inputs needs to be explored. The expression of glutamate receptors in the surviving glutamatergic synapses in the parkinsonian STN would be a factor that is influenced by a major loss of glutamatergic inputs. Addressing this question using ultra-high resolution freeze substitution or freeze fracture EM techniques would be an interesting research direction to pursue (Nusser et al., 1998; Masugi-Tokita et al., 2007). Also, it would be interesting to see whether there

are any morphological changes occurring to the terminal-post synaptic target complex in such pathological conditions (Villalba and Smith, 2011).

4.2.8. Common pathological mechanisms affecting the integrity of glutamatergic afferents to the striatum and subthalamic nucleus in the dopamine-denervated state

At first glance, one could conclude that the partial degeneration of the corticosubthalamic projection reported in our study mirror pathological changes of the glutamatergic corticostriatal system in the parkinsonian state (Ingham et al., 1989; Zaja-Milatovic et al., 2005; Raju et al., 2008; Villalba et al., 2009; Mathai and Smith, 2011) However, additional information is needed to make such comparison. First, and foremost, although a significant loss of glutamatergic synapses has been reported in the striatum of 6-OHDA-treated rats, there is no direct evidence that these synapses were those of cortical terminals. In fact, previous studies have demonstrated an increase or no significant change in the prevalence of vGluT1-containing terminals in the striatum of MPTP-treated parkinsonian monkeys (Raju et al., 2008). Along the same line, human postmortem studies revealed an increase of vGluT1 protein expression in the striatum of PD patients (Kashani et al., 2007). Furthermore, we need to explore whether there are any changes in the synaptic transmission, long term plasticity, and functional specificity of the corticosubthalamic projection as seen in case of the corticostriatal system in parkinsonian animals (Calabresi et al., 1993; Florio et al., 1993; Onn and Grace, 1999; Calabresi et al., 2000; Onn et al., 2000; Strafella et al., 2005; Calabresi et al., 2007).

4.2.9. Impact of the loss of corticosubthalamic terminals on the efficacy of STN-DBS

The cerebral cortex is antidromically activated during STN-DBS (Li et al., 2007). Whether this antidromic drive is an important factor in mediating the therapeutic benefits of STN-DBS is not clearly known. With the knowledge that corticosubthalamic inputs are lost in parkinsonism, it would be important to correlate the integrity of the corticosubthalamic system with the efficacy of the procedure in patients.

## 4.3. Concluding Remarks

This thesis work has resulted in some key findings regarding the changes in the glutamatergic inputs to the STN in the parkinsonism state. The STN, which has long been considered to be an important nucleus of the basal ganglia, has been a subject of deeper investigation ever since the advent of subthalamotomy and STN-DBS to treat advanced-stage parkinsonian patients. Understanding the pathological changes occurring to extrinsic inputs leading to the STN has been an important point to address. This thesis has partly addressed this issue by characterizing changes occurring to the glutamatergic component of the STN afferents. Importantly, a reduced innervation of the STN by glutamatergic inputs in parkinsonism has been the most important finding of this thesis. The impact of such a denervation on the activity of the basal ganglia needs to be further explored. Also, some of the findings of this thesis could aid computational modeling studies in understanding the intrinsic dynamics of STN activity. Moreover, recognizing that the glutamatergic inputs to the STN are affected by dopaminergic denervation, in addition to the well-known changes happening to the glutamatergic inputs to the striatum, warrants detailed studies of changes occurring to all the basal ganglia projection systems

in parkinsonism. A clear understanding of the progression of some of these pathological changes and the local versus network effects of dopamine loss would help us better understand the pathophysiology of the disease. Finally, whether these findings translate to changes occurring in the actual human disease must be explored.

# 5. References

Afsharpour S (1985) Light microscopic analysis of Golgi-impregnated rat subthalamic neurons. J Comp Neurol 236:1-13.

Albin RL, Young AB, Penney JB (1989) The functional anatomy of basal ganglia disorders. Trends Neurosci 12:366-375.

Alexander GE, DeLong MR, Strick PL (1986) Parallel organization of functionally segregated circuits linking basal ganglia and cortex. Annu Rev Neurosci 9:357-381.

Alexander GE, Crutcher MD, DeLong MR (1990) Basal ganglia-thalamocortical circuits: parallel substrates for motor, oculomotor, "prefrontal" and "limbic" functions. Prog Brain Res 85:119-146.

Alvarez L, Macias R, Pavon N, Lopez G, Rodriguez-Oroz MC, Rodriguez R, Alvarez M, Pedroso I, Teijeiro J, Fernandez R, Casabona E, Salazar S, Maragoto C, Carballo M, Garcia I, Guridi J, Juncos JL, DeLong MR, Obeso JA (2009) Therapeutic efficacy of unilateral subthalamotomy in Parkinson's disease: results in 89 patients followed for up to 36 months. J Neurol Neurosurg Psychiatry 80:979-985.

Alvarez VA, Sabatini BL (2007) Anatomical and physiological plasticity of dendritic spines. Annu Rev Neurosci 30:79-97.

Arias-Carrion O, Poppel E (2007) Dopamine, learning, and reward-seeking behavior. Acta Neurobiol Exp (Wars) 67:481-488.

Barroso-Chinea P, Castle M, Aymerich MS, Lanciego JL (2008) Expression of vesicular glutamate transporters 1 and 2 in the cells of origin of the rat thalamostriatal pathway. J Chem Neuroanat 35:101-107.

Barroso-Chinea P, Castle M, Aymerich MS, Perez-Manso M, Erro E, Tunon T, Lanciego JL (2007) Expression of the mRNAs encoding for the vesicular glutamate transporters 1 and 2 in the rat thalamus. J Comp Neurol 501:703-715.

Baudrexel S, Witte T, Seifried C, von Wegner F, Beissner F, Klein JC, Steinmetz H, Deichmann R, Roeper J, Hilker R (2011) Resting state fMRI reveals increased subthalamic nucleus-motor cortex connectivity in Parkinson's disease. Neuroimage 55:1728-1738.

Bergman H, Wichmann T, DeLong MR (1990) Reversal of experimental parkinsonism by lesions of the subthalamic nucleus. Science 249:1436-1438.

Bergman H, Wichmann T, Karmon B, DeLong MR (1994) The primate subthalamic nucleus. II. Neuronal activity in the MPTP model of parkinsonism. J Neurophysiol 72:507-520.

Beurrier C, Congar P, Bioulac B, Hammond C (1999) Subthalamic nucleus neurons switch from single-spike activity to burst-firing mode. J Neurosci 19:599-609.

Bevan MD, Bolam JP (1995) Cholinergic, GABAergic, and glutamate-enriched inputs from the mesopontine tegmentum to the subthalamic nucleus in the rat. J Neurosci 15:7105-7120.

Bevan MD, Wilson CJ (1999) Mechanisms underlying spontaneous oscillation and rhythmic firing in rat subthalamic neurons. J Neurosci 19:7617-7628.

Bevan MD, Francis CM, Bolam JP (1995) The glutamate-enriched cortical and thalamic input to neurons in the subthalamic nucleus of the rat: convergence with GABA-positive terminals. J Comp Neurol 361:491-511.

Bevan MD, Atherton JF, Baufreton J (2006) Cellular principles underlying normal and pathological activity in the subthalamic nucleus. Curr Opin Neurobiol 16:621-628.

Bevan MD, Magill PJ, Terman D, Bolam JP, Wilson CJ (2002) Move to the rhythm: oscillations in the subthalamic nucleus-external globus pallidus network. Trends Neurosci 25:525-531.

Bogenpohl J, Galvan A, Hu X, Wichmann T, Smith Y (2013) Metabotropic glutamate receptor 4 in the basal ganglia of parkinsonian monkeys: ultrastructural localization and electrophysiological effects of activation in the striatopallidal complex. Neuropharmacology 66:242-252.

Bourne SK, Eckhardt CA, Sheth SA, Eskandar EN (2012) Mechanisms of deep brain stimulation for obsessive compulsive disorder: effects upon cells and circuits. Front Integr Neurosci 6:29.

Bronstein JM et al. (2011) Deep brain stimulation for Parkinson disease: an expert consensus and review of key issues. Arch Neurol 68:165.

Calabresi P, Centonze D, Bernardi G (2000) Electrophysiology of dopamine in normal and denervated striatal neurons. Trends Neurosci 23:S57-63.

Calabresi P, Mercuri NB, Sancesario G, Bernardi G (1993) Electrophysiology of dopamine-denervated striatal neurons. Implications for Parkinson's disease. Brain 116 ( Pt 2):433-452.

Calabresi P, Picconi B, Tozzi A, Di Filippo M (2007) Dopamine-mediated regulation of corticostriatal synaptic plasticity. Trends Neurosci 30:211-219.

Campbell GA, Eckardt MJ, Weight FF (1985) Dopaminergic mechanisms in subthalamic nucleus of rat: analysis using horseradish peroxidase and microiontophoresis. Brain Res 333:261-270.

Chudasama Y, Baunez C, Robbins TW (2003) Functional disconnection of the medial prefrontal cortex and subthalamic nucleus in attentional performance: evidence for corticosubthalamic interaction. J Neurosci 23:5477-5485.

Dierssen G, Bergmann LL, Gioino G, Cooper IS (1961) Hemiballism following surgery for Parkinson's disease. A clinicoanatomical study of a case. Arch Neurol 5:627-637.

Do MT, Bean BP (2003) Subthreshold sodium currents and pacemaking of subthalamic neurons: modulation by slow inactivation. Neuron 39:109-120.

Do MT, Bean BP (2004) Sodium currents in subthalamic nucleus neurons from Nav1.6-null mice. J Neurophysiol 92:726-733.

Fan KY, Baufreton J, Surmeier DJ, Chan CS, Bevan MD (2012) Proliferation of external globus pallidus-subthalamic nucleus synapses following degeneration of midbrain dopamine neurons. J Neurosci 32:13718-13728.

Feger J, Bevan M, Crossman AR (1994) The projections from the parafascicular thalamic nucleus to the subthalamic nucleus and the striatum arise from separate neuronal populations: a comparison with the corticostriatal and corticosubthalamic efferents in a retrograde fluorescent double-labelling study. Neuroscience 60:125-132.

Ferraye MU, Debu B, Fraix V, Krack P, Charbardes S, Seigneuret E, Benabid AL, Pollak P (2011) Subthalamic nucleus versus pedunculopontine nucleus stimulation in Parkinson disease: synergy or antagonism? J Neural Transm 118:1469-1475.

Florio T, Di Loreto S, Cerrito F, Scarnati E (1993) Influence of prelimbic and sensorimotor cortices on striatal neurons in the rat: electrophysiological evidence for converging inputs and the effects of 6-OHDA-induced degeneration of the substantia nigra. Brain Res 619:180-188.

Fremeau RT, Jr., Voglmaier S, Seal RP, Edwards RH (2004) VGLUTs define subsets of excitatory neurons and suggest novel roles for glutamate. Trends Neurosci 27:98-103.

Fremeau RT, Jr., Troyer MD, Pahner I, Nygaard GO, Tran CH, Reimer RJ, Bellocchio EE, Fortin D, Storm-Mathisen J, Edwards RH (2001) The expression of vesicular glutamate transporters defines two classes of excitatory synapse. Neuron 31:247-260.

Fujiyama F, Unzai T, Nakamura K, Nomura S, Kaneko T (2006) Difference in organization of corticostriatal and thalamostriatal synapses between patch and matrix compartments of rat neostriatum. Eur J Neurosci 24:2813-2824.

Fujiyama F, Kuramoto E, Okamoto K, Hioki H, Furuta T, Zhou L, Nomura S, Kaneko T (2004) Presynaptic localization of an AMPA-type glutamate receptor in corticostriatal and thalamostriatal axon terminals. Eur J Neurosci 20:3322-3330.

Galvan A, Smith Y (2011) The primate thalamostriatal systems: Anatomical organization, functional roles and possible involvement in Parkinson's disease. Basal Ganglia 1:179-189.

Galvan A, Hu X, Smith Y, Wichmann T (2010) Localization and function of GABA transporters in the globus pallidus of parkinsonian monkeys. Exp Neurol 223:505-515.

Galvan A, Hu X, Smith Y, Wichmann T (2011) Localization and pharmacological modulation of GABA-B receptors in the globus pallidus of parkinsonian monkeys. Exp Neurol 229:429-439.

Garber JC, Barbee RW, Bielitzki JT, Clayton LA, Donovan JC, Hendriksen CFM, Kohn DF, Lipman NS, Locke PA, Melcher J, Quimby FW, Turner PV, Wood GA, Würbel H (2010) Guide for the Care and Use of Laboratory Animals, 8 Edition. Washington, D.C.: The National Academies Press.

Gill SS, Heywood P (1997) Bilateral dorsolateral subthalamotomy for advanced Parkinson's disease. Lancet 350:1224.

Gras C, Herzog E, Bellenchi GC, Bernard V, Ravassard P, Pohl M, Gasnier B, Giros B, El Mestikawy S (2002) A third vesicular glutamate transporter expressed by cholinergic and serotoninergic neurons. J Neurosci 22:5442-5451.

Graveland GA, Williams RS, DiFiglia M (1985) A Golgi study of the human neostriatum: neurons and afferent fibers. J Comp Neurol 234:317-333.

Gross RE (2008) What happened to posteroventral pallidotomy for Parkinson's disease and dystonia? Neurotherapeutics 5:281-293.

Guridi J, Obeso JA (2001) The subthalamic nucleus, hemiballismus and Parkinson's disease: reappraisal of a neurosurgical dogma. Brain 124:5-19.

Haber SN, Fudge JL, McFarland NR (2000) Striatonigrostriatal pathways in primates form an ascending spiral from the shell to the dorsolateral striatum. J Neurosci 20:2369-2382.

Hadipour-Niktarash A, Rommelfanger KS, Masilamoni GJ, Smith Y, Wichmann T (2012) Extrastriatal D2-like receptors modulate basal ganglia pathways in normal and Parkinsonian monkeys. J Neurophysiol 107:1500-1512.

Hallworth NE, Wilson CJ, Bevan MD (2003) Apamin-sensitive small conductance calcium-activated potassium channels, through their selective coupling to voltage-gated calcium channels, are critical determinants of the precision, pace, and pattern of action potential generation in rat subthalamic nucleus neurons in vitro. J Neurosci 23:7525-7542.

Hammond C, Yelnik J (1983) Intracellular labelling of rat subthalamic neurones with horseradish peroxidase: computer analysis of dendrites and characterization of axon arborization. Neuroscience 8:781-790.

Hassani OK, Feger J (1999) Effects of intrasubthalamic injection of dopamine receptor agonists on subthalamic neurons in normal and 6-hydroxydopamine-lesioned rats: an electrophysiological and c-Fos study. Neuroscience 92:533-543.

Haynes WI, Haber SN (2013) The organization of prefrontal-subthalamic inputs in primates provides an anatomical substrate for both functional specificity and integration: implications for Basal Ganglia models and deep brain stimulation. J Neurosci 33:4804-4814.

Hazrati LN, Parent A (1991) Projection from the external pallidum to the reticular thalamic nucleus in the squirrel monkey. Brain Res 550:142-146.

Hazrati LN, Parent A, Mitchell S, Haber SN (1990) Evidence for interconnections between the two segments of the globus pallidus in primates: a PHA-L anterograde tracing study. Brain Res 533:171-175.

Helmich RC, Aarts E, de Lange FP, Bloem BR, Toni I (2009) Increased dependence of action selection on recent motor history in Parkinson's disease. J Neurosci 29:6105-6113.

Helmstaedter M, Mitra PP (2012) Computational methods and challenges for large-scale circuit mapping. Curr Opin Neurobiol 22:162-169.

Henderson JM, Carpenter K, Cartwright H, Halliday GM (2000) Degeneration of the centre median-parafascicular complex in Parkinson's disease. Ann Neurol 47:345-352.

Hornykiewicz O (1998) Biochemical aspects of Parkinson's disease. Neurology 51:S2-9.

Humphries MD, Gurney K (2012) Network effects of subthalamic deep brain stimulation drive a unique mixture of responses in basal ganglia output. Eur J Neurosci 36:2240-2251.

Hur EE, Zaborszky L (2005) Vglut2 afferents to the medial prefrontal and primary somatosensory cortices: a combined retrograde tracing in situ hybridization study [corrected]. J Comp Neurol 483:351-373.

Ingham CA, Hood SH, Arbuthnott GW (1989) Spine density on neostriatal neurones changes with 6-hydroxydopamine lesions and with age. Brain Res 503:334-338.

Ingham CA, Hood SH, Taggart P, Arbuthnott GW (1998) Plasticity of synapses in the rat neostriatum after unilateral lesion of the nigrostriatal dopaminergic pathway. J Neurosci 18:4732-4743.

Inoue K, Koketsu D, Kato S, Kobayashi K, Nambu A, Takada M (2012) Immunotoxin-mediated tract targeting in the primate brain: selective elimination of the cortico-subthalamic "hyperdirect" pathway. PLoS One 7:e39149.

Iwahori N (1978) A Golgi study on the subthalamic nucleus of the cat. J Comp Neurol 182:383-397.

Jahfari S, Waldorp L, van den Wildenberg WP, Scholte HS, Ridderinkhof KR, Forstmann BU (2011) Effective connectivity reveals important roles for both the hyperdirect (fronto-subthalamic) and the indirect (fronto-striatal-pallidal) fronto-basal ganglia pathways during response inhibition. J Neurosci 31:6891-6899.

Joel D, Weiner I (1994) The organization of the basal ganglia-thalamocortical circuits: open interconnected rather than closed segregated. Neuroscience 63:363-379.

Kaneko T, Fujiyama F (2002) Complementary distribution of vesicular glutamate transporters in the central nervous system. Neurosci Res 42:243-250.

Kashani A, Betancur C, Giros B, Hirsch E, El Mestikawy S (2007) Altered expression of vesicular glutamate transporters VGLUT1 and VGLUT2 in Parkinson disease. Neurobiol Aging 28:568-578.

Kita H (1992) Responses of globus pallidus neurons to cortical stimulation: intracellular study in the rat. Brain Res 589:84-90.

Kita H, Chang HT, Kitai ST (1983) The morphology of intracellularly labeled rat subthalamic neurons: a light microscopic analysis. J Comp Neurol 215:245-257.

Kita T, Kita H (2012) The subthalamic nucleus is one of multiple innervation sites for long-range corticofugal axons: a single-axon tracing study in the rat. J Neurosci 32:5990-5999.

Kliem MA, Pare JF, Khan ZU, Wichmann T, Smith Y (2010) Ultrastructural localization and function of dopamine D1-like receptors in the substantia nigra pars reticulata and the internal segment of the globus pallidus of parkinsonian monkeys. Eur J Neurosci 31:836-851.

Kubota Y, Hatada S, Kondo S, Karube F, Kawaguchi Y (2007) Neocortical inhibitory terminals innervate dendritic spines targeted by thalamocortical afferents. J Neurosci 27:1139-1150.

Lacey CJ, Boyes J, Gerlach O, Chen L, Magill PJ, Bolam JP (2005) GABA(B) receptors at glutamatergic synapses in the rat striatum. Neuroscience 136:1083-1095.

Lavoie B, Parent A (1994a) Pedunculopontine nucleus in the squirrel monkey: projections to the basal ganglia as revealed by anterograde tract-tracing methods. J Comp Neurol 344:210-231.

Lavoie B, Parent A (1994b) Pedunculopontine nucleus in the squirrel monkey: distribution of cholinergic and monoaminergic neurons in the mesopontine tegmentum with evidence for the presence of glutamate in cholinergic neurons. J Comp Neurol 344:190-209.

Levesque JC, Parent A (2005) GABAergic interneurons in human subthalamic nucleus. Mov Disord 20:574-584.

Li JL, Xiong KH, Dong YL, Fujiyama F, Kaneko T, Mizuno N (2003) Vesicular glutamate transporters, VGluT1 and VGluT2, in the trigeminal ganglion neurons of the rat, with special reference to coexpression. J Comp Neurol 463:212-220.

Li S, Arbuthnott GW, Jutras MJ, Goldberg JA, Jaeger D (2007) Resonant antidromic cortical circuit activation as a consequence of high-frequency subthalamic deep-brain stimulation. J Neurophysiol 98:3525-3537.

Liguz-Lecznar M, Skangiel-Kramska J (2007) Vesicular glutamate transporters (VGLUTs): the three musketeers of glutamatergic system. Acta Neurobiol Exp (Wars) 67:207-218.

Lindefors N, Ungerstedt U (1990) Bilateral regulation of glutamate tissue and extracellular levels in caudate-putamen by midbrain dopamine neurons. Neurosci Lett 115:248-252.

Magill PJ, Bolam JP, Bevan MD (2000) Relationship of activity in the subthalamic nucleus-globus pallidus network to cortical electroencephalogram. J Neurosci 20:820-833.

Mallet N, Pogosyan A, Sharott A, Csicsvari J, Bolam JP, Brown P, Magill PJ (2008) Disrupted dopamine transmission and the emergence of exaggerated beta oscillations in subthalamic nucleus and cerebral cortex. J Neurosci 28:4795-4806.

Mallet N, Micklem BR, Henny P, Brown MT, Williams C, Bolam JP, Nakamura KC, Magill PJ (2012) Dichotomous organization of the external globus pallidus. Neuron 74:1075-1086.

Masilamoni GJ, Bogenpohl JW, Alagille D, Delevich K, Tamagnan G, Votaw JR, Wichmann T, Smith Y (2011) Metabotropic glutamate receptor 5 antagonist protects dopaminergic and noradrenergic neurons from degeneration in MPTP-treated monkeys. Brain 134:2057-2073.

Masugi-Tokita M, Tarusawa E, Watanabe M, Molnar E, Fujimoto K, Shigemoto R (2007) Number and density of AMPA receptors in individual synapses in the rat cerebellum as revealed by SDS-digested freeze-fracture replica labeling. J Neurosci 27:2135-2144.

Mathai A, Smith Y (2011) The corticostriatal and corticosubthalamic pathways: two entries, one target. So what? Front Syst Neurosci 5:64.

Mathai A, Pare JF, Jenkins S, Smith Y (2009) Glutamatergic inputs to the subthalamic nucleus: A quantitative analysis of the synaptic microcircuitry of vGluT1- and vGluT2-containing terminals in nonhuman primates. In: 39th Annual Meeting of the Society for Neuroscience. Chicago, IL.

Mathai A, Pare JF, Jenkins S, Smith Y (2010) Glutamatergic inputs to the subthalamic nucleus: A quantitative analysis of the synaptic microcircuitry of vGluT1- and vGluT2-containing terminals in normal and Parkinsonian nonhuman primates. In: Xth Triennial Meeting of the International Basal Ganglia Society. Long Branch, NJ.

Mathai A, Ma Y, Wichmann T, Smith Y (2011) Glutamatergic inputs to the subthalamic nucleus degenerate in experimental parkinsonism. In: 41st Annual Meeting of the Society for Neuroscience. Washington, DC.

McIntyre CC, Savasta M, Kerkerian-Le Goff L, Vitek JL (2004) Uncovering the mechanism(s) of action of deep brain stimulation: activation, inhibition, or both. Clin Neurophysiol 115:1239-1248.

McMillan J, Galvan A, Wichmann T, Bloomsmith M (2010) The use of positive reinforcement during pole and collar training of rhesus macaques (Macaca

mulatta). Journal of the American Association for Laboratory Animal Science 49:705-706.

Meshul CK, Cogen JP, Cheng HW, Moore C, Krentz L, McNeill TH (2000) Alterations in rat striatal glutamate synapses following a lesion of the cortico- and/or nigrostriatal pathway. Exp Neurol 165:191-206.

Middleton FA, Strick PL (1994) Anatomical evidence for cerebellar and basal ganglia involvement in higher cognitive function. Science 266:458-461.

Middleton FA, Strick PL (2002) Basal-ganglia 'projections' to the prefrontal cortex of the primate. Cereb Cortex 12:926-935.

Mink JW (1996) The basal ganglia: focused selection and inhibition of competing motor programs. Prog Neurobiol 50:381-425.

Mink JW, Thach WT (1993) Basal ganglia intrinsic circuits and their role in behavior. Curr Opin Neurobiol 3:950-957.

Miyachi S, Lu X, Imanishi M, Sawada K, Nambu A, Takada M (2006) Somatotopically arranged inputs from putamen and subthalamic nucleus to primary motor cortex. Neurosci Res 56:300-308.

Monakow KH, Akert K, Kunzle H (1978) Projections of the precentral motor cortex and other cortical areas of the frontal lobe to the subthalamic nucleus in the monkey. Exp Brain Res 33:395-403.

Nambu A, Tokuno H, Takada M (2002) Functional significance of the cortico-subthalamo-pallidal 'hyperdirect' pathway. Neurosci Res 43:111-117.

Nambu A, Takada M, Inase M, Tokuno H (1996) Dual somatotopical representations in the primate subthalamic nucleus: evidence for ordered but reversed body-map

transformations from the primary motor cortex and the supplementary motor area. J Neurosci 16:2671-2683.

Nambu A, Tokuno H, Hamada I, Kita H, Imanishi M, Akazawa T, Ikeuchi Y, Hasegawa N (2000) Excitatory cortical inputs to pallidal neurons via the subthalamic nucleus in the monkey. J Neurophysiol 84:289-300.

Nusser Z, Hajos N, Somogyi P, Mody I (1998) Increased number of synaptic GABA(A) receptors underlies potentiation at hippocampal inhibitory synapses. Nature 395:172-177.

Onn SP, Grace AA (1999) Alterations in electrophysiological activity and dye coupling of striatal spiny and aspiny neurons in dopamine-denervated rat striatum recorded in vivo. Synapse 33:1-15.

Onn SP, West AR, Grace AA (2000) Dopamine-mediated regulation of striatal neuronal and network interactions. Trends Neurosci 23:S48-56.

Orieux G, Francois C, Feger J, Hirsch EC (2002) Consequences of dopaminergic denervation on the metabolic activity of the cortical neurons projecting to the subthalamic nucleus in the rat. J Neurosci 22:8762-8770.

Orieux G, Francois C, Feger J, Yelnik J, Vila M, Ruberg M, Agid Y, Hirsch EC (2000) Metabolic activity of excitatory parafascicular and pedunculopontine inputs to the subthalamic nucleus in a rat model of Parkinson's disease. Neuroscience 97:79-88.

Parent A, Hazrati LN (1995) Functional anatomy of the basal ganglia. I. The cortico-basal ganglia-thalamo-cortical loop. Brain Res Brain Res Rev 20:91-127.

Parent M, Parent A (2005) Single-axon tracing and three-dimensional reconstruction of centre median-parafascicular thalamic neurons in primates. J Comp Neurol 481:127-144.

Parent M, Parent A (2006) Single-axon tracing study of corticostriatal projections arising from primary motor cortex in primates. J Comp Neurol 496:202-213.

Paxinos G, Huang X-F, Toga AW (1999) The Rhesus Monkey Brain in Stereotaxic Coordinates, 1 Edition. San Diego: Academic Press.

Pelloux Y, Baunez C (2013) Deep brain stimulation for addiction: why the subthalamic nucleus should be favored. Curr Opin Neurobiol 23:713-720.

Peters A, Palay SL, Webster Hd (1991) The Fine Structure of the Nervous System: Neurons and their Supporting Cells, 3 Edition. New York: Oxford University Press.

Pifl C, Bertel O, Schingnitz G, Hornykiewicz O (1990) Extrastriatal dopamine in symptomatic and asymptomatic rhesus monkeys treated with 1-methyl-4-phenyl-1,2,3,6-tetrahydropyridine (MPTP). Neurochem Int 17:263-270.

Rafols JA, Fox CA (1976) The neurons in the primate subthalamic nucleus: a Golgi and electron microscopic study. J Comp Neurol 168:75-111.

Raju DV, Shah DJ, Wright TM, Hall RA, Smith Y (2006) Differential synaptology of vGluT2-containing thalamostriatal afferents between the patch and matrix compartments in rats. J Comp Neurol 499:231-243.

Raju DV, Ahern TH, Shah DJ, Wright TM, Standaert DG, Hall RA, Smith Y (2008) Differential synaptic plasticity of the corticostriatal and thalamostriatal systems in an MPTP-treated monkey model of parkinsonism. Eur J Neurosci 27:1647-1658.

Ranck JB, Jr. (1975) Which elements are excited in electrical stimulation of mammalian central nervous system: a review. Brain Res 98:417-440.

Rektor I, Balaz M, Bockova M (2009) Cognitive activities in the subthalamic nucleus. Invasive studies. Parkinsonism Relat Disord 15 Suppl 3:S83-86.

Rommelfanger KS, Wichmann T (2010) Extrastriatal dopaminergic circuits of the Basal Ganglia. Front Neuroanat 4:139.

Sadikot AF, Parent A, Francois C (1992) Efferent connections of the centromedian and parafascicular thalamic nuclei in the squirrel monkey: a PHA-L study of subcortical projections. J Comp Neurol 315:137-159.

Shen KZ, Johnson SW (2000) Presynaptic dopamine D2 and muscarine M3 receptors inhibit excitatory and inhibitory transmission to rat subthalamic neurones in vitro. J Physiol 525 Pt 2:331-341.

Shepherd GM (2013) Corticostriatal connectivity and its role in disease. Nat Rev Neurosci 14:278-291.

Shimamoto SA, Ryapolova-Webb ES, Ostrem JL, Galifianakis NB, Miller KJ, Starr PA (2013) Subthalamic nucleus neurons are synchronized to primary motor cortex local field potentials in Parkinson's disease. J Neurosci 33:7220-7233.

Shink E, Bevan MD, Bolam JP, Smith Y (1996) The subthalamic nucleus and the external pallidum: two tightly interconnected structures that control the output of the basal ganglia in the monkey. Neuroscience 73:335-357.

Smeal RM, Keefe KA, Wilcox KS (2008) Differences in excitatory transmission between thalamic and cortical afferents to single spiny efferent neurons of rat dorsal striatum. Eur J Neurosci 28:2041-2052.

Smith Y (2011) Anatomy and Synaptic Connectivity of the Basal Ganglia. In: Youmans Neurological Surgery, 6 Edition (Winn HR, ed), pp 854-863. Philadelphia: Saunders.

Smith Y, Hazrati LN, Parent A (1990) Efferent projections of the subthalamic nucleus in the squirrel monkey as studied by the PHA-L anterograde tracing method. J Comp Neurol 294:306-323.

Smith Y, Wichmann T, DeLong M (2013) Corticostriatal and Mesocortical Dopamine Systems: Do Species Differences Matter? Nature Reviews Neuroscience (In press).

Smith Y, Bevan MD, Shink E, Bolam JP (1998) Microcircuitry of the direct and indirect pathways of the basal ganglia. Neuroscience 86:353-387.

Smith Y, Wichmann T, Factor SA, DeLong MR (2012) Parkinson's disease therapeutics: new developments and challenges since the introduction of levodopa. Neuropsychopharmacology 37:213-246.

Stephens B, Mueller AJ, Shering AF, Hood SH, Taggart P, Arbuthnott GW, Bell JE, Kilford L, Kingsbury AE, Daniel SE, Ingham CA (2005) Evidence of a breakdown of corticostriatal connections in Parkinson's disease. Neuroscience 132:741-754.

Strafella AP, Ko JH, Grant J, Fraraccio M, Monchi O (2005) Corticostriatal functional interactions in Parkinson's disease: a rTMS/[11C]raclopride PET study. Eur J Neurosci 22:2946-2952.

Stuart G, Spruston N (1998) Determinants of voltage attenuation in neocortical pyramidal neuron dendrites. J Neurosci 18:3501-3510.

Teagarden MA, Rebec GV (2007) Subthalamic and striatal neurons concurrently process motor, limbic, and associative information in rats performing an operant task. J Neurophysiol 97:2042-2058.

Tepper JM, Wilson CJ, Koos T (2008) Feedforward and feedback inhibition in neostriatal GABAergic spiny neurons. Brain Res Rev 58:272-281.

Villalba RM, Smith Y (2011) Differential structural plasticity of corticostriatal and thalamostriatal axo-spinous synapses in MPTP-treated Parkinsonian monkeys. J Comp Neurol 519:989-1005.

Villalba RM, Smith Y (2013) Differential striatal spine pathology in Parkinson's disease and cocaine addiction: a key role of dopamine? Neuroscience 251:2-20.

Villalba RM, Lee H, Smith Y (2009) Dopaminergic denervation and spine loss in the striatum of MPTP-treated monkeys. Exp Neurol 215:220-227.

Villalba RM, Wichmann T, Smith Y (2013) Neuronal loss in the caudal intralaminar thalamic nuclei in a primate model of Parkinson's disease. Brain Struct Funct.

Weston MC, Nehring RB, Wojcik SM, Rosenmund C (2011) Interplay between VGLUT isoforms and endophilin A1 regulates neurotransmitter release and short-term plasticity. Neuron 69:1147-1159.

Wichmann T, DeLong MR (1996) Functional and pathophysiological models of the basal ganglia. Curr Opin Neurobiol 6:751-758.

Wichmann T, DeLong MR (2003) Pathophysiology of Parkinson's disease: the MPTP primate model of the human disorder. Ann N Y Acad Sci 991:199-213.

Wichmann T, Kliem MA, DeLong MR (2001) Antiparkinsonian and behavioral effects of inactivation of the substantia nigra pars reticulata in hemiparkinsonian primates. Exp Neurol 167:410-424.

Wilson CJ, Bevan MD (2011) Intrinsic dynamics and synaptic inputs control the activity patterns of subthalamic nucleus neurons in health and in Parkinson's disease. Neuroscience 198:54-68.

Wylie SA, Ridderinkhof KR, Bashore TR, van den Wildenberg WP (2010) The effect of Parkinson's disease on the dynamics of on-line and proactive cognitive control during action selection. J Cogn Neurosci 22:2058-2073.

Yelnik J, Percheron G (1979) Subthalamic neurons in primates: a quantitative and comparative analysis. Neuroscience 4:1717-1743.

Zaja-Milatovic S, Milatovic D, Schantz AM, Zhang J, Montine KS, Samii A, Deutch AY, Montine TJ (2005) Dendritic degeneration in neostriatal medium spiny neurons in Parkinson disease. Neurology 64:545-547.